

Development of biodegradable nanostructured polymer materials by using block copolymer technology for packaging applications





GIPUZKOAKO
INGENIARITZA
ESKOLA
ESCUELA
DE INGENIERÍA
DE GIPUZKOA

Development of biodegradable nanostructured polymer materials by using block copolymer for packaging applications.

Miriam Gallur Blanca

PhD Program of Renewable Materials Engineering

Department of Chemical and Environmental Engineering

Thesis supervisors:

Dr Susana Aucejo

Dr Agnieszka Tercjak

Donostia-San Sebastián, 2022

Confidential

(c)2022 MIRIAM GALLUR BLANCA

Dedicado a todos los miembros de mi familia, la de casa y la de mi segunda casa, ITENE.

SUMMARY

SUMMARY

This investigation work is focused on preparation and characterization of novel polymeric materials based on PLDA homopolymer and both commercial and synthesized PLLA-b-PCL diblock copolymer with improved properties to be use for packaging applications. This manuscript consists of a short Introduction and Motivation and Objectives, following 7 Chapters related to experimental part of this investigation work and is finished with General Conclusions, Future Work and Scientific Production.

In Chapter 1, the miscibility between PLDA and PCL homopolymers is evaluated since PCL homopolymer as a good candidate to improve brittleness of PLDA. For this purpose, first a procedure for obtaining homopolymer films by solvent casting technology is checked. Using this procedure, several PLDA/PCL polymer blends are produced and characterized to analyse PLDA/PCL miscibility.

Chapter 2 deals with the use of a semi-crystalline PLLA-b-PCL diblock copolymer as a polymer blend component to introduce a PCL block in a PLDA homopolymer. Several PLLA-b-PCL/PLDA polymer blends with different PLLA-b-PCL content is produced by solvent casting and studied. Main characterization is focused on the effect of the PLLA-b-PCL on the properties of PLDA polymer matrix, concretely on the possibility of its self-assembly and the morphologies obtained, as well as the improvement of barrier properties if compared with neat PLDA homopolymer.

Chapter 3 explores the use of the PLLA-b-PCL as polymer blend compatibilizer to improve the miscibility of PLDA-PCL polymer blend components. The investigation work in this Chapter is oriented to the double miscibility between each block of PLLA-b-PCL diblock copolymer with PLDA and PCL homopolymers, respectively. Two specific ratios of PLDA-PCL are chosen for preparation of PLLA-b-PCL/PLDA-PCL polymer blends with different content of PLLA-b-PCL diblock copolymers. PLLA-b-PCL/PLDA-PCL polymer blends is characterized to analyse the effect of the PLLA-d-PCL as compatibilizer on the final morphology, thermal and barrier properties.

Chapter 4 takes advantage of the results obtained in Chapter 2 using a commercial diblock copolymer, the investigation work is focused on the synthesis of PLLA-b-PCL diblock copolymer on laboratory scale with the same characteristics as the commercial one. In this Chapter, the

optimization of polymerization reaction conditions of synthesis on laboratory scale of PLLA-b-PCL diblock copolymer is established and the possibility of nanostructuring of polymer blend by addition of PLLA-b-PCL diblock copolymer is verified. Moreover, an evaluation of three different PLDA:PCL ratios (1:1, 2:1 and 3:1) is done as well as preparation and characterization of mechanical, thermal and barrier properties of PLLA-b-PCL/PLDA polymer blends using synthesized PLLA-b-PCL diblock copolymers with different PLLA:PCL ratios. This Chapter allow to choose the synthesis procedure and the ratio of the PLLA-b-PCL diblock copolymer for its upscale in Chapter 5.

Chapter 5 is focused on the scale up process of synthesized PLLA-b-PCL diblock copolymer on preindustrial scale. For this purpose, it was necessary to study the kinetic of the polymerization reaction to control the final molecular weight and ratio between blocks of PLLA-b-PCL diblock copolymer if compared with commercial PLLA-b-PCL diblock copolymer. The optimization of polymerization reaction is done taking into account the reduction of the cost of the reactives, as well as the time of each polymerization step. Synthesized PLLA-b-PCL is characterized to achieve similar properties to this of commercial block copolymer.

In Chapter 6, synthesized on preindustrial scale PLLA-b-PCL diblock copolymer named DBC is used to produce novel DBC/PLDA polymer blends using conventional thermoplastics processing technologies such as extrusion compound, extrusion cast and injection on preindustrial scale. Before the extrusion, a preliminary extrusion simulation is performed, and the optimized extrusion parameters is used to produce the DBC/PLDA polymer blends. Moreover, in this Chapter, the food safety of polymeric materials is tested to verify their use for food packaging applications and the biodegradability and compostability to guarantee that DBC does not modify these properties.

Finally, in Chapter 7 a validation of the developed DBC/PLDA polymer blends for being use as a packaging material is done. For this purpose, two different package types were used on preindustrial scale, in particular a thermoformed tray and a vacuum bag. Thus, two specific products with different shelf-life, concretely fresh pastry and cure ham are selected to this validation. A preliminary study of both shelf-life is carried out including an organoleptic study with internal panellist to evaluate the consumer acceptance of the new developed materials.

TABLE OF CONTENTS

<i>I. INTRODUCTION</i>	3
<i>II. MOTIVATION AND OBJECTIVES</i>	23
<i>III. CHAPTERS</i>	29
CHAPTER 1. Evaluation of miscibility of poly (L-D-lactic acid) and poly (ϵ -caprolactone) polymer blends	33
CHAPTER 2. Preparation and characterization of polymer blends based on poly (L-D-lactic acid) and poly (L-lactic acid-b- ϵ -caprolactone) diblock copolymer	61
CHAPTER 3. Preparation and characterization of polymer blends based on poly (L-D-lactic acid), poly(ϵ -caprolactone) homopolymers and a poly (L-lactic acid-b- ϵ -caprolactone) diblock copolymer as compatibilizer agent.....	101
CHAPTER 4. Synthesis and characterization of tailored made poly (L-lactic-b- ϵ -caprolactone) diblock copolymers	137
CHAPTER 5. Scale up process of the synthesis of tailored made poly ((L-lactic acid-b- ϵ -caprolactone) diblock copolymer.....	187
CHAPTER 6. Production on preindustrial scale and characterization of DBC/PLDA polymer blends.....	213
CHAPTER 7. Packaging production pilot trials of developed DBC/PLDA polymer blend and its validation with food products.....	265
<i>IV. GENERAL CONCLUSIONS, FUTURE WORKS AND SCIENTIFIC PRODUCTION</i>	297
<i>V. ANNEXES</i>	309
<i>VI. ACKNOWLEDGEMENTS</i>	335

I.INTRODUCTION

I.INTRODUCTION

I.1. PACKAGING MATERIALS CURRENT SCENARIO	7
I.2. FOOD PACKAGING REQUIREMENTS AND MATERIALS	8
I.2.1. Packaging types and definition	8
I.2.2. Current materials used in food packaging applications	9
I.3. BIOPLASTICS AND BIOPOLYMERS	10
I.3.1. Bioplastics future scenario and definitions	10
I.3.2. Poly (lactic acid) (PLA)	15
I.4. DIBLOCK COPOLYMERS.....	16
I.5. REFERENCES	19

I.1. PACKAGING MATERIALS CURRENT SCENARIO

In last era, the use of conventional polymers in the different industries has reached alarming levels. Conventional polymeric materials are present in our daily lives and in the different products that surround us. This is mainly due to their great properties, such as versatility, durability, low cost and because they allow the industry to meet the demands of the customers of different industries such as packaging, building and construction, household, leisure, automotive or electrical among others. Specially for the packaging industry conventional materials are presented in a huge number of applications due to its lightness, transparency and high barrier properties which made them safe materials to contain and transport food and other goods.

During the last years, the global production of fossil-based or conventional polymers reached almost 368 million tons, representing an increase of about 10 million tons, with respect to the global production of fossil-based polymers in 2018, being only in Europe 58 million tons. Regarding the percentage by industry, as it is shown in Figure I.1 packaging represent the major consumer, ~40 %, compared with the second one that is construction ~20 % or automotive which represent only ~10% [1].

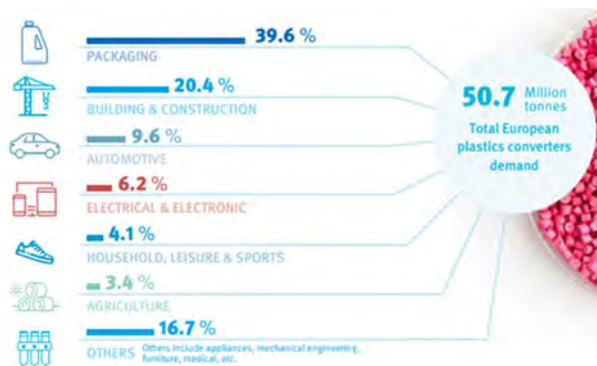


Figure I.1. Conventional polymer materials production by industries in Europe. *Source: PlasticsEurope Market Research Group (PEMRG) and Conversio Market & Strategy.GmbH.*

It is well-known that since 2015 the EU started to reduce conventional polymer production and to control their consumption, indeed, in 2015, the EU Action Plan for the Circular Economy was defined, in order to protect the environment from plastic pollution and encourage the reuse and the recyclability. This change allows to industries and to consumers to know the

principles of circular economy, and to learn about how to collaborate in all the different steps of the conventional polymers (plastics) life, from the plastics production, conversion into products, consumption, waste collection and finally the different waste treatments to valorize polymer wastes including the recycling.

During last years, different actions were carried out in this line and results showed a progress in the change from linear to circular economy, some numbers indicated that more than 10 million tons of post-consumer plastic waste were sent to recycling since 2018, 4.6 million tons of this post-consumer plastic has been used in new plastics products and compared to 2018, the quantity of recycled plastic used in packaging items has been increased by 43% [2]. These improvements also have been driven by the European Strategy for Plastics in a Circular Economy [3] and concretely in the field of packaging because of by 2030 all packaging plastic must be reusable or capable of being recycled in a profitable way. From this, its derived the Directive 2018/852 [4], which modifies the old directive 94/62/EC on packaging and packaging waste, establishes the minimum reuse and recycling of plastic waste for the medium and long term of: 50% by 2025 and 55% by 2030, as well as a recycling of a minimum of 70% by weight of all packaging waste. This change has driven the interest of looking for real sustainable packaging materials and to substitute the use of synthetic polymers by natural biopolymers, being one of the most promising applications these related to packaging.

However, packaging technology is a wide science field which requires knowledge not only in materials science, also in food science and in the interactions which could be between the packaging materials and the food which contains them.

I.2. FOOD PACKAGING REQUIREMENTS AND MATERIALS

I.2.1. Packaging types and definition

Packaging types can be divided mainly in three which are represented in the industry. First one is the primary packaging, which is the packaging that is in direct contact with the product. Most of the times primary packaging is named unit of packaging and could be the unique packaging that direct contain the product (ie: tray with fresh meat, bag with pastry, jar with marmalade) [5]. The second one is the named secondary packaging which group several primary packages and that can be used to transport the primary packages (ie: cardboard box with several bags with pastry). And the third one is tertiary packaging which are usually used to transport a high

number of secondary packaging and are for example containers or a pallet. In this investigation work the research was focus on the development of materials to reach the primary packaging requirements. The main basic functions of a packaging are summarized below:

1. Containment. The packaging must contain the product and maintain its integrity. This means the original properties during the different processes that involved the supply chain of the product from the package action until the final dispensing of the product including the transport.
2. Protection. Packaging must protect the product to external influences that could damage the product changing the chemical, biological or physical properties of the food/product.
3. Communication. The package must inform the consumers providing information about legal requirements but also about marketing information such as, nutritional facts or prizes.
4. Convenience. Convenience means to provide the consumer a desired functionality, such as easy to hand and to dispose, easy to open or to reclose and also the visibility (consumers need to see the product inside the package). In this decade packages with food ready to eat are examples of packaging designed to accomplish with the consumer convenience and demands.

In recent years, in addition with the conventional functions of a package consumers aligned with the EU recommendations also demand the development of packaging more sustainable with the environment and using natural materials which can be ease recycle or reintroduced in the environment like biodegradable and compostable materials.

I.2.2. Current materials used in food packaging applications

As it was explained before the majority of the materials used for primary packaging applications, are made of synthetic polymers such as poly (propylene) (PP), poly (ethylene) (PE), poly (styrene) (PS) or poly (ethylene terephthalate) (PET). In Table I.1 the distribution of the most used polymers for packaging applications by polymer type and examples of its main applications are summarized.

Type	(%)	Main uses
PP	19.7	Food packaging with medium oxygen barrier and high humidity barrier requirements (sweet and snacks unit flexible bags, thermal resistant trays to be used in oven or microwaves for food ready to eat)

PE (LDPE, LLDPE)	17.4	One use supermarket bag, general trays and films for food products with medium oxygen and water vapour barrier requirements.
PE (HDPE, MDPE)	12.9	Rigid food packaging with medium barrier requirements milk bottles, shampoo
PET	8.4	Rigid and flexible packaging with high oxygen and water vapour barrier requirements such as bottle for water, juices, soft drinks.
PS	6.1	Semi-rigid food packaging with high medium barriers (dairy products, fishery trays)

I.3. BIOPLASTICS AND BIOPOLYMERS

I.3.1. Bioplastics future scenario and definitions

Exploring alternatives for substituting synthetic polymer packaging materials is one of the joined objectives of the research and the industry. Both agree the need to use polymeric materials from renewable sources. With this aim during last decade, several new sustainable materials have been developed and commercialize. These materials are general named bioplastics, and nowadays although they represent only 1 % of the more than 368 million tons of plastic produced annually, the demand is continuously growing. Figure I.2 shows the evolution of the expected global production of bioplastics for the next years up to 2025 [6].



Figure I.2. Forecast of bioplastics up to 2025. Source: European Bioplastics, nova-Institute (2021).

As it is forecast a high increased is expected from the next years in the production of bioplastics from 2.11 million tons in 2019 to about 2.42 million tons by 2024, being this increase a revolution in the field of materials.

According to the definition of the European Bioplastics association, bioplastics materials involved a family of several polymers that have in common that are either biobased, biodegradable, or both [7].

There are many definitions of what it means biobased materials, (materials which are fully or partly extracted from biomass) and biodegradable materials (a material which degrades in a controlled condition according to defined standards). On the same way it is well-known that not all biobased materials are biodegradable as well as all biodegradable materials have been obtained from biomass.

There are many classifications of bioplastics however one of them is by origin. In this investigation work the classification by origin was chosen to define bioplastics materials. Taking into account this classification, bioplastics can be divided in the following subgroups:

- Natural biopolymers which are polymers directly extracted from the nature, such as cellulose.
- Biopolymers which are polymers which can be produced by synthetic polymerization but using natural monomers extracted from the nature or the biomass, such as PLA.
- Biopolymers produced by fermentation technologies using biomass and microorganisms such as PHB.

Natural biopolymers mainly include those made from polysaccharides (such as cellulose or starch). The first type of biopolymers includes biopolymers such as poly (lactic acid) (PLA), which is extracted from biomass and biopolyethylene (BioPE), which is synthesized using ethylene monomer produced from bioethanol. The third type is related to biopolymers, which are produced from bacterial fermentation or microorganisms, such as poly (hydroxyalkanoates) (PHAs). According to ISO 17088, EN 13432/ 14995 or ASTM 6400 or 6868, a compostable polymer is a polymer that undergoes degradation by biological processes during specific composting conditions to be transformed in CO₂, H₂O, inorganic compounds, and organic biomass. These materials must be disintegrated avoiding visual contamination and must be safe for being used as a compost material, because of that they can not contain toxic residues such as hard metals or hazardous substances. Therefore, the evaluation of

compostability following the current standards have four main steps to be accomplished, chemical characteristics, biodegradability, disintegration, and ecotoxicity or evaluation of the generated compost quality.

As can be understood from the definition a biopolymer synthesized from biomass can be biodegradable and compostable like as poly (lactic acid) or can not be biodegradable or compostable such as BioPE. On the contrary there are biodegradable and compostable polymers which have a synthetic or fossil-based origin such as poly (ϵ -caprolactone).

Commercial bioplastics available in the industry, their producers, and their brand names are summarized in Table I. 2.

Table I. 2. Commercial bioplastics available at industrial scale, producers, and brand names.

Biodegradable			
Origin	Polymer	Brand	Producer
Renewable	Starch	Mater Bi Bioplast Biolice Cereplast Piopar Solanyl Vegeplast EverCorn Amitroplast Plantic Gialene Tapioplast	Novamont Biotec GmbH & Co. KG Limagrain Céréales Ingrédients Biopolymer Technologies Rodenburg Biopolymers Vegemat Japan Cornstarch Co. Agrana Plantic – Kuraray Roquette DKSH
	Cellulose	Biograde Tenite Fasal Bioceta NatureFlex Tipa	FKuR Eastman Fasal Wood Keg Mazzucchelli Futamura Tipa Compostable Packaging
	PHAs (PHB/PHBV/PHBH)	Enmat Enmat PHACT Biocycle Biopol Mirel NODAX Kaneka PHBH MINERV-PHA Biomer grades Bioplastech Sogreen	TianAn Helian Polymers B. V. / PHAradox CJ Bio PHB-ISA Metabolix Metabolix - ADM Danimer Scientific Kaneka Bio-ON Biomer Bioplastech

		DAN*NA PHA BluePHA	Tianjin Green bioscience Artificial Nature BluePHA Co. Ltd
	PLA	PLA-Ingeo Luminy Renew Lacea Lacty Eco plastic Heplon Ecoloju Hycail Revode Bioshrink Terramac TE	NatureWorks LLC TotalEnergies Corbion Futero Mitsui Chemicals Shimadzu Toyota Chronopol Mitsubishi Hycail Hysun Biomaterials Co. Ltd Alesco GmbH & Co. KG Unitika Ltd
	PLA/PCL blend	Vyloecol BE	Toyobo
	PLA/copolyester blend	Bioflex Ecovio Floreon	FKuR BASF Floreon
	recycled PLA	LOOPLA Galactic Luminy rPLA PLA recycled rPLA	Galactic TotalEnergies Corbion Gianeco S.r.l. LoopLife Polymers – Despriet Gebroeders NV
	PBAT	Fepol Ecoflex Origo Bio (Eatar Bio) Ecoworld M-Vera TRBF Biogenpol Ecovio Biopar	Far eastern new century BASF Novamont Jinhui Zhaolong BIO-FED Jiangsu Torise Biomaterials ANKOR Bioplastics BASF Biopolymer Technologies AG

Non - renewable	PBS	BioPBS FZ Skygreen SG100	Mitsubishi Chemicals (MCP) Sk Chemicals
	PBSA	BioPBS FD Skygreen SG 200	Mitsubishi Chemicals (MCP) Sk Chemicals
	PVOH	Nichigo G-Polymer Elvanol Poval Selvol	Nippon Goshei Kuraray Kuraray Sekisui Specialty Chemicals
	PCL	Tone Capa Celgreen Pvaxx	Union Carbide Corporation Solvay Daycel Reliance Industries
Non biodegradable			
Renewable	Bio-PE	Green PE Terralene	Braskem FKuR
	Bio-PP	Green PP	Braskem
	Bio-PET	Eastlon PET Green PET BioPET	FKuR Braskem Avantium
	Bio-PA	EcoPAXX Vestamid Terra HS Grilamid 2s Ultramid S Balance Zytel RS Hiprolon Kalix Agimid Rilsan Terez Eco Amilan	DSM Evonik – FkuR EMS Grivory BASF DuPont Arkema Solvay Agiplast Arkema Ter Plastics Polymer Group Toray Plastics

In this investigation work, PLDA and PCL have been selected used. PLA has a renewable origin and it biodegradable and compostable according to mentioned standards and PCL hasn't come from renewable origin but it is biodegradable and compostable according to mentioned standards.

1.3.2. Poly (lactic acid) (PLA)

The demand of biopolymers to be used as packaging materials lead to poly (lactic acid) as one of the most promising candidates, indeed PLA was called the frontrunner of the bioplastics due its attractive mechanical properties which have been comparable with some synthetic polymers [8]. PLA is a bioplastic synthesized using monomers from renewable sources. The first PLA generation was obtained from sources such as corn or sugar beets agricultural sources, second generation of PLA was produced using agricultural or sources which no compete with human food. Nowadays there are several studies which corroborated the use of agroindustrial wastes to produce lactic acid by chemical hydrolysis of wastes such as the last production research of *El-Sheshtawy et al.*[9] which use agroindustrial wastes as cotton textiles or coffee pulp. These new ways of producing PLA allowed to reduce the PLA cost and to increase the availability in the market. PLA was selected in this investigation work because of its production capacity and its market availability, its processability, PLDA can be processed using conventional processing technologies such as extrusion compounding, extrusion cast or injection which are commonly used in the packaging industry [10] and decisively due to its natural properties which compared with other biopolymers were similar to synthetic polymers. These properties are high young modulus, high scratch resistance, high transparency, good sealability, good printability, certified industrial compostability. However, PLA present some drawbacks such as high hydrophilicity which it means poor oxygen and water vapour barrier properties, brittleness, low impact strength and low heat resistance.

Looking to these drawbacks and despite the benefits of PLA compared with other biopolymers it is necessary to improve PLA properties to be used as packaging material.

In this sense different research along the last years have been done, such as the development of nanocomposites, [8],[11], [12],[13], [14] or using other biopolymers or bioplastics to developed PLA polymer blends with improved properties, such as the use of PBS to improve thermal resistance [15] or the use of PCL to improve PLA ductility [16] among others. However high molecular polymer blends such as PLA and PCL normally, are immiscible [17] and it was necessary to use modifiers like as surfactants or other additives which finally decrease other properties such as mechanical ones [18],[19]. In this investigation work PCL bioplastic was selected to improve PLA due to PCL inherent properties such as low glass transition temperature (- 63 °C) and its low melting temperature (~ 60 °C) [20] which could improve PLA

brittleness. However, the use of PCL homopolymer was refuted and other alternatives as the use of copolymers containing PCL blocks were used.

I.4. DIBLOCK COPOLYMERS

Block copolymers materials (BCP) are polymeric materials composed of two or more chemically different, generally immiscible, polymer units linked by covalent bonds. The polymer units which constitute BCP are usually named blocks. Depending on the number of blocks, block copolymers could be diblock, triblock etc. [21].

The difference between a polymer blend and a block copolymer is that block copolymers are materials capable of self-assembling into different microstructures at the nanometer scale, leading to different morphologies and these morphologies could have a wide variety of mechanical, optical or electrical properties [22]. This characteristic of block copolymers is because of they have been considered future promising materials, since it is possible to tailored made different block copolymers combining specific blocks to obtain desired properties.

In this investigation work, a diblock copolymer (DBC) has been chosen as main material, concretely a symmetric block copolymer (A-B) composed of a linear block of poly (L-lactic acid) covalently bonded to a block of poly (ϵ -caprolactone) (PLLA-b-PCL). In this case both blocks of the diblock copolymer (PLLA and PCL) are crystalline and both homopolymers are immiscible.

The thermodynamic incompatibility between the two blocks of the DBC usually generates a segregation between blocks polymer chains, named self-assembly, as it was mentioned before. This separation allow DBC to adopt different morphologies such as spheres, cylinders, lamellar and gyroidal ones as it was described by *Hu et al.* [23].

The segregation of the block copolymers has been demonstrated that is governed by three controllable parameters which are, the degree of polymerization (N) of both polymers blocks, the Flory-Huggins interaction parameter (χ_N) between blocks and the volumetric fraction of each of the blocks at DBC.

Depending on the parameter χ_N and evaluating different theories on the phase separation of block copolymers, three types of regimes can be distinguished: weak segregation limit (WSL) for χ_N below 10; intermediate segregation region (ISR) for values of χ_N between 10 and 50 and

finally, for high values of χ_N ($\chi_N \rightarrow \infty$) the strong segregation regime (SSL). Those different regimes led to different morphologies as it is shown in Figure I. 3.

In this case and due to its crystalline nature the microphase separation will be a competition between the segregation and the crystallization processes. The effect of how the different crystallinity of the DBC could affect the final morphology was studied by several authors such as *Navarro-Baena et al.* [24], *Peponi et al.* [25] and *Hamley et al.* [26] and in particular using block copolymers containing PLA and PCL as a blocks. In this investigation work the use of PLLA-b-PCL diblock copolymer will be studied. Numerous studies have determinate that PLLA-b-PCL are weakly segregated in the melt depending on the composition and the molecular weight of each block [27], [28], consequently it is expected not to reach an ordered structure like showed in Figure I. 3.

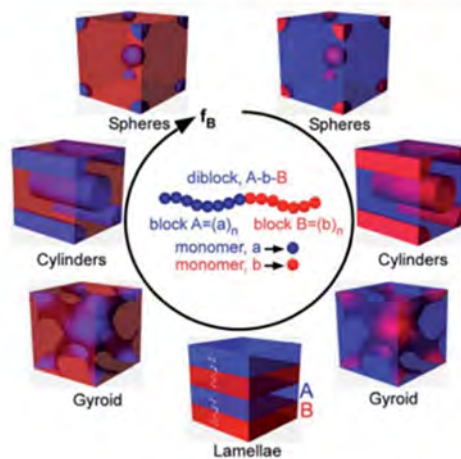


Figure I. 3. Phase diagram of a symmetric diblock copolymer [23].

During last decade, numerous applications of the use of BCP in different fields of research have been reported. The tailored synthesis of BCP made them similar to a bottom-up nanomaterial synthesis playing with the self-assembling and taking advantage of that to developed advanced materials.

Some examples of the wide range of applications which could be developed using block copolymers are thin films for electronic devices nanostructured membranes for filtering, photonic materials and batteries among or old applications as a surfactants in products for

detergency or pharmacy [23]. DBC have been used also to improved epoxy properties such as *Cano et al.* [29] or to develop nanostructured unsaturated polyesters using triblocks copolymers such as *Builes et al.* [30]. The use of DBC in the field of compatibilizer for conventional thermoplastics polymer blends have been also explored, mainly focus on materials such as Nylon -6, PP or PS by using reactive blending such as *Jiang et al.* [31] or polymer blending to improve polymer blends compatibility such as described *Müller et al.* [32] for blends of PMMA and PS.

However, it has been during the last decade when it is reported the use of DBC as compatibilizer of natural polymers by polymer blending, as it was reported by *Chang et al.*[33] using PI-b-PLLA diblock copolymer as a compatibilizer for PLLA and soybean oil polymer blends. In this investigation work the PLLA-b-PCL diblock copolymer will be use by polymer blending as compatibilizer for PLDA and PCL homopolymer components.

The use of DBC as a component in a polymer blend and not as an additive to nanostructure biodegradable and compostable materials such as PLDA hasn't extensively studied,in this investigation work it will be studied and almost by using conventional processing technologies at preindustrial scale.

I.5. REFERENCES

1. Europe, P. Plastics – the Facts 2020. *PlasticEurope* 2020, 16.
2. Plastics Europe The Circular Economy for Plastics. 2022, 1–36.
3. European Commission A European Strategy for Plastics in a Circular Economy. 2018.
4. Directiva (UE) 2018/852 Del Parlamento Europeo y Del Consejo de 30 de Mayo de 2018.
5. Singh, E.; Osmani, R.A.M.; Jhadav, S.; Kazi, H.; Vaghela, R. *Bionanocomposites in Food Packaging Applications and Their Risk Assessment for Public Health*; LTD, 2022; ISBN 9780323885287.
6. Global Production Capacities of Bioplastics 2021.
7. Marienstrabe-Berlin What Are Bioplastics. *Eur. Bioplastics* 2015, 1–2.
8. Raquez, J.M.; Habibi, Y.; Murariu, M.; Dubois, P. Polylactide (PLA)-Based Nanocomposites. *Prog. Polym. Sci.* 2013, 38, 1504–1542, doi:10.1016/j.progpolymsci.2013.05.014.
9. El-Sheshtawy, H.S.; Fahim, I.; Hosny, M.; El-Badry, M.A. Optimization of Lactic Acid Production from Agro-Industrial Wastes Produced by *Kosakonia Cowanii*. *Curr. Res. Green Sustain. Chem.* 2022, 5, 100228, doi:10.1016/j.crgsc.2021.100228.
10. Lorenzo, M.L. Di; Androsch, R. *Aplicaciones Industriales Poli(Ácido Láctico)*; 2018; ISBN 9783319754581.
11. Jacob, J.; Lawal, U.; Thomas, S.; Valapa, R.B. *Biobased Polymer Composite from Poly(Lactic Acid): Processing, Fabrication, and Characterization for Food Packaging*; Elsevier Inc., 2020; ISBN 9780128187951.
12. Nofar, M. Multiphase Polylactide Blends: Toward a Sustainable and Green Environment. *Multiph. Polylactide Blends Towar. a Sustain. Green Environ.* 2021, 1–391, doi:10.1016/B978-0-12-824150-9.00011-X.
13. Zhu, B.; Wang, Y.; Liu, H.; Ying, J.; Liu, C.; Shen, C. Effects of Interface Interaction and Microphase Dispersion on the Mechanical Properties of PCL/PLA/MMT Nanocomposites Visualized by Nanomechanical Mapping. *Compos. Sci. Technol.* 2020, 190, 108048, doi:10.1016/j.compscitech.2020.108048.
14. Feijoo, J.L.; Cabedo, L.; Giménez, E.; Lagaron, J.M.; Saura, J.J. Development of

- Amorphous PLA-Montmorillonite Nanocomposites. *J. Mater. Sci.* 2005, *40*, 1785–1788, doi:10.1007/s10853-005-0694-8.
15. Deng, Y.; Thomas, N.L. Blending Poly(Butylene Succinate) with Poly(Lactic Acid): Ductility and Phase Inversion Effects. *Eur. Polym. J.* 2015, *71*, 534–546, doi:10.1016/j.eurpolymj.2015.08.029.
 16. Wu, D.; Zhang, Y.; Zhang, M.; Zhou, W. Phase Behavior and Its Viscoelastic Response of Polylactide/Poly(ϵ -Caprolactone) Blend. *Eur. Polym. J.* 2008, *44*, 2171–2183, doi:10.1016/j.eurpolymj.2008.04.023.
 17. Maglio, G.; Malinconico, M.; Migliozi, A.; Groeninckx, G. Immiscible Poly(L-Lactide)/Poly(ϵ -Caprolactone) Blends: Influence of the Addition of a Poly(L-Lactide)-Poly(Oxyethylene) Block Copolymer on Thermal Behavior and Morphology. *Macromol. Chem. Phys.* 2004, *205*, 946–950, doi:10.1002/macp.200300150.
 18. Bondeson, D.; Oksman, K. Dispersion and Characteristics of Surfactant Modified Cellulose Whiskers Nanocomposites. *Compos. Interfaces* 2007, *14*, 617–630, doi:10.1163/156855407782106519.
 19. Przybysz-Romatowska, M.; Haponiuk, J.; Formela, K. Poly(ϵ -Caprolactone)/Poly(Lactic Acid) Blends Compatibilized by Peroxide Initiators: Comparison of Two Strategies. *Polymers (Basel)*. 2020, *12*, doi:10.3390/polym12010228.
 20. Akoumeh, R.; Elzein, T.; Martínez-Campos, E.; Reviriego, F.; Rodríguez-Hernández, J. Fabrication of Porous Films from Immiscible Polymer Blends: Role of the Surface Structure on the Cell Adhesion. *Polym. Test.* 2020, *91*, doi:10.1016/j.polymertesting.2020.106797.
 21. Bates FS, F.G.. Block Copolymer Thermodynamics: Theory and Experiment. *Annu. Rev. Physics-Chemistry* 1990, *41*, 525–557.
 22. Bates FS, F.G.. Block Copolymers—Designer Soft Materials. *Phys. Today* 1999, *52*, 32–38.
 23. Hu, H.; Gopinadhan, M.; Osuji, C.O. Directed Self-Assembly of Block Copolymers: A Tutorial Review of Strategies for Enabling Nanotechnology with Soft Matter. *Soft Matter* 2014, *10*, 3867–3889, doi:10.1039/c3sm52607k.
 24. Navarro-Baena, I.; Marcos-Fernandez, A.; Kenny, J.M.; Peponi, L. Crystallization Behavior of Diblock Copolymers Based on PCL and PLLA Biopolymers. *J. Appl. Crystallogr.* 2014, *47*, 1948–1957, doi:10.1107/S1600576714022468.
 25. Peponi, L.; Navarro-Baena, I.; Castelletto, V.; Kenny, J.M.; Marcos-Fernández, A. Effect of the Molecular Weight on the Crystallinity of PCL-b-PLLA Di-Block Copolymers.

- Polymer (Guildf)*. 2012, 53, 4561–4568, doi:10.1016/j.polymer.2012.07.066.
26. Hamley, I.W.; Castelletto, V.; Castillo, R. V.; Müller, A.J.; Martin, C.M.; Pollet, E.; Dubois, P. Crystallization in Poly(L-Lactide)-b-Poly(ε-Caprolactone) Double Crystalline Diblock Copolymers: A Study Using x-Ray Scattering, Differential Scanning Calorimetry, and Polarized Optical Microscopy. *Macromolecules* 2005, 38, 463–472, doi:10.1021/ma0481499.
 27. Kim, J.K.; Park, D.J.; Lee, M.S.; Ihn, K.J. Synthesis and Crystallization Behavior of Poly(L-Lactide)-Block-Poly(ε-Caprolactone) Copolymer. *Polymer (Guildf)*. 2001, 42, 7429–7441, doi:10.1016/S0032-3861(01)00217-8.
 28. Michell, R.M.; Müller, A.J.; Spasova, M.; Dubois, P.; Burattini, S.; Greenland, B.W.; Hamley, I.W.; Hermida-Merino, D.; Cheval, N.; Fahmi, A. Crystallization and Stereocomplexation Behavior of Poly(D - And L -Lactide)-b-Poly(N,N-Dimethylamino-2-Ethyl Methacrylate) Block Copolymers. *J. Polym. Sci. Part B Polym. Phys.* 2011, 49, 1397–1409, doi:10.1002/polb.22323.
 29. Cano, L.; Builes, D.H.; Tercjak, A. Morphological and Mechanical Study of Nanostructured Epoxy Systems Modified with Amphiphilic Poly(Ethylene Oxide-b-Propylene Oxide)-b-Ethylene Oxide) Triblock Copolymer. *Polymer (Guildf)*. 2014, 55, 738–745, doi:10.1016/j.polymer.2014.01.005.
 30. Builes DH, Hernández-Ortiz JP, Corcuera MA, Mondragon I, T.A. Effect of Poly(Ethylene Oxide) Homopolymer and Two Different Poly(Ethylene Oxide-b- Poly(Propylene Oxide)-b-Poly(Ethylene Oxide) Triblock Copolymers on Morphological, Optical, and Mechanical Properties of Nanostructured Unsaturated Polyester. *ACS Appl Mater Interfaces*. 2014, 22, 1073–1081, doi:10.1021/am4046266.
 31. G. Jiang, H. Wu, S. Guo Using of BC as Surfactants. *Polym. Eng. Sci.* 2010, 50, 2273–2286.
 32. Schacher, F.H.; Rugar, P.A.; Manners, I. Functional Block Copolymers: Nanostructured Materials with Emerging Applications. *Angew. Chemie - Int. Ed.* 2012, 51, 7898–7921, doi:10.1002/anie.201200310.
 33. K. Chang, M. L. Robertson, M.A.H. PLA and Soybean Copolymers. *ACS Appl. Mater.* 2009, 1, 2390–2399.

II. MOTIVATION AND OBJECTIVES

II. MOTIVATION AND OBJECTIVES

II.1. MOTIVATION AND OBJECTIVES..... 27

II.1. MOTIVATION AND OBJECTIVES

The need of development of novel packaging materials is increased over the last decade. This need is most pronounced in the field of sustainable materials like as bioplastics. Known bioplastics and its blends do not reach the high requirements demanded to materials currently used for packaging applications. In particular, there are some food packaging applications, where the use of commercial biodegradable polymers is still not possible. Food packaging materials with high oxygen and water vapour barrier properties to avoid food degradation, for instance dried snacks, fall into this category.

Another example are foodstuffs that require barrier and long shelf-life, such as sauces. Products that have to be packed while hot, and hence need temperature-resistant packages, are another example.

Therefore, the opportunity exists to develop new bioplastics meeting the demanded requirements, especially biodegradable and compatible materials as they represent a more environmentally friendly alternative from an end of life point of view.

In addition, latest technologies to develop packaging materials must be aligned with the European Strategy for Plastics in a Circular Economy and the packaging waste directives (Directive 2018/852) which indicate that by 2030 all materials should be reusable or recyclable, including organic recycling as a solution for compostable materials.

The aim of this investigation work is the development of biodegradable and compostable packaging materials based on bioplastics, such as PLDA, with improved properties compared with commercial PLA by using diblock copolymers as cutting-edge technology to develop nanostructured materials.

To reach this goal extensive research has been performed from laboratory to preindustrial scale with the aim to demonstrate that the use of diblock copolymers is an up scalable technology and that developed nanostructured DBC/PLDA polymer blends are validated to be used for some food packaging applications.

Thanking above into account, the main objective of this investigation work is to improve properties of neat PLDA homopolymer to develop novel polymeric materials for food packaging applications. With this aim a commercial and synthesized PLLA-b-PCL diblock copolymer will be used to validate, from laboratory to preindustrial scale, the possibility of

development of novel polymer blends based on PLDA modified with these block copolymers for a new biodegradable and compostable polymeric materials for food packaging applications.

The specific objectives of this investigation work are the following:

- Study of the miscibility between PLDA and PCL homopolymers,
- Evaluation of the possibility of the addition of a semi-crystalline commercial PLLA-b-PCL diblock copolymer to improve miscibility between PCL block and PLDA homopolymer and to develop nanostructured PLLA-b-PCL/PLDA polymer blends,
- Evaluation of the possibility of the use of commercial PLLA-b-PCL diblock copolymer as polymer blend compatibilizer to improve miscibility between PLDA and PCL homopolymers,
- The synthesis of the PLLA-b-PCL diblock copolymer on the laboratory and preindustrial scale with properties similar to commercial PLLA-b-PCL diblock copolymer,
- The analysis of the nanostructuring of PLDA matrix using synthesized at laboratory scale PLLA-b-PCL block copolymer,
- The evaluation of the possibility of scale up of synthesized PLLA-b-PCL diblock copolymer on preindustrial scale using facilities of pilot plant of ITENE,
- The production of DBC/PLDA polymer blends on preindustrial scale using conventional processing technologies such as extrusion compounding, extrusion cast and injection. Here, the aim is also to corroborate the nanostructured DBC/PLDA polymer blends are able to reach the same properties as these achieved on laboratory scale,
- The evaluation of food safety and the biodegradability and compostability of developed DBC/PLDA polymer blends employing standard tests.

III. CHAPTERS

CHAPTER 1

Evaluation of miscibility of poly (L-D-lactic acid) and poly (ϵ -caprolactone) polymer blends

Poly (L-D-lactic acid) (PLDA) is one of the aliphatic polyesters most intensively studied for packaging applications during the last decade. This is due to its good mechanical properties, high availability, competitive cost, and its excellent biodegradability and compostability under industrial conditions. However, the main drawback of PLDA is its brittleness. This weakness could be improved by blending with more flexible polymer components. Poly (ϵ -caprolactone) (PCL) is a biodegradable aliphatic polyester with a low glass transition temperature and a high elongation at break, being one of the most promising candidates to modify the brittleness of PLDA. However, PLDA is usually immiscible with PCL, and thus PLDA/PCL polymer blends do not reach an intrinsic blend and consequently their expected improvement of the mechanical properties are not achieved. The aim of this Chapter is the evaluation of the miscibility between PLDA and PCL. A study of miscibility between PLDA and PCL homopolymers has been carried out, for this purpose, three protocols to obtain PLDA/PCL polymer blend films have been developed and a thermal study by DSC and TGA has been done to prove that PLDA and PCL polymers are not miscible or are miscible only up to a percentage. The result of this Chapter will allow to better understand the effect of the addition of poly (L-lactic-b- ϵ -caprolactone) diblock copolymer to increase PLDA/PCL polymer blend miscibility, which will be described in more details in Chapters 2 and 3.

CHAPTER 1. Evaluation of miscibility of poly (L-D-lactic acid) and poly (ϵ -caprolactone) polymer blends

1.1. INTRODUCTION AND OBJECTIVES	35
1.2. MATERIALS AND METHODS	39
1.2.1. Materials	39
1.2.2. Experimental methods	40
1.2.2.1. Study of different solvent casting conditions for preparation of PLDA homopolymer films	40
1.2.2.2. Preparation of PLDA/PCL polymer blends films by solvent casting	41
1.2.3. Characterization techniques	41
1.2.3.1. Films appearance	41
1.2.3.2. Gel permeation chromatography (GPC)	41
1.2.3.3. Differential scanning calorimetry (DSC)	42
1.2.3.4. Thermogravimetric analysis (TGA)	43
1.3. RESULTS AND DISCUSSION	43
1.3.1. <i>Characterization of commercial PLDA and PCL homopolymers</i>	43
1.3.1.1. Appearance of the films	43
1.3.1.2. Gel permeation characterization	44
1.3.1.3. Differential scanning calorimetry	44
1.3.2. <i>The evaluation of different protocols used for preparation of PLDA/PCL polymer blend films by solvent casting</i>	45
1.3.2.1. Characterization of PLDA homopolymer films thermal properties by DSC	46
1.3.2.2. Determination of solvent residual content in PLDA homopolymer films	48
1.3.3. <i>Miscibility of PLDA/PCL polymer blends films</i>	51
1.4. CONCLUSIONS	55
1.5. REFERENCES	56

1.1. INTRODUCTION AND OBJECTIVES

Poly (lactic acid) (PLA) is a linear aliphatic polyester, synthesized from the lactic acid. PLA has been widely studied during the last decade due to its wide range of properties if compared with other commercial biopolymers. The main benefits of PLA are its renewability, biocompatibility, biodegradability, and compostability under industrial conditions. Good processability (if compared with other compostable polymers), mechanical properties, thermal resistance and barrier properties of PLA make it one of the most widely used in biodegradable and compostable packaging applications. As was mentioned above, PLA could be synthesized by ring opening polymerization (ROP) of lactide dimer or by direct polycondensation of lactic acid monomer [1]. The main drawbacks of the polycondensation of lactic acid monomer is, on the one hand, the removal of the side reaction products such as water and, on the other hand, the reaction high viscosity which led to a low molecular weight PLA homopolymer. Therefore, the most efficient method for synthesis of PLA is the ROP of lactide dimer [2], which results in high molecular weight PLA [3]. At industrial scale, companies such as Natureworks or Total Corbion PLA use a combination of both methods to synthesize PLA, starting from a polycondensation of lactic acid monomer to produce the lactide dimer and then following ROP to produce the final PLA with the desirable molecular weight.

The lactic acid monomer possesses chiral activity, which depends on the asymmetric carbon position. This is responsible for presence of two different stereoisomers configurations L-lactic acid monomer and D-lactic acid monomer (see Figure 1.1), and described with details elsewhere by *Duana et al.* [4], *Lunt et al.* [5] and *Auras et al.* [6].

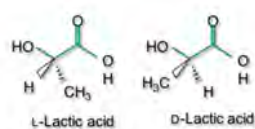


Figure 1.1. Stereoisomers of L-lactic acid and D-lactic acid monomers. *Source: adapted from Auras et al.* [6].

Moreover, the lactic acid monomer can be transformed in the lactide dimer and has three different forms depending on the carbon position: D-lactide, meso-lactide and L-lactide, as shown in Figure 1.2.

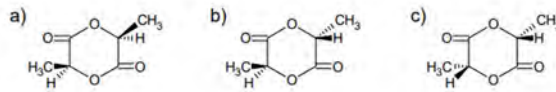


Figure 1.2. Stereoisomers of lactide dimers, a) D-lactide, b) meso-lactide, c) L-lactide. *Source: adapted from Auras et al. [6].*

The polymerization reaction of PLA by ROP can lead to different stereoisomers polymer configurations as shown in Table 1.1.

Table 1.1. PLA stereoisomers configurations.	
PLA Type	Configuration Structure
Isotactic PLA	<p style="text-align: center;">For L-lactide or D-lactide, all sequences are the same.</p> <p style="text-align: center;">Isotactic PLLA</p> <p style="text-align: center;">Isotactic PDLA</p>
Syndiotactic PLA	<p style="text-align: center;">The stereocenters have alternating positions, first L-lactide, second D-lactide, and their following the same sequence.</p>
Tactic PLA	<p style="text-align: center;">The stereocenters have a random configuration, if the lactide is the meso-lactide the name should be isotactic stereoblock.</p>

These different stereoisomers configurations open the possibility to fabricate different types of commercial PLA with different final properties. However, from the industrial point of view, the production of neat PLLA or PDLA homopolymers is quite expensive. Consequently, most of

the commercial grades of PLA used for packaging applications consist of a mixture of PLLA with a small amount of PDLA (low wt%). The difference between the amounts of each stereoisomer is due to the fact that in the nature is easier to find L-lactic acid form than D-lactic acid form [7]. As expected, the different amount of PLLA or PDLA is responsible for different final properties of PLA and, as a consequence, for diverse applications in the market.

Most of the commercial grades PLA available in the market consist of high amount of PLLA homopolymer and very low amount of PDLA, less than 8 wt%. The increase of the D-lactic acid monomer in commercial PLA led to decrease of crystallinity degree, and, as a consequence, thermal and mechanical properties are affected since this polymer become almost amorphous. Surprisingly, D-lactic polymer is used as nucleating agent to improve PLDA commercial grades as has been reported by *Park et al.* [8] and *Aliotta et al.* [9]. Both research groups reported a positive effect on crystallinity and mechanical properties, with the increase of D-lactic polymer content in these polymer blends.

In this investigation work the selected commercial PLA grade is a poly (L-D-lactic acid) (PDLA) which contains ~2 wt% of D-lactic acid monomer. The Young modulus of this PDLA polymer is ~3GPa and a tensile strength ~50 and 70 MPa. Thus, the mechanical properties are optimal compared with some commercial conventional polyesters such as PET or some polyolefins such as PS [10], however its elongation at break is ~4 %, being this value the main drawback of this commercial PLA. This weakness can affect the final PLDA polymer toughness and can be improved by either blending or copolymerization with more flexible or ductile polymers components. Several research have been done in this direction by authors such as *Rasal et al.* [11] and *Fortelny et al.* [12] among others.

Poly (ϵ -caprolactone) (PCL) is a fossil based aliphatic polyester, synthesized similarly as poly (lactic acid) by ROP of ϵ -caprolactone monomer. As reported in the literature, in the case of PCL several organic metal complex catalysts can be used [13]. PCL homopolymer is a ductile, and semi-crystalline polymer with a low glass transition temperature (-60 °C), a low melting transition temperature (60 °C) and a high elongation at break (≥ 600). Taking this into account, the blending of PCL with PLA can result in reduction of PLA glass transition temperature due to plasticization effect of PCL, which also can affect PLA brittleness. Many research groups investigated polymer blends of PLA with different flexible biodegradable polyesters such as poly (butylene succinate) (PBS), poly (3-hydroxybutyrate) (P3HB), poly (hydroxybutyrate-co-3-hydroxyvalerate) (PHBV), poly (butylene adipate-co-terephthalate) (PBAT), among other to

avoid PLA brittleness. In this filed authors such as *J.M.Raquez et al.* [14], *Barakat et al.* [15], or *Hongwei Bai et al.* [16] have been published a comprehensive reviews. Moreover, several routes have been deeply explored to produce PLA blends being the most studied the polycondensation (in both solution or melt), the chemical chain extension by using reactive extrusion or the ROP followed by a functionalization with an aliphatic polyester chain.

The main drawback of polymer blend of PLA with different polyesters is still poor impact resistance due to micrometric phase separation and poor interfacial adhesion between the two polymer blend components. This behaviour can be better understood by study the miscibility and compatibility between polymer blend components. The miscibility between polymer blend components takes place when the resulted blends is homogeneous not only at micrometric but also at nanoscale level. Therefore, any microphase separation can not be detected. This effect was observed for some polymers such as PLA with poly (methyl methacrylate) (PMMA) blends [17]. Several studies have been carried out to evaluate the miscibility between PLA/PCL polymer blends and, as expected, it was demonstrated by authors such as *Yokohara et al.* [18], *Jiao et al.* [19] or *Broz et al.* [20] among others like *Jerome et al.* [21], *Delgado-Aguilar et al.* [22] and *Przybysz-Romatowska et al.* [23], that high molecular weight PLA is usually immiscible with high molecular weight PCL, even at temperatures higher than their melt temperatures. Thus, the immiscibility between PLDA and PCL provoked microphase separation and spherical morphology for PLDA/PCL polymer blends can be detected. Moreover, the properties of polymer blends are lower if compare with the properties of homopolymer components.

To predict polymer blend components immiscibility, the glass transition temperature (T_g) of each component should be calculated. The T_g of each polymer blend component can be analyse by several techniques, but the most common technique is differential scanning calorimetry (DSC). As it is well known, for partially miscible polymer blends, the multiple T_g 's will showed intermediate temperature values (if compared to the T_g of each polymer blend component) corresponding to partially miscible phases rich in one of polymer blend components. The variation in binary blend T_g can be modeled by the Fox-Flory equation (see Equation 1.1)

$$T_{g12} = T_{g1}(w_1) + T_{g2}(w_2) \quad \text{Equation 1.1}$$

where T_{g12} is the T_g of the polymer blend, T_{g1} and T_{g2} are the T_g 's of polymer blend components, and w_1 and w_2 are the weight percent (wt%) of each component in the polymer

blend. This equation is a simple equation that does not take into account specific interactions between the polymer blend components like as Gordon-Taylor equation [24].

The term of *compatibility* is a different term than *miscibility*. *Compatibility* considers the final properties of the polymer blend and for example if blending results in the improvement of the mechanical properties or barrier properties of developed polymer blend, this polymer blend is compatible either if this polymer blend is not miscible or partially miscible.

With the same objective that presented research groups works, several companies have been working on the improvement of PLA toughness without decrease its transparency. In the patent of Shimadzu Corporation [25], blending technology has been used to prepare PLA blends with less than 40 wt% of PCL or PBS resulted in slight improvement in mechanical properties In the patent of Mitsubishi Plastics [26], biodegradable polymer films have been prepared based on PLA and a flexible aliphatic polyesters (PCL, PBS, or poly (butylene succinate adipate) (PBSA), which correspond to commercial products such as Placel® H7 (Daicel Chem), Bionolle® 1010 (Showa High Polymer K.K) and Bionolle® 3010 (Showa High Polymer K.K) with the $T_g \leq 0$ °C. Obtained in this way polymer blend films possessed high impact strength, dimensional and chemical stability under heat as well as humidity conditions. Moreover, these films do not reach barrier properties and neither thermal resistance. Thus, developed polymer blends do not provide sufficient flexibility (Young modulus of 1 GPa or less) for PLA, and polymer blends require the addition of higher amount of the flexible aliphatic polyester, for example, ≥ 60 wt% PBS. As a result, the main characteristics of PLA such as barrier and mechanical resistance or toughness are mostly loosed.

The main objective of this Chapter is the evaluation of the miscibility between PLDA/PCL polymer blend components prepared by solvent casting. For this propose several blends of PLDA/PCL was produced at laboratory scale using different procedure and miscibility between blend components has been studied. The main aim was also to maintain the transparency and low residual solvent content in obtained polymer blend films.

1.2. MATERIALS AND METHODS

1.2.1. Materials

Poly (L-D-lactic acid) (PLDA) 7032 D with 2 wt% content of PDLA was supplied by Natureworks LLC. Poly (ϵ -caprolactone) (PCL) Capa 100 was produced by Perstop and formerly supplied by

Solvay. Chloroform and dichloromethane were purchased from Sigma-Aldrich. The chemical structure of PLDA and PCL is shown in the Figure 1.3 and Figure 1.4, respectively.

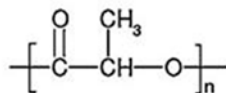


Figure 1.3. Chemical structure of PLDA.

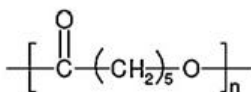


Figure 1.4. Chemical structure of PCL.

1.2.2. Experimental methods

In this Chapter all investigated polymer blend films were obtained by solvent casting preparation method. To determine the appropriate solvent and evaporation conditions several experiments for PLDA homopolymer have been carried out with the aim of choose the best protocol for the preparation of the transparent PLDA/PCL polymer blend films. The main requirements for the best protocol were low residual solvent content and homogeneous polymer blend films.

1.2.2.1. Study of different solvent casting conditions for preparation of PLDA homopolymer films

PLDA homopolymer was used to evaluate the different solvent casting conditions to prepare polymer films. PLDA homopolymer films were prepared using as solvent both chloroform and dichloromethane. First, 10 g of PLDA homopolymer was dissolved under stirring (100 rpm) at room temperature during 30 min. Then, the solution was casted onto Petri dishes and were dried. The drying protocol consisted in two consecutive steps with different conditions.

- Step 1: drying at temperature of 23 °C and relative humidity (RH) of 50 %.
- Step 2: drying at temperature of 25 °C under vacuum with controlled p (660 mbar), a hysteresis loop of 80 and varying the time.

Details of each protocol condition is summarized in Table 1.2.

Table 1.2. Different conditions tested for preparation of PLDA homopolymer films by solvent casting method. S1 correspond to step 1 and S2 correspond to step 2.				
Protocols	S1: Laboratory ambient RH (50%)		S2: Under vacuum p (660 mbar)	
	T (°C)	t (h)	T (°C)	t (h)
Protocol 1	23	2.5	25	48
Protocol 2	23	24	25	12
Protocol 3	23	2.5	40	48

1.2.2.2. Preparation of PLDA/PCL polymer blends films by solvent casting

PLDA/PCL polymer blends with different weight ratio (70:30, 50:50 and 30:70) between homopolymers were prepared by solvent casting following the experimental procedure described in Section 1.2.2.1. For the drying step, protocol 2 was used:

- Step 1: drying during 24 h at T of 23 °C and RH of 50 %.
- Step 2: drying during 2 h at T of 25 °C under vacuum with controlled p (660 mbar) and a hysteresis loop of 80.

All investigated PLDA/PCL blends are summarized in Table 1.3.

Table 1.3. PLDA/PCL polymer blend films and its weight relation between blend components.		
Sample name	PLDA (%)	PCL (%)
PLDA	100	0
PLDA/PCL 70:30	70	30
PLDA/PCL 50:50	50	50
PLDA/PCL 30:70	30	70
PCL	0	100

1.2.3. Characterization techniques

1.2.3.1. Films appearance

The appearance of PLDA homopolymer films and PLDA/PCL polymer blend films were visually analysed in this investigation work.

1.2.3.2. Gel permeation chromatography (GPC)

The number average molecular weight (M_n) and the weight average molecular weight (M_w) distributions of commercial PLDA and PCL homopolymers were determined by gel permeation chromatography (GPC) using a Perkin Elmer Series 200 equipped with a refractive index detector. Tetrahydrofuran (THF) was used as mobile phase at a flow rate of 1 mL/min. Specimen concentrations were 0.1 g/mL THF. The injected volume was 200 μ L and the flow rate was 1.5 mL/min at 7.1 MPa. The M_n , M_w and the polydispersity index (PDI) values of investigated samples were calculated using polystyrene as standard.

1.2.3.3. Differential scanning calorimetry (DSC)

DSC measurement was performed using a Mettler Toledo DSC822e equipment, provided with a robotic arm and an electric intracooler as a refrigeration unit. Investigated films with a weight between 5-10 mg were sealed in aluminum pans.

The observed inflection point of the heat flow signal change was chosen to evaluate the glass transition temperature (T_g). The cold crystallization temperature (T_{cc}) was settled as the maximum exothermic peak during the heating scan and the melting temperature (T_m) observed during the 1st and 2nd heating scans was settle as the maximum of the endothermic peak, taking the area under the peak to analyse the melting enthalpy (ΔH_m). In general, first scanning is performed to avoid the thermal history and, as a consequence, the thermal transitions of investigated films were determinate from the second scan.

Moreover, crystallization temperature (T_c) calculated from the cooling scan was taken as the minimum of the exothermic peak observed in this scan, and the crystallization enthalpy (ΔH_c) was calculated from the area under this exothermic peak.

Before each measurement, the films were conditioned at 50 % RH and at 23 °C. All performed measurements were carried out under nitrogen gas at a flow rate of 50 mL/min.

Two different methods were used:

Method 1 was used to analyse thermal properties of both PLDA and PCL homopolymers including the crystallization of PLDA homopolymer films, which were obtained by solvent casting using two different solvents. The measurement was performed with a heating/cooling rate of 20 °C/min. First heating scan was in the temperature range from 25 °C to 250 °C, cooling scan from 250 °C to 0 °C and the second heating scan from 0 °C to 250 °C.

Method 2 was used to evaluate the miscibility of PLDA/PCL polymer blends components used the following procedure:

- Cycle 1 (1st heating scan): from 25 °C to 250 °C using a heating rate of 20 °C/min.
- Cycle 2 (cooling): from 250 °C to -60 °C using a heating rate of 100 °C/min.
- Cycle 3 (2nd heating scan): from -60 °C to 250 °C using a heating rate of 10 °C/min.

DSC technique was also used for the calculation of the homopolymers and polymer blend film degree of crystallinity (χ_c). This calculation was performed following the Equation 1.2.

$$X_c = \frac{(\Delta H_m - \Delta H_{cc})}{\Delta H_m^0} \times 100 \quad \text{Equation 1. 2}$$

In this equation, the term ΔH_m correspond to the experimental enthalpy of the melting transition, ΔH_{cc} correspond to the experimental enthalpy of the cold crystallization transition, and ΔH_m^0 is the theoretical melting transition enthalpy of the 100 % crystalline polymer. The ΔH_m^0 of PLA is 93.0 J/g [27]. In this case the χ_c of PCL was not calculated since the objective of this research work was related to the improvement of PLDA homopolymer properties.

1.2.3.4. Thermogravimetical analysis (TGA)

TGA of PLDA homopolymer and PLDA/PCL polymer blends films were carried out using a Mettler Toledo TGA/SDTA/851 (Mettler Toledo, Columbus, OH, USA). Samples of ~7.5 mg were heated from 25 °C to 700 °C at a heating rate of 10 °C/min and under nitrogen atmosphere. The TGA curves were plotted as the weight loss as a function of temperature. The results showed the onset temperature (T_{onset}) which is the beginning of weight loss as a function of the temperature and the degradation temperature (T_{deg}) which is defined as the temperature at the end of the degradation.

1.3. RESULTS AND DISCUSSION

1.3.1. Characterization of commercial PLDA and PCL homopolymers

1.3.1.1. Appearance of the films

PLDA homopolymer films and PLDA/PCL polymer blend films were homogeneous at macroscopic level. Moreover, PLDA/PCL polymer blend films showed high transparency. Thus, any macrophase separation and any macro crystallization was observed.

1.3.1.2. Gel permeation characterization

M_w , M_n and PDI of both commercial PLDA and PCL homopolymers were determined by GPC and results are showed in Table 1.4. The high M_n and M_w of PLDA homopolymer is slightly lower than M_n and M_w of PCL homopolymer being PDI very similar equal to 1.5 and 1.39 for PLDA and PCL, respectively.

Table 1.4.PLDA and PCL homopolymers molecular weights obtained by GPC.

Sample name	M_n (g/mol)	M_w (g/mol)	PDI
PLDA	111.790	168.704	1.50
PCL	100.865	140.038	1.39

1.3.1.3. Differential scanning calorimetry

Thermal transitions of both PLDA and PCL homopolymers were analysed by DSC. The method used was *Method 1* described in Section 1.2.3.3. In Figure 1.5, DSC thermograms of PLDA and PCL homopolymers are represented.

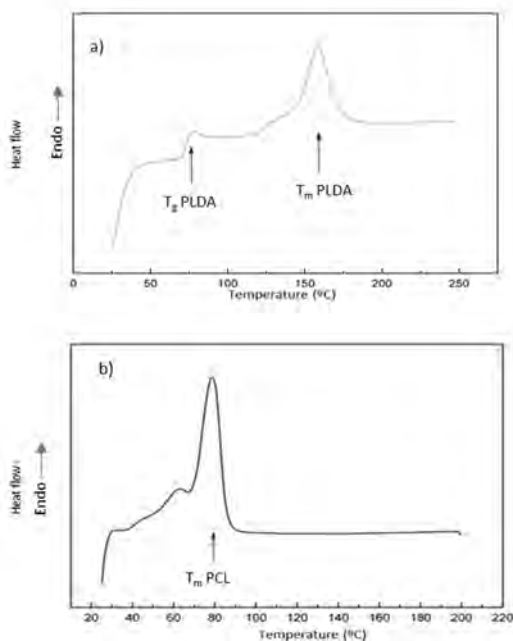


Figure 1.5. DSC thermograms of a) PLDA and b) PCL homopolymers.

As can be easily observed the T_g of PLDA homopolymer was identified at 66 °C and the T_m at 157 °C with its corresponding melting transition enthalpy of 30 J/g. PCL homopolymer showed the T_m at 78 °C and its corresponding melting transition enthalpy was 40 J/g. All thermal transitions are summarized in Table 1 5.

Sample name	T_g (°C)	T_m (°C)	ΔH_m (J/g)
PLDA	73	145	349
PCL	-	79	54

1.3.2. The evaluation of different protocols used for preparation of PLDA/PCL polymer blend films by solvent casting

The different protocols of preparation PLDA/PCL polymer blend films were studied to select the most appropriate conditions to avoid crystallization of PLDA and PCL polymer blends components during film preparation but also to evaluate the solvent residual content in prepared films. The solvent residual contents were analysed by TGA. The χ_c is one of the most important parameters of a polymer since it has strong influence on the mechanical properties [30] and affect other important properties, such as gas permeability [31] related with the polymer barrier properties against oxygen and water vapour among other gases.

Taken this into account, in this Chapter different PLDA homopolymer films were obtained by varying the preparation conditions previously mentioned in Section 1.2.2.1. Different conditions were employed since the χ_c and the solvent residual content are important parameters to control the preparation process due to their strong influence on the final properties of obtained PLDA and PCL homopolymer films. The list of tested films is summarized in Table 1.6. The investigated films were denominated as PLDA-formula of solvent- P_x protocol number.

Previous experiments to determine the best protocol were made using only PLDA homopolymer. Once adequate protocol was selected PLDA/PCL polymer blends were prepared and characterized.

Sample name	Solvent	Protocol (see Table2, Chapter 1)
PLDA-CHCl ₃ P ₁	Chloroform	1

PLDA-CHCl ₃ P ₂	Chloroform	2
PLDA-CHCl ₃ P ₃	Chloroform	3
PLDA-CH ₂ Cl ₂ P ₁	Dichloromethane	1
PLDA-CH ₂ Cl ₂ P ₂	Dichloromethane	2
PLDA-CH ₂ Cl ₂ P ₃	Dichloromethane	3

1.3.2.1. Characterization of PLDA homopolymer films thermal properties by DSC

The χ_c of a polymer is temperature dependent due to this reason it is necessary to carry out polymer characterization measurements at the same conditions, in this way, it is possible to compare the properties of different polymeric materials.

The evaluation of the χ_c of PLDA homopolymer by DSC was performed following the *Method 1* described in Section 1.2.3.3. To evaluate the thermal history of PLDA homopolymer films and how the solvent influence on the final crystallization of PLDA homopolymer, the first heating scan was considered.

To evaluate the effect of different drying protocols on the preparation of PLDA homopolymer films, the relaxation enthalpy or physical ageing should be considered. PLA as a semi-crystalline polymer has an enthalpy relaxation behaviour. This behaviour is observed when PLA is storage in conditions near its T_g it means around 53-55 °C. This phenomenon is called relaxation enthalpy or physical ageing as showed by *Huang et al.* [28] and *Turner et al.* [29]. The T_g of obtained PLDA homopolymer film is around 60 °C, consequently, drying or storage PLDA homopolymer at a temperature lower and close to the T_g (for example in protocol 3 the storage temperature was 40 °C of the polymer will result in the presence of the relaxation enthalpy or physical ageing.

As reported several years ago by different research groups [30], [31], [32] relaxation enthalpy or physical ageing has strong influence on the polymeric material properties, such as the mechanical properties, barrier resistance, optical properties, and the crystallization behaviour. Taking this into account, it is necessary to evaluate if the protocols chosen to obtain PLDA homopolymer films will provoke the relaxation enthalpy or physical ageing of PLDA homopolymer films.

In Table 1.7 main thermal transitions of PLDA homopolymer films prepared by different protocols are summarized.

Sample name	Relaxation enthalpy	T _g (°C)	T _{cc} (°C)	T _m (°C)	ΔH _m (J/mol)	X _c (%)
PLDA-CHCl ₃ P1	Not	37	110	150	9.4	10
PLDA-CHCl ₃ P2	Not	-	130	150	1.9	2
PLDA-CHCl ₃ P3	Yes	47	130	151	2.3	2.5
PLDA-CH ₂ Cl ₂ P1	Yes	48	130	151	2.3	2.5
PLDA-CH ₂ Cl ₂ P2	Yes	50	130	150	1.9	2
PLDA-CH ₂ Cl ₂ P3	Yes	50	-	150	6.0	6.5

In Figure 1.6, DSC thermograms of different PLDA homopolymer films prepared using chloroform as solvent are showed. DSC thermograms proved that films prepared by protocol 3 presented a higher enthalpy relaxation if compared to films prepared by protocol 1 and 2. *Cowie et al.* [45] reported that the enthalpy relaxation affect the segmental mobility caused volume relaxation and the reduction of the free volume. A smaller free volume led to smaller enthalpy relaxation. This effect was observed for some investigated PLDA homopolymer films. T_{cc} of PLDA homopolymer films prepared by protocol 2 and 3, appeared at higher temperature if compared to the T_{cc} of PLDA homopolymer films prepared by protocol 1. This effect could be related with the X_c which is lower for film prepared by protocol 1. The T_ms of PLDA homopolymer films prepared by three different protocols was the same.

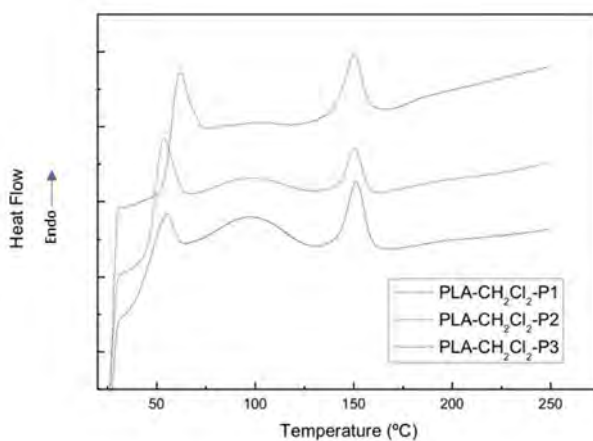


Figure 1.6. DSC thermograms of PLDA homopolymer films prepared by solvent casting using chloroform as solvent.

Thermograms of PLDA homopolymer films prepared by solvent casting using dichloromethane as solvent are showed in Figure 1.7. DSC results indicated that all films possessed a high

relaxation enthalpy or physical ageing compared with those obtained using chloroform. In addition, the T_g s of these films were shifted to higher temperatures compared with the T_g of PLDA homopolymer films prepared by protocols 1-3 using chloroform as solvent. The T_{cc} , T_m and X_c values were similar to those obtained using chloroform as solvent. As was also demonstrated by *Rhim et al.* [33], dichloromethane (DCM) dissolved PLDA homopolymer films and led to films with lower X_c however it can not be used in industrial applications since it is highly toxic and carcinogenic. In 1999 the EU presented a report of *Tukker et al.* [34], where were exposed the advantages and drawbacks of the use of DCM in the industry and its market restrictions due to the fact that DCM is a toxic and volatile compound which can be found in the ground waters and waste waters of several industries like as textile, pharmaceutical, metal-working, and chemical and petroleum industries. Moreover, *Shestakova et al.* [35] demonstrated its potentially carcinogenic effect on animals and humans. On the other hand, to control the X_c of PLDA homopolymer films it is necessary a balance between solvent fast evaporation and residual solvent content. Thus, the residual solvent content caused the relaxation enthalpy as it was deduced from DSC results presented in Figure 1.6. and Figure 1.7. To complete the solvent selection TGA measurements were carried out and the results were presented below.

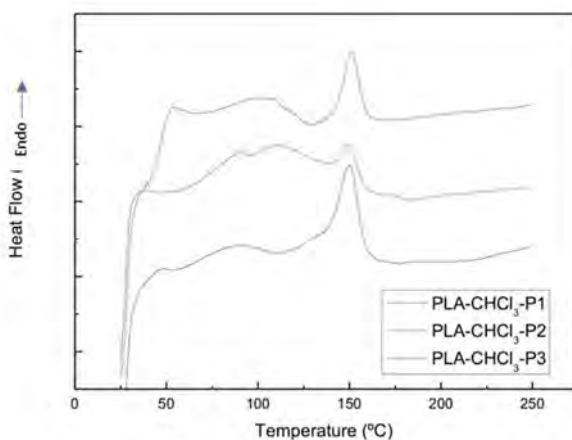


Figure 1.7. DSC thermograms of PLDA homopolymer films prepared by solvent casting using dichloromethane as solvent.

1.3.2.2. Determination of solvent residual content in PLDA homopolymer films

To evaluate the final solvent content of all prepared PLDA homopolymer films, TGA analyses were carried out following the procedure describe in Section 1.2.3.4. TGA thermograms allow also to study thermal stability of PLDA homopolymer films prepared by different protocols. All

prepared PLDA homopolymer films showed a slight weight loss between 80 °C and 100 °C related to the removal of the solvent, which was captured during each film preparation [36]. After this weight loss, a one-step thermal degradation was observed for all prepared PLDA homopolymer films prepared by protocol 1, 2 and 3, respectively, as observed from TGA thermograms showed in Figure 1.8, Figure 1.9 and Figure 1.10. The residual content corresponding to polymer impurities was calculated at 700 °C. The % of solvent content, the T_{deg} and the final residue content of PLDA homopolymer films prepared by protocol 1, 2 and 3 are showed in Table 1. 8, Table 1.9 and Table 1.10, respectively.

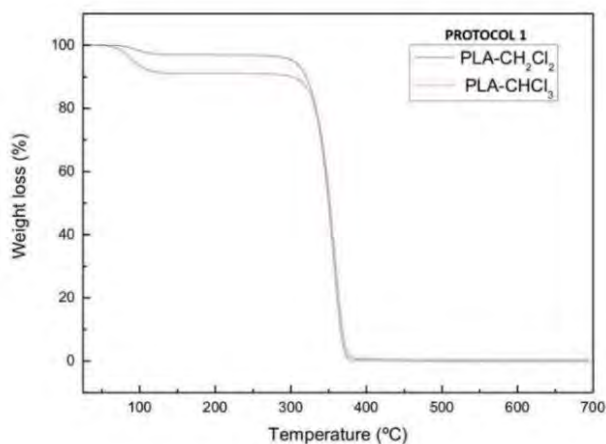


Figure 1.8. TGA curves of PLDA homopolymer films prepared by protocol 1.

Sample name	Solvent	T_{onset} (° C)	Solvent content (%)	Polymer content (%)	T_{deg} (° C)	Residue content (%)
PLDA-CHCl ₃ P1	Chloroform	80	9	91	310	0.43
PLDA-CH ₂ Cl ₂ P1	Dichloromethane	90	3	97	300	0.01

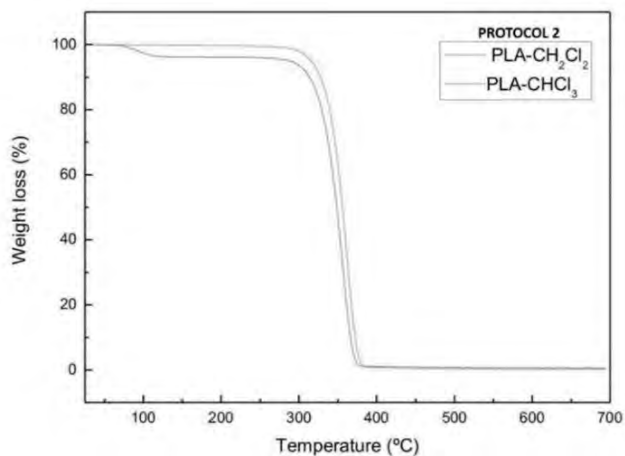


Figure 1.9. TGA curves of PLDA homopolymer films prepared by protocol 2.

Table 1.9. T_{onset} and T_{deg} of PLDA homopolymer films obtained by protocol 2.

Sample name	Solvent	T_{onset} (° C)	Solvent content (%)	Polymer content (%)	T_{deg} (° C)	Residue content (%)
PLDA-CHCl ₃ P2	Chloroform	-	-	99	300	0.4
PLDA-CH ₂ Cl ₂ P2	Dichloromethane	80	4	95	290	0.7

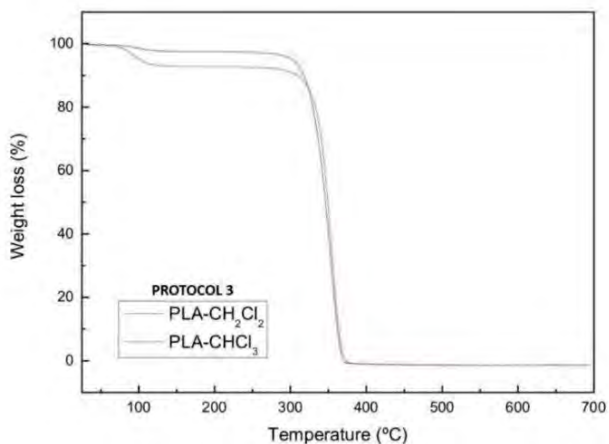


Figure 1.10. TGA curves of PLDA homopolymer films prepared by protocol 3.

Table 1.10. T_{onset} and T_{deg} of PLDA homopolymer films obtained by protocol 3.

Sample name	Solvent	T_{onset} (° C)	Solvent content (%)	Polymer content (%)	T_{deg} (° C)	Residue content (%)
PLDA-CHCl ₃ P3	Chloroform	80	7	94	300	1.26
PLDA-CH ₂ Cl ₂ P3	Dichloromethane	100	2	98	300	1.38

The lowest content of residual solvent was obtained using protocol 2, if compared with the other protocols the residual solvent content in protocol 2 was less than 1 % in chloroform. In all the protocols the T_{onset} was around 80 °C - 100 °C and the T_{deg} of PLDA homopolymer films was ~300 °C. These results demonstrated that type of protocol does not affect highly to T_{onset} and T_{deg} . Thus, taken into account the results of the comparison between relaxation enthalpy studied by DSC, and final solvent content studied by TGA, the protocol 2 was selected for preparation of PLDA/PCL polymer blend films and, as a consequence, all investigated in this Chapter polymer blends were prepared by solvent casting using chloroform as solvent.

1.3.3. Miscibility of PLDA/PCL polymer blends films

Miscibility between polymer blend components has strong effect on the final properties of polymer blends. In the introduction of this Chapter the difference between miscibility and compatibility was explained. In this investigation work, DSC technique was used to determinate the T_g s of PLDA/PCL polymer blends and discuss the miscibility between both blend components.

For this purpose, several PLDA/PCL polymer blends varying the ratio between PLDA and PCL homopolymers were prepared. The preparation was carried out following the protocol 2 explained in detail in Section 1.2.2.1.

As it is explained in the introduction using the Fox–Flory equation: $T_{g12} = T_{g1} (w_1) + T_{g2} (w_2)$ (Equation 1.1), it is possible to estimate values according to the miscibility of a polymer blends. In polymer blends which are miscible in amorphous phase it is expected to see a single T_g with an intermediate temperature between that of each individual homopolymers, while immiscible or partially miscible polymer blends showed multiple T_g 's. In the case of a completely immiscible polymer blends, the T_g 's of the single homopolymers will remained at

same temperature as it was demonstrated by authors such as *Chen et al.* [37] and *Perrin et al.* [38].

But not only T_g serves to analyse miscibility between polymer blends, T_{cc} and T_m also indicate changes in the miscibility, in addition if any displacement of both temperatures is observed during the heating scan it means that any change in the homopolymer is occurring, so an effect related with the miscibility is occurring.

PLDA/PCL polymer blend films were analysed by DSC using method 2 described in Section 1.2.3.3. DSC thermograms of PLDA/PCL polymer blend films and neat PLDA and PCL homopolymers are shown in Figure 1.11.

As one can be observed, during the 1st heating PLDA homopolymer film showed the T_g at 50 °C, the small peak of T_{cc} at 118 °C and the main peak corresponding to the T_m at 150 °C. Under the same DSC conditions, PCL homopolymer film had only the T_m at 64 °C. PLDA homopolymer and the PLDA/PCL with the weight ratio 70:30 polymer blend showed a T_g around 48-50 °C, those values are under the theoretical PLDA T_g values found in bibliography of 55-58 °C, by for example *Bai et al.* [16] and *Park et al.* [39] but as it was very near to the stabilization effect of the equipment during the heating scan it is not clearly showed in the thermogram.

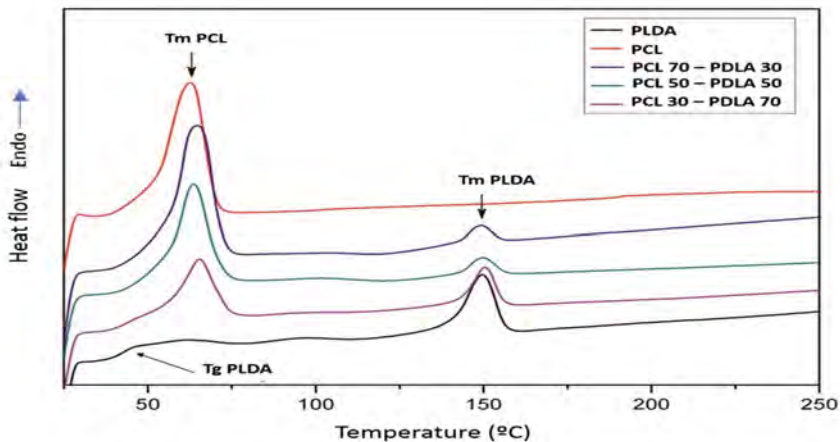


Figure 1.11. DSC thermograms of PLDA/PCL polymer blends during 1st heating scan.

The thermal transitions corresponding to PLDA/PCL appeared in the temperature range similar to the temperature range of neat PLDA and PLC homopolymers. Thus, only small variation of the T_m of PLDA or the T_m of PCL rich phases in polymer blends can be detected if compared

with corresponding T_m of polymer blend components. This displacement is caused by the weight ratio between polymer blend components, but it is not caused by miscibility.

A decrease in the peak area of melting transitions of both PCL and PLDA rich phase is clearly observed in Figure 1.11. This behaviour corresponds to a decrease of their enthalpies related with the weight ratio between PLDA/PCL polymer blend components and, therefore, the lower amount of each blend component if compared to the wt% of corresponding homopolymer. Regarding the T_g as parameter to identify the miscibility, under DSC conditions, it was not possible to observe it, probably since the T_g of PLDA is in the same temperature range as the PCL T_m . Table 1.11 summarized main thermal transitions of PLDA and PCL phases calculated from the 1st DSC heating scan.

Sample name	T_g PCL (°C)	T_m PCL (°C)	ΔH_m PCL (J/g)	T_m PLDA (°C)	ΔH_m PLDA (J/g)
PLDA	50	-	-	150	6.56
PCL	-	64	57	-	-
PCL/PLDA 70:30	-	65	57	149	3.53
PCL/PLDA 50:50	-	64	13	150	1.24
PCL/PLDA 30:70	48	65	22	150	1.27

After the 1st scan, polymer blends were cooling very quick (quenched). This quenching was done running from the liquid state (250 °C) down to -60 °C using the possible maximum speed. This treatment was done to maintain the polymer structure in the amorphous phase. When both polymers do not mix well, the amorphous portion of each polymer phase, as reflected by the T_g would maintain their original properties and both T_g will be observed as showed by *Hofman et al.* [40]. The T_g of PCL is -60 °C [41]. For investigated polymer blends and due to the equipment used was not possible to identify the T_g of PCL rich phase but it was possible to identify the T_g of PLDA rich phase and any displacement of the T_g of PLDA rich phase if compared to the T_g of PLDA homopolymer was observed. This means that PLDA/PCL polymer blend components was not miscibility as will be also see analysing the thermogram corresponding to the 2nd heating scan.

Figure 1.12. shows PLDA/PCL polymer blends thermal transitions after the quenching. Under this condition, PLDA homopolymer showed only the T_g at 59 °C due to all PLDA was in amorphous phase after the quenching step. PCL homopolymer showed the T_m at 56 °C. The T_g

of PLDA homopolymer was found ~ 55 °C and it was observed like a shoulder before the melting transition of PCL started. The T_m of PCL homopolymer was at ~ 60 °C. Any displacement of melting transition of each PLDA/PCL polymer blend components if compared to the melting transitions of PLDA and PCL homopolymers was detected. The Hoffman's law [42] predicted that at least one displacement of one of the melting transitions could indicate a slight miscibility. But it is not observed in the studied PLDA/PCL polymer blends.

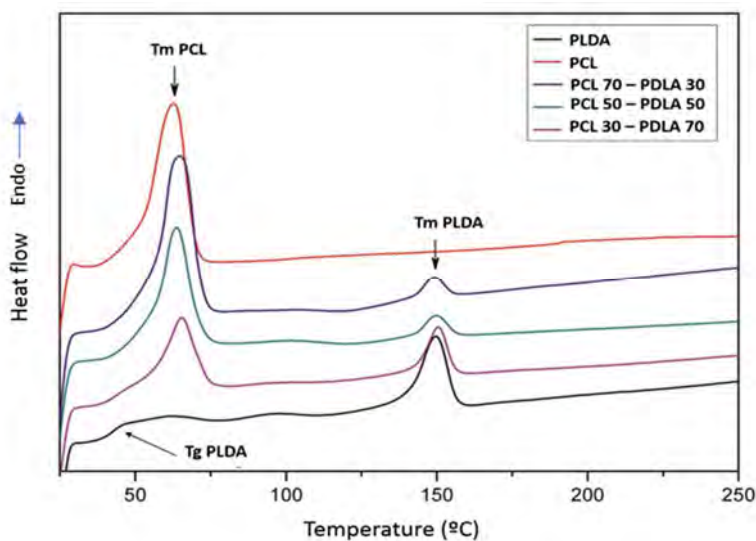


Figure 1.12. DSC thermograms of PLDA/PCL polymer blends during 2nd heating scan.

Main thermal transitions values related to each PLDA/PCL blend component phase are summarized in Table 1.12.

Sample name	T_g PCL (°C)	T_m PCL (°C)	ΔH_m PCL (J/g)	T_m PLDA (°C)	ΔH_m PLDA (J/g)
PLDA	59	-	-	-	-
PCL	-	56	41	-	-
PCL/PLDA 70:30	-	56	41	149	6
PCL/PLDA 50:50	-	56	28	149	1.24
PCL/PLDA 30:70	-	56	15	150	5

1.4. CONCLUSIONS

In this Chapter, a protocol to obtain PLDA/PCL polymer films by solvent casting was developed and PLDA/PCL polymer blends were prepared using such protocol and further characterized.

From this Chapter the following conclusions can be drawn:

- The best protocol for preparation of PLDA and PCL homopolymer films was chosen taking into account degree of crystallinity (χ_c), relaxation enthalpy and T_{deg} and % of residual solvent content.
- DSC and TGA results allowed to conclude that employment of protocol 2 using chloroform led to the lowest enthalpy relaxation of PLDA and the lowest residual content amount maintaining almost unaffected the T_{deg} and χ_c .
- Thermal results showed that although varying the percentages of PCL and PLDA in the PLDA/PCL polymer blend, T_g , T_{cc} and T_m of each homopolymer of the blend didn't present any change compared with PLDA and PCL homopolymers indicating lack of miscibility between both homopolymers.
- Obtained results showed that PLDA/PCL blends were immiscible and is necessary to find other solutions how to add PCL to PLDA to reach correct physical blending and to improve PLDA brittleness by taking advantage of the PCL flexibility.

1.5. REFERENCES

1. K. Jem, J. van der Pol, S. de V. Microbial Lactic Acid, Its Polymer Polypoly (Lactic Acid), and Their Industrial Applications. In *Plastics from bacteria, natural functions and applications*; Chen, G.-Q., Ed.; Springer-Verlag Berlin Heidelberg, 2010; p. 450.
2. A. Södergård, M.S.. *Prog. Polym. Sci.* 2002, 27, 1123–1163.
3. S. A, S.M. Industrial Production of High Molecular Weight Poly(Lactic Acid). In *Poly(lactic acid): synthesis, structures, properties, processing, and application*; Auras R, Lim LT, Selke SEM, Tsuji H, Ed.; New Jersey, 2010; pp. 27–41.
4. B. G, Q. Duana, Y.L. *RSC Adv.* 2015, 5, 13437–13442.
5. J.Lunt No Title. *Polym. Degrad. Stab* 1998, 59, 145152.
6. Auras, R.; Harte, B.; Selke, S. An Overview of Polylactides as Packaging Materials. *Macromol. Biosci.* 2004, 4, 835–864, doi:10.1002/mabi.200400043.
7. P.R. Gruber, E.S. Hall, J.H. Kolstad, M.L. Iwen, R.D. Benson, R.L.B. Continuous Process for Manufacture of Lactide Polymers with Controlled Optical Purity 1992.
8. Park, H.S.; Hong, C.K. Relationship between the Stereocomplex Crystallization Behavior and Mechanical Properties of PLLa/Pdla Blends. *Polymers (Basel)*. 2021, 13, doi:10.3390/polym13111851.
9. Aliotta, L.; Cinelli, P.; Coltelli, M.B.; Righetti, M.C.; Gazzano, M.; Lazzeri, A. Effect of Nucleating Agents on Crystallinity and Properties of Poly (Lactic Acid) (PLA). *Eur. Polym. J.* 2017, 93, 822–832, doi:10.1016/j.eurpolymj.2017.04.041.
10. HITACHI SHIPBUILDING ENG CO; TOHOKU ELEC–TRIC POWER CO; UNIV NAGOYA NAT UNIV CORP; NATUREWORKS LLC No Title 2013.
11. R. M. Rasal, A. V. Janorkar, D.E.H. No Title. *Prog. Polym. Sci.* 2010, 35, 338–356.
12. Fortelny, I.; Ujcic, A.; Fambri, L.; Slouf, M. Phase Structure, Compatibility, and Toughness of PLA/PCL Blends: A Review. *Front. Mater.* 2019, 6, 1–13, doi:10.3389/fmats.2019.00206.
13. Liu, H.; Zhang, J. Research Progress in Toughening Modification of Poly(Lactic Acid). *J. Polym. Sci. Part B Polym. Phys.* 2011, 49, 1051–1083, doi:10.1002/polb.22283.
14. J.M. Raquez, K.S.Anderson, K.M.Schreck, M.A.H. No Title. *Polym. Rev.* 2008, 48, 85–108.

15. I. Barakat, P. Dubois, R. Jerome, P.T. No Title. *Macromolecules* 1991, 24, 6542–6545.
16. Bai, H.; Xiu, H.; Gao, J.; Deng, H.; Zhang, Q.; Yang, M.; Fu, Q. Tailoring Impact Toughness of Poly(L-Lactide)/Poly(ϵ -Caprolactone) (PLLA/PCL) Blends by Controlling Crystallization of PLLA Matrix. *ACS Appl. Mater. Interfaces* 2012, 4, 897–905, doi:10.1021/am201564f.
17. S. Modi, K. Koelling, Y. *J Appl Polym Sci* 2012, 124, 3074–3081.
18. T. Yokohara, M.Y. *Eur Polym J* 2008, 44, 677–685.
19. L. Jiao, C.L. Huang, J.B. Zeng, Y.Z. Wang, X.L.W. No Title. *Thermochim Acta* 2012, 539, 16–22.
20. Broz, M.E.; VanderHart, D.L.; Washburn, N.R. Structure and Mechanical Properties of Poly(D,L-Lactic Acid)/Poly(ϵ -Caprolactone) Blends. *Biomaterials* 2003, 24, 4181–4190, doi:10.1016/S0142-9612(03)00314-4.
21. Koning, C.; Van Duin, M.; Pagnouille, C.; Jerome, R. Strategies for Compatibilization of Polymer Blends. *Prog. Polym. Sci.* 1998, 23, 707–757, doi:10.1016/S0079-6700(97)00054-3.
22. Delgado-Aguilar, M.; Puig, R.; Sazdovski, I.; Fullana-i-Palmer, P. Polylactic Acid/Polycaprolactone Blends: On the Path to Circular Economy, Substituting Single-Use Commodity Plastic Products. *Materials (Basel)*. 2020, 13, 1–18, doi:10.3390/ma13112655.
23. Przybysz-Romatowska, M.; Haponiuk, J.; Formela, K. Poly(ϵ -Caprolactone)/Poly(Lactic Acid) Blends Compatibilized by Peroxide Initiators: Comparison of Two Strategies. *Polymers (Basel)*. 2020, 12, doi:10.3390/polym12010228.
24. M. Gordon, J. S. Taylor, J. Gordon-Taylor Equation. *Appl. Chem.* 1952, 2, 495.
25. Shimadzu Corporation Patent
26. Mitsubishi Plastics Patent.
27. Park, S.D.; Todo, M.; Arakawa, K.; Koganemaru, M. Effect of Crystallinity and Loading-Rate on Mode I Fracture Behavior of Poly(Lactic Acid). *Polymer (Guildf)*. 2006, 47, 1357–1363, doi:10.1016/j.polymer.2005.12.046.
28. R-M.Ho, P-Y.Hsieh, W-H.Tseng, C-C. Lin, B-H.Huang, B.L. No Title. *Macromolecules* 2003, 36, 9085.
29. J.F. Turner, A. Riga, A. O'Connor, J. Zhang, J.J.C. No Title. *J. Therm. Anal. Calorim.* 2004,

- 75, 257–268.
30. J. M. Hutchinson No Title. *Prog. Polym. Sci.* 1995, 20, 703–760.
 31. X. Monnier, A. Siter, E.D. No Title. *Thermochim Acta* 2017, 648, 13–22.
 32. M. Pluta, M. Murariu, M. Alexandre, A. Galeski, P.D. No Title. *Polym. Degrad. Stab.* 2008, 93, 925–931.
 33. J.W. Rhim, A.K. Mohanty, S.P.S. No Title. *J. Appl. Polym. Sci.* 2006, 101, 3736–3742.
 34. Global Production Capacities of Bioplastics 2021.
 35. Shestakova, M.; Sillanpää, M. Removal of Dichloromethane from Ground and Wastewater: A Review. *Chemosphere* 2013, 93, 1258–1267, doi:10.1016/j.chemosphere.2013.07.022.
 36. L. Yu, K. Dean, L.L. No Title. *Prog. Polym. Sci.* 2006, 31, 576–602.
 37. C-C. Chen, J-Y. Chueh, H. Tseng, H-M. Huang, S.-Y.L. No Title. *Biomaterials* 2003, 24, 1167–1173.
 38. D. E. Perrin, J.P.E. Polycaprolactone. In *Handbook of Biodegradable Polymers*; A. J. Domb, J. Kost, D.M.W., Ed.; HAP: Australia, 1997; pp. 63–77.
 39. Choi, N.S.; Kim, C.H.; Cho, K.Y.; Park, J.K. Morphology and Hydrolysis of PCL/PLLA Blends Compatibilized with P(LLA-Co-ECL) or P(LLA-b-ECL). *J. Appl. Polym. Sci.* 2002, 86, 1892–1898, doi:10.1002/app.11134.
 40. D. Hofman, J. Ulbrich, D. Fritsch, D.P. No Title. *Polymer (Guildf)*. 1996, 37.
 41. A. Leiva, L. Gargallo, A. González, E. Araneda, D.R. No Title. *Eur. Polym. J.* 2006, 42, 316–321.
 42. J. Urquijo, G.Guerrica-Echevarria, J.E. No Title. *J. Appl. Polym. Sci.* 2015, 132.
 43. Todo, M.; Takayam, T. Fracture Mechanisms of Biodegradable PLA and PLA/PCL Blends. *Biomater. - Phys. Chem.* 2011, doi:10.5772/24199.
 44. T. Takayama, M. Todo, H. Tsuji No Title. *J. Mech. Behav. Biomed. Mater.* 2011, 4, 255.
 45. Cowie ,J.M.G.; Harris, S.I., *Macromolecules*. 1998, 31, 2611

CHAPTER 2

Preparation and characterization of polymer blends based on poly (L-D-lactic acid) and poly (L-lactic acid-b- ϵ -caprolactone) diblock copolymer

In this Chapter the polymer blending technology was used with the aim of study the effect of the addition of PCL block of diblock copolymer on the brittleness of PLDA homopolymer. For this purpose, polymer blends based on PLDA modified with a semi-crystalline poly (L-lactic acid-b- ϵ -caprolactone) (PLLA-b-PCL) diblock copolymer were prepared. Commercial PLLA-b-PCL diblock copolymer was chosen taking results obtained in Chapter 1 into account and the fact that PLLA block can act as compatibilizer with PLDA matrix and PCL block can improved final properties of PLDA. PLLA-b-PCL/PLDA polymer blends with different PLLA-b-PCL content were prepared by spin coating for the morphology studied, solvent casting and extrusion cast to produce probes for testing transparency, thermal and barrier properties. Moreover, the effect of the PCL block content on the crystallinity and the morphology of the PLLA-b-PCL/PLDA polymer blends have been deeply studied to check the effectiveness of the incorporation of PCL block. Moreover, the effect of the PLLA-b-PCL diblock copolymer addition on the improvement of final polymer blends properties such as thermal resistance, oxygen and water vapour permeability were also investigated in this Chapter.

CHAPTER 2. Preparation and characterization of polymer blends based on poly (L-D-lactic acid) and poly (L-lactic acid-b- ϵ -caprolactone) diblock copolymer

2.1. INTRODUCTION AND OBJECTIVES	63
2.2. MATERIALS AND METHODS	66
2.2.1. Materials	66
2.2.1.1. Poly (L-D-lactic acid)	66
2.2.1.2. Poly (L-lactic acid-b- ϵ -caprolactone) diblock copolymer	66
2.2.2. Experimental methods	67
2.2.2.1. Preparation of PLLA-b-PCL/PLDA polymer blends by solvent casting	67
2.2.2.2. Preparation of PLLA-b-PCL/PLDA polymer blends by spin coating	68
2.2.2.3. Preparation of PLLA-b-PCL/PLDA by extrusion	68
2.2.3. Characterization techniques	69
2.2.3.1. Gel permeation chromatography (GPC)	69
2.2.3.2. Differential scanning calorimetry (DSC)	69
2.2.3.3. Appearance, transparency, and PLLA-b-PCL/PLDA polymer blend films thickness	69
2.2.3.4. Atomic force microscopy (AFM)	70
2.2.3.5. Wide angle X-ray diffraction (WAXS)	70
2.2.3.6. Thermogravimetric analysis (TGA)	70
2.2.3.7. Oxygen and water vapour permeability measurements (OTR and WVTR)	71
2.3. RESULTS AND DISCUSSION.....	71
2.3.1. <i>Characterization of PLLA-b-PCL diblock copolymer</i>	71
2.3.1.1. Gel permeation characterization	72
2.3.1.2. Differential scanning calorimetry	72
2.3.2. <i>Appearance, transparency and thickness of PLLA-b-PCL/PLDA polymer blends</i>	74
2.3.3. <i>Morphology of PLLA-b-PCL/PLDA polymer blends by AFM</i>	76
2.3.4. <i>Crystallinity of PLLA-b-PCL/PLDA polymer blends by DSC and WAXS</i>	82
2.3.5. <i>Thermogravimetric analyses</i>	85
2.3.6. <i>Oxygen and water vapour barrier properties of PLLA-b-PCL/PLDA polymer blends</i>	87
2.4. CONCLUSIONS	92
2.5. REFERENCES	94

2.1. INTRODUCTION AND OBJECTIVES

As was mentioned in Chapter 1, PLA is one of the aliphatic polyesters most intensively studied for packaging applications due to its remarkable physical properties as well as its biocompatibility [1][2], and its excellent biodegradability properties [3], which strongly depend on its stereochemistry and its molecular weight. In addition, this aliphatic polyester is easily processed by conventional thermoplastic technologies such as extrusion, injection or injection blowing to produce films [4], sheets, cups, or bottles [5]. PLA find brought range of industrial applications due to its physical properties. One of these applications of PLA for consumer product is application in packaging industry, possible due to its transparency, low toxicity and environmentally sustainability [6]. Nevertheless, as it was explained in Chapter 1, there are some drawbacks, such as its brittleness which affect its mechanical properties like as toughness, crystallization behaviour which provokes problems on its processability and its low gas barrier properties that limits its current use in some packaging applications [7].

Different technologies have been studied to improve these weaknesses of PLA. To reach this objective, different authors reported improvements of PLA by the blending with more flexible polymers such as monomeric or small molecules, oligomeric, polymeric plasticizers or a mix of them as was described by *Liu et al.* [8], the use of natural additives which improve ductility and offer other properties like antioxidant activity as was studied by *Lukic et al.* [9] or antimicrobial activity studied by *Muller et al.* [10] who increase the plasticizer effect on PLA using natural antimicrobial additives. The use of compatibilizers has been also studied to improve PLA blends with other biopolymers with optimal miscibility as was studied by *Ljungberg et al.* [11]. Also, several authors have been focusing their research on PLA properties using nanotechnology. The use of different types of nano-reinforcements has been extensively studied by several authors, *Cabedo et al.* [12], *Raquez et al.* [2] and *Tenn et al.* [13] studied the use of inorganic nano-reinforcements like nanoclays to improve mechanical and barrier properties of PLA. Also the author of this investigation work participated in several patents for improving PLA barrier properties for packaging applications [14], [15] reaching improvements of 30 % in oxygen barrier permeability. Other authors used organic nano-reinforcements like nanocellulose to improve PLA barrier properties such as *Petersson et al.* [16] *Oksman et al.* [17] or *Zimmerman et al.* [18].

As is well known, the polymer blending technology consist of melting the PLA with other thermoplastics and it is well known as one of the most practical and cost-effectiveness

technology to improve its final properties. To improve the toughness of PLA several experiments blending PLA with soft or rubbery materials like as PCL have been studied [19]. These routes in which polymer blend remains miscible will improve PLA flexibility and then processability, but the effectiveness of the blending technology is strongly controlled by the final morphology of the blend. The success of the blending technology depends on the miscibility between blend components since the lack of miscibility have strong effect on the final morphology resulting in poor final properties of polymer blends as it was explained in Chapter 1. In the case of partial miscibility between polymer blend components, typical sea island morphology is commonly observed, and such lack of miscibility could impact in the final mechanical polymer blend properties, which will be worse than those of the homopolymers separately. This effect was observed for PLDA/PCL polymer blends extensively studied.

The use of DBC has been used in conventional polymer matrices to produce nanostructured nanocomposites such as *Builes et al.* [20] described for unsaturated polyesters and other polymers. Most of the authors like as *Peponi et al.* [21] identified the change of the matrices morphology caused by the addition of diblock or triblock copolymer on the polymer formulation, obtaining unexpected properties in macro properties like as thermal resistance.

PLDA/PCL polymer blends prepared and characterized in Chapter 1 showed lack of miscibility between PLDA and PCL component, consequently blending with block copolymer as blend component seems to be interesting and new possibility to explore in present Chapter.

The use of diblock copolymers open the possibility to design polymer blends with enhanced final properties. In particular, the mechanical and barrier properties of semi-crystalline polymer materials such as PLA strongly depends on their crystallinity. Therefore, it is possible to tailor polymer materials leading to the desired final properties by designing nanostructured polymer blends using block copolymers as a component of the formulation of the polymer blend. This used was not extended reported in bibliography, in addition, the majority of the authors such as *Armentano et al.*[22] in their work describe other nanostructured PLA materials with improved properties but using nano-reinforcements such as nanoclays.

As describe in more details in Chapter 1, PCL could be an excellent candidate for improving PLA brittleness, due its low glass transition temperature (- 65 °C) and its large elongation at break (≥ 600 %) if it was compatible with PLA. However as it was demonstrated in Chapter 1, high molecular weight PLA is usually immiscible with PCL, even at temperatures higher than their melt temperatures [23]. Consequently, as mentioned above, the main objective of this

Chapter was to explore the use of a diblock copolymer based on PLA and PCL blocks to prepare polymer blends with PLDA homopolymer by polymer blending technology.

Diblock copolymers (DBC) have been considered novel materials since it is easy to tailor made their main properties such as thermal or mechanical by selecting to be used chemically different blocks or adjusting the ratio of the constituting blocks. Here, it should be mentioned that in this case both blocks of the diblock copolymer (PCL and PLLA) are crystalline, consequently the microphase separation will be a competition between self-assembly and crystallization processes.

Self-assembly of diblock copolymers is usually driven by the thermodynamic repulsion between covalently bonded polymer chains of the different blocks, which as a result provokes the different microphase segregation below the order-disorder transition temperature and then the different morphologies at nanoscale are achieved. The self-assembly between immiscible constituent blocks of DBC generates nanoscale microstructures producing promising nanostructured materials with unexpected properties as it has been demonstrated by several authors such as *Builes et al.* [24] and *Cano et al.* [25] which used copolymers to improve mechanical and thermal properties of different matrices. Most of them such as *Peponi et al.* [21] identified the change of the matrices morphology caused by the addition of diblock or triblock copolymer on the polymer formulation.

Segregation strength dominates final DBC morphology in the melt, while any crystallization can be confined within the copolymer microdomain structure for strongly segregated systems, in the case of weakly segregated melts or homogenous systems, the crystallization can drive the formation of the final structure as has been observed by *Navarro-Baena et al.* [26]. As it is well known the segregation of DBCs depends strongly on both the Flory-Huggins interaction parameter (χN) of each block and the degree of polymerization of DBC and it is necessary to take into account polymer solubility parameters to predict that any other force could drive block segregation.

Blending polymers with block copolymers allow to obtain nanostructured polymer blends with different microphase separated domain sizes, which results in different morphologies which could provoke different final properties as was described by *Gomez-Hermoso-de-Mendoza et al.* [27] improving mechanical properties of TiO₂/cellulose acetate by the addition of poly(ethylene oxide-b-propylene oxide-b-ethylene oxide) (EPE) triblock copolymer and

Wasanasuk *et al.* [28] who identified changes in the PLA crystallinity by changes in the PLA morphology.

In this Chapter, polymer blends based on semi-crystalline biodegradable PLDA modified with PLLA-b-PCL diblock copolymer, which was able to self-assembly due to partial miscibility between PLLA block and PLDA matrix, were prepared and characterized. In the literature one can find information about low χ_N values for different PLLA-b-PCL diblock copolymers, confirming that this diblock copolymer showed weak segregation in the melt [29].

The main objective of the investigation work presented in this Chapter was study the influence of the addition of PLLA-b-PCL diblock copolymer on the final properties of PLLA-b-PCL/PLDA polymer blends if compare with PLDA homopolymer.

2.2. MATERIALS AND METHODS

2.2.1. Materials

2.2.1.1. Poly (L-D-lactic acid)

Poly (L-D-lactic acid) (PLDA) homopolymer used in the investigation work developed in this Chapter was the same as in Chapter 1. The details of this PLDA are describe in Chapter 1, Section 1.2.1.

2.2.1.2. Poly (L-lactic acid-b- ϵ -caprolactone) diblock copolymer

Poly (L-lactic acid-b- ϵ -caprolactone) diblock copolymer (PLLA-b-PCL) with the trade name P635 was provided by Polymer Source Inc. PLLA-b-PCL diblock copolymer is a double semi-crystalline diblock copolymer with M_n equal 60.000 and weight ratio between blocks 2:1 and with a chemical structure showed in Figure 2.1.

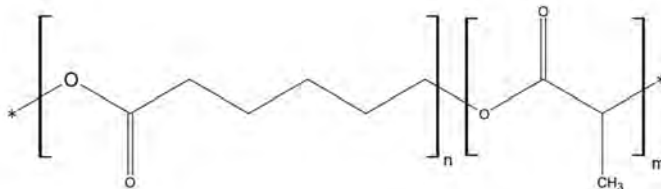


Figure 2.1.Chemical structure of PLLA-b-PCL diblock copolymer.

2.2.2. Experimental methods

As it is shown in Table 2.1., PLLA-b-PCL/PLDA polymer blends with different weight ratio between polymer blend components were obtained.

All investigated PLLA-b-PCL/PLDA polymer blends were prepared at laboratory scale. Different polymer processing technologies were used for preparation of these polymer blends depending on the properties to analyse. The technology used for preparation of the polymer blends for physico-chemical, mechanical properties and thermal was solvent casting and for barrier properties extrusion cast method. For morphological analyses investigated polymer blends were prepared by spin coating technology.

As mentioned before, different PLLA-b-PCL/PLDA polymer blends were prepared varying the PLLA-b-PCL diblock copolymer content, and as a consequence, the amount of PCL block segment, which represents the immiscible block segment in investigated polymer blends, and which will be responsible for the final morphology of polymer blends.

Sample name	PLDA (wt%)	PLLA-b-PCL (wt%)	PCL block (wt%)
PLDA	100	0	
PLLA-b-PCL/PLDA 10:90	90	10	3.3
PLLA-b-PCL/PLDA 20:80	80	20	6.6
PLLA-b-PCL/PLDA 30:70	70	30	9.9
PLLA-b-PCL/PLDA 40:60	60	40	13.2
PLLA-b-PCL/PLDA 50:50	50	50	16.5
PLLA-b-PCL/PLDA 70:30	30	70	23
PLLA-b-PCL/PLDA 80:20	20	80	26.4
PLLA-b-PCL	0	100	33

2.2.2.1. Preparation of PLLA-b-PCL/PLDA polymer blends by solvent casting

PLLA-b-PCL/PLDA polymer blends were obtained using solvent casting method. All investigated polymer blends were prepared by dissolving 10 g of each polymer blend component in chloroform under stirring (100 rpm) at room temperature during 30 min. Then, 5 mL of each solution was cast onto Petri dishes and dried following protocol 2 described in Chapter 1, Section 1.2.2.1.

Obtained PLLA-b-PCL/PLDA polymer blend films were homogeneous and all of them presented high transparency. PLLA-b-PCL/PLDA polymer blend films were stored in a silica gel desiccator during 24 h before being tested.

2.2.2.2. Preparation of PLLA-b-PCL/PLDA polymer blends by spin coating

PLLA-b-PCL/PLDA polymer blend films were spin coated using a P6700 spin-coater supplied by Cookson Electronics. These polymer blend films were prepared from a solution containing 1 wt% of each polymer in chloroform. In order to prepare each polymer blend films, a volume of 20 μL of each polymer blend solution were coated onto a glass support, and the spin-coater cycle program was as follows: 1.000 rpm for 60 s and 4.000 rpm for 20 s. Residual chloroform was removing by evaporation at room temperature. Films were stored in a silica gel desiccator during 24 h before the measurements.

2.2.2.3. Preparation of PLLA-b-PCL/PLDA by extrusion

PLLA-b-PCL/PLDA polymer blend films were prepared also by extrusion at laboratory scale. Previously to the processing step, PLDA homopolymer and PLLA-b-PCL diblock copolymer were dried in different conditions:

- PLDA homopolymer was dried during 3 h at 90 °C in a vacuum oven. Taken into account that PLDA is a high humidity sensitive polymer, this condition ensures that PLDA is completely dried before being fed into the extruder to avoid degradation caused by an excess of humidity during the extrusion step.
- PLLA-b-PCL diblock copolymer was dried at 40 °C during 15 min in a conventional oven. The difference on the selected conditions was due to PCL block segment of PLLA-b-PCL diblock copolymer which T_m is ~ 60 °C.

Once the components were mixed in the desired ratio between the different polymer blend components, the blend was processed using a twin screw mini-extruder Micro 15 cc Twin Screw Compounder (DSM Xplore). The processing conditions in this case were 199 °C, at 100 rpm for 4 min. Once the processing time is finished, the nozzle was opened, and the film was collected by a film winding system. To control the control of the thickness, only the winding speed was used. The optimal conditions of the extrusion process were optimized playing with rotation speed of the screws (rpm), torque (N) and temperature of the three zones of the extruder jacket.

The temperature profile, processing speed and residence time are summarized in Table 2.2.

Temperature zone 1 (°C)	Temperature zone 2 (°C)	Temperature zone 3 (°C)	Melting temperature (°C)	Screw speed (rpm)	Residence time (min)
200	205	210	200	100	4

Extruded PLLA-b-PCL/PLDA polymer blend films were obtained to determine oxygen and water vapour transmission rate values in order to compare the difference in gases permeability by using different processing technologies and to identify how the solvent volume could affect the gas barrier final results.

2.2.3. Characterization techniques

2.2.3.1. Gel permeation chromatography (GPC)

M_n and PDI of PLLA-b-PCL block copolymer was determined by the same GPC equipment as one used for PLDA and PCL homopolymers characterization in Chapter 1, Section 1.2.3.2.

2.2.3.2. Differential scanning calorimetry (DSC)

DSC was performed using a DSC Q 2000 from TA Instruments Inc. equipped with an autosampler. Nitrogen was used as purge gas (20 mL/min). DSC technique was used to determine the thermal transitions of PLLA-b-PCL/PLDA polymer blends and their neat components. DSC measurement was performed with the heating/cooling scan rate equal to 10 °C/min in the temperature range from -90 °C to 250 °C. The T_g , T_{cc} and T_m were calculated in the same way as describe in Chapter 1, Section 1.2.3.3. T_{cc} and T_m were determined from heating scans while T_c was determined from the cooling scans. To avoid thermal history, the samples were heated above the melting temperature of polymer blend components priori to each measurement.

2.2.3.3. Appearance, transparency, and PLLA-b-PCL/PLDA polymer blend films thickness

The appearance of solvent casted films was analysing by using printed logo templates to identify the transparency. Additionally, the transparency was measured by a UV-Vis-V-630 spectrophotometer (Jasco). All measurements were done at 600 nm and results were given as

a percent transmittance (% T), which is the percentage of the light transmitted by the investigated films related to the reference blank which was, in this case, the air.

The thickness of the PLLA-b-PCL/PLDA polymer blend films obtained by solvent casting and extrusion techniques were measured using a micrometer (mod. 644, Mitutoyo Kanagawa) with a sensitivity of $\pm 2 \mu\text{m}$. The thickness was calculated as average value from measurements taken at five different locations on each polymer blend film and following the standard *UNE EN ISO 4593:2010 Plastics - Film and sheeting - Determination of thickness by mechanical scanning*.

2.2.3.4. Atomic force microscopy (AFM)

The morphology of the investigated polymer blend films was studied using atomic force microscopy (AFM). AFM images were achieved by operating in tapping mode with a scanning probe microscope (Nanoscope IIIa, MultimodeTM from Veeco) equipped with an integrated silicon tip/cantilever with a resonance frequency of $\sim 300\text{kHz}$ from the same manufacturer. Height and phase images were obtained under ambient conditions with typical scan speeds of 0.8 - 1.6 line/s, using a scanner head with a maximum range of $16 \mu\text{m} \times 16 \mu\text{m}$. For analysis of the observed surface structures, Nanoscope image processing software was used.

2.2.3.5. Wide angle X-ray diffraction (WAXS)

WAXS analysis of PLLA-b-PCL/PLDA polymer blends films were performed using a Bruker AXS D5005 diffractometer equipped with Cu hollow cathode ($\lambda = 0.154 \text{ nm}$) and an oscillation detector. The WAXS diffraction pattern was measured from 10° to 25° (2θ) at a scan rate of $0.02^\circ/\text{min}$.

2.2.3.6. Thermogravimetric analysis (TGA)

Thermogravimetric analyses of PLLA-b-PCL/PLDA polymer blend films were carried out using a TGA Q5000 from TA Instruments Inc. described in more details in Chapter 1, Section 1.2.2. The only difference in samples analysis by TGA was that the heating range was from 25°C to 900°C .

2.2.3.7. Oxygen and water vapour permeability measurements (OTR and WVTR)

The OTR of investigated PLLA-b-PCL/PLDA polymer blend films prepared by different processing techniques (solvent casting and extrusion cast) was measured according to ASTM standard method D3985 using an OX-TRAN 2/21 ST (Mocon Inc). The OTR measurements were performed at 23 °C and at 0 % RH and p equal to 1 atm e. Before testing OTR the polymer blend probes were conditioned in pure nitrogen inside the chamber to remove traces of atmospheric oxygen. The OTR results were presented in ($\text{cm}^3 / \text{m}^2 \text{ day}^1$). Oxygen permeability ($\text{cm}^3 \mu\text{m} / \text{m}^2 \text{ day}^1 \text{ Pa}$) was calculated by multiplying the oxygen transmission rate by the film thickness (μm).

Water vapour transmission rate (WVTR) was measured according to ASTM F-1249 using a Permatran W 3/33 SG+ module (Mocon, Inc.). Samples were exposed to 90 % RH and tested at 38 ± 1 °C. Polymer blend films were conditioned in the testing cell for 12 h. Water vapour permeability ($\text{g} \mu\text{m} / \text{m}^2 \text{ day}^1 \text{ Pa}$) was calculated by multiplying the water vapour transmission rate by the films thickness (μm).

All measurements were done in duplicate; samples were masked to 5 cm x 5 cm exposed area and the OTR and WVTR values were collected when the equilibrium was reached.

2.3. RESULTS AND DISCUSSION

2.3.1. Characterization of PLLA-b-PCL diblock copolymer

PLLA-b-PCL diblock copolymer is a semi-crystalline diblock copolymer composed by two blocks, PLLA and PCL. As indicated by supplier, Polymer Source Inc, this block copolymer was synthesized by the ROP using Sn catalyst and methoxy diethylene glycol as initiator.

Moreover, Polymer Source Inc. specified molecular weight and main thermal characterization of this PLLA-b-PCL diblock copolymer in the technical data sheet for each block of this diblock copolymer. However, to confirm the physico-chemical characterization of PLLA-b-PCL diblock copolymer, under measurement conditions employed in this work all necessary measurements were performed.

2.3.1.1. Gel permeation characterization

The M_n of each block of PLLA-b-PCL diblock copolymer extracted from GPC together with the PDI are shown in Table 2.3. As expected, the experimentally determined values are equal to these provide by Polymer Source Inc.

Sample name	M_n		PDI	
	PLLA-b-PCL	PLLA block		PCL block
PLLA-b-PCL	60.000	20.000	40.000	1.45

2.3.1.2. Differential scanning calorimetry

Table 2.4 showed the thermal transitions provided by Polymer Source Inc.

Sample name	T_g (°C)	T_m (°C)	T_c (°C)
PCL block	-67	55	31
PLLA block t	-	158	-

As describe in the Chapter 1, Section 1.2.3.3, the χ_c of polymeric materials was calculated from DSC results used Equation 1.2. [30]. In the case of a diblock copolymer, the χ_c of each block of block copolymer should be considered. At it is well known, thermoplastics can be divided in crystalline and amorphous polymers. The semi-crystalline thermoplastic possess glass, melting and crystallization transition while the amorphous thermoplastic has only glass transition. Consequently, depends on the nature of blocks of block copolymer one can expect amorphous or semi-crystalline blocks.

The PLLA-b-PCL diblock copolymer consists of two crystalline blocks. As a consequence, it is necessary to quantify the contribution of each block to the final crystallinity. For this purpose, the χ_c of each block of PLLA-b-PCL diblock copolymer was calculated using Equation 2.1.

$$X_c = \frac{(\Delta H_{m(block)})}{\Delta H_m^o} \times W_{block} \quad \text{Equation 2. 1}$$

In this equation, the term $\Delta H_{m \text{ block}}$ corresponds to experimental enthalpy of the melting transition of each crystalline block, and the ΔH_m^o is theoretical melting transition enthalpy of

100 % crystalline polymeric material. Follow the literature, the ΔH_m^0 of PLA was equal 93.0 J/g [31] and the ΔH_m^0 of PCL was equal 150 J/g [32].

To evaluate the χ_c of each block of PLLA-b-PCL diblock copolymer a specific DSC procedure was used. The 1st step was an isothermal ramp at 190 °C during 5 min followed crystallization scan from 190 °C to 0 °C at a heating rate of 10 °C/min as 2nd step. The 3rd step consists of heating scan from 0 °C to 200 °C at a heating rate of 10 °C/min.

Once the PLLA-b-PCL diblock copolymer was melted a controlled crystallization ramp was performed in order to ensure complete crystallization of each block. In this scan the onset crystallization temperature and the crystallization peak of PCL block were identified together with the T_c of PLLA block. After that, a heating ramp was performed to obtain the T_m s of both blocks and the T_g -of PLLA block. Figure 2.2 showed DSC thermogram of PLLA-b-PCL diblock copolymer.

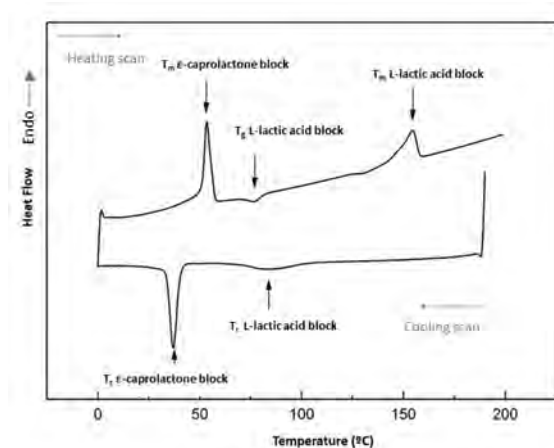


Figure 2.2. DSC thermogram of PLLA-b-PCL diblock copolymer.

In Table 2.5. PLLA-b-PCL copolymer thermal transitions are summarized:

Table 2.5. Thermal transitions of PLLA-b-PCL diblock copolymer obtained by DSC.					
Sample name	Cooling scan		Heating scan		
	T_g (°C)	T_c (°C)	T_m (°C)	ΔH_m (J/mol)	T_g (°C)
PLLA block	-	80	155	20	80
PCL block	-	35	54	30	-

Here it should be pointed out that, 1st heating scan corresponding to thermal history was not plotted in DSC thermogram. DSC results allowed to clearly identify the T_c of the PLLA block of PLLA-b-PCL diblock copolymer at ~ 80 °C and T_c of PCL block at ~ 40 °C while the T_m of PCL block can be easily observed at ~ 56 °C. Moreover, the T_g of PLLA block was detected ~ 80 °C. Additionally, at 125 °C a slight shoulder could be observed related to T_{cc} of PLLA block of PLLA-b-PCL diblock copolymer before its T_m at ~ 155 °C. All transitions related with PLLA block are higher than those corresponding to neat PLDA homopolymer. This behaviour can be explained due to possible co-crystallization process.

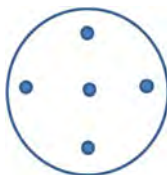
As mentioned before, the X_c of each block was calculated following the equation 1. The mass fraction for each block (w) was determined from the relation between the M_n of each block extracted from GPC results and the weight of the PLLA-b-PCL diblock copolymer used for DSC measurement (0.8 mg).

The calculated $w_{\text{PCL block}}$ value was 0.334 while $w_{\text{PLLA block}}$ was 0.666. Taking these values into account the $X_{c\text{PCL}}$ was equal 0.06 % and $X_{c\text{PLLA}}$ was 0.15 %.

These results will be useful to understand the effect of the PLLA-b-PCL diblock copolymer addition on the final properties of PLLA-b-PCL/PLDA polymer blends.

2.3.2. Appearance, transparency and thickness of PLLA-b-PCL/PLDA polymer blends

As it was described in Section 2.2.3.3. the thickness of the films was measured using a micrometer. As the PLLA-b-PCL/PLDA polymer blends were obtained casted onto a round Petri dish, the average thickness was calculated from measurements taken at five different points on each film as it is shown in Scheme 2.1. The average of the centered point was also evaluated.



Scheme 2.1. Scheme of points to measure thickness of solvent casted PLLA-b-PCL/PLDA polymer blend films.

All PLLA-b-PCL/PLDA polymer blend films prepared by solvent casting have a thickness ~ 100 μm . The thickness of extruded polymer blend films was measured using the same micrometer

and controlled by adjusting extruder parameters. The average thickness of each extruded PLLA-b-PCL/PLDA polymer blend film was $\sim 120 \mu\text{m}$.

Table 2.6. summarized the average thickness of solvent casted PLLA-b-PCL/PLDA polymer blend films.

Table 2.6. Thickness of solvent casted PLLA-b-PCL/PLDA polymer blend films.		
Samples name	Thickness (mm)*	Centered point (mm)*
Neat PLDA	110 ± 5	112 ± 1
PLLA-b-PCL/PLDA 10:90	103 ± 4	111 ± 1.5
PLLA-b-PCL/PLDA 20:80	103 ± 7	112 ± 6
PLLA-b-PCL/PLDA 30:70	112 ± 6	118 ± 2.6
PLLA-b-PCL/PLDA 40:60	109 ± 7	117 ± 3
PLLA-b-PCL/PLDA 50:50	118 ± 6	114 ± 2.8
PLLA-b-PCL/PLDA 70:30	116 ± 5	114 ± 1.5
PLLA-b-PCL/PLDA 80:20	107 ± 8	110 ± 3

Moreover, as shown in Figure 2.3, all solvent casted PLLA-b-PCL/PLDA polymer blend films were transparent at room temperature.

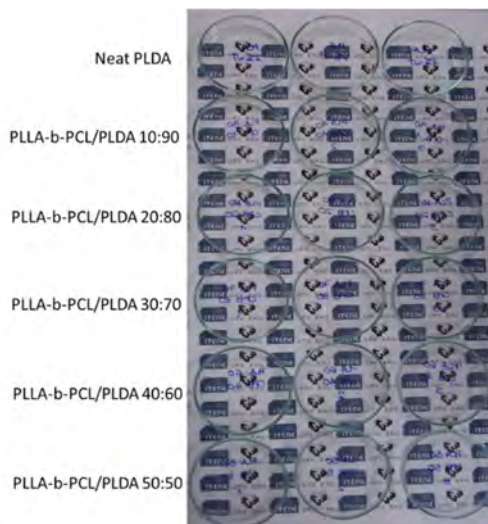


Figure 2.3. Digital image of the transparency of solvent casted PLLA-b-PCL/PLDA polymer blend films.

UV-Vis measurements were carried out to determine the transmittance of investigated films. The transmittance values of PLLA-b-PCL/PLDA polymer blends as well as PLDA and PCL homopolymers are reported in Table 2.7. Obtained transmittance values of PLLA-b-PCL/PLDA

polymer blend films were lower if compared to transmittance value of neat PLDA homopolymer. However, even adding 70 wt% of PLLA-b-PCL diblock copolymer into PLLA-b-PCL/PLDA polymer blend, the transmittance was high reaching almost 90 %. Thus, the addition of PLLA-b-PCL block does not affect drastically the transparency of investigated PLLA-b-PCL/PLDA polymer blends and simultaneously improve final properties of PLLA-b-PCL/PLDA polymer blends if compared to neat PLDA homopolymer.

Table 2.7. Transparency of PLLA-b-PCL/PLDA polymer blend films taken at 600 nm wavelength.

Sample name	Transmittance (%)
PLDA	99
PLLA-b-PCL/PLDA (10:90)	99
PLLA-b-PCL/PLDA (30:70)	98
PLLA-b-PCL/PLDA (50:50)	92
PLLA-b-PCL/PLDA (70:30)	90
PCL	84

2.3.3 Morphology of PLLA-b-PCL/PLDA polymer blends by AFM

The morphology of investigated PLLA-b-PCL/PLDA polymer blends with 20, 30, 50, 70, and 80 wt% of PLLA-b-PCL diblock copolymer content was analysed by AFM. All polymer blends were transparent at room temperature (see Figure 2.3) indicating the absence of macroscopic phase separation. In the case of PLLA-b-PCL diblock copolymer, even if this DBC consists of two polymeric blocks, PLLA and PCL, are unable to separate at macroscopic length scale spontaneously. This DBC could be self-assembled at a nanoscale level forming different well-organized structures within the PLDA as matrix. Thus, the maximum distance for these ordered structures can be the maximum size of both chains of the constituent block. The final morphology will depend on the number of monomeric units of each block of DBC together with the molar ratio of both blocks. The Flory-Huggins interaction parameter (χN), the molecular weight and the volume fraction of the immiscible block (ϕ) [33], as well as the preparation conditions among other influence the generated morphologies. As it is shown in Figure 2.4., AFM phase images clearly exhibit microphase separation of immiscible PCL block rich phase. The AFM phase images allow to distinguish a continuous brighter region attributed to PLLA block/PLDA matrix and darker, spherical domains of separated at nanoscale PCL block rich phase.

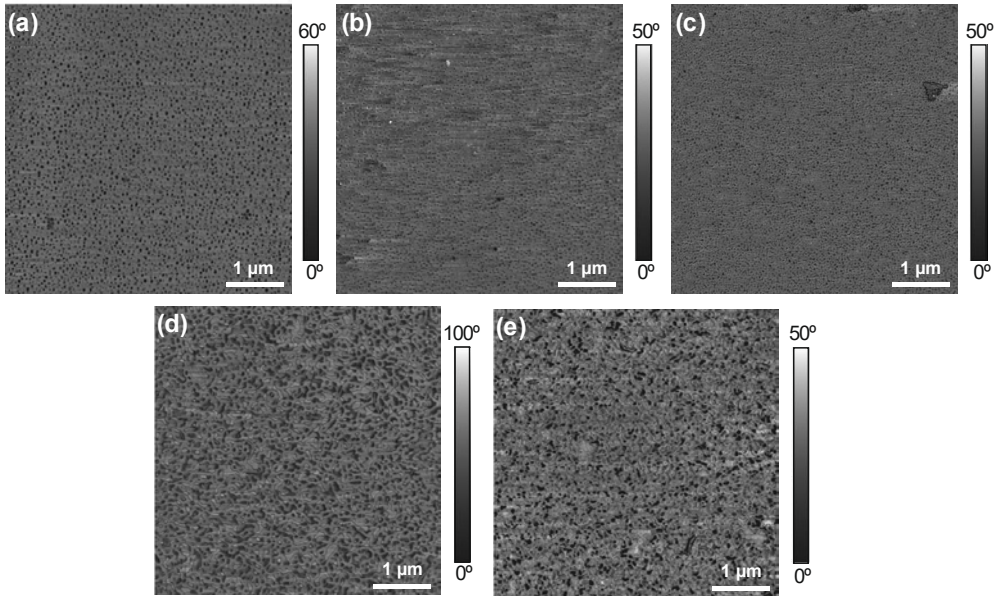


Figure 2.4. AFM phase images of PLLA-b-PCL/PLDA polymer blends with different contents of DBC: (a) 20, (b) 30, (c) 50, (d) 70 and (e) 80 wt%.

Thus, the nanometer scale spherical domains were ascribed to PCL block rich phase since the PLLA block of the DBC is partially miscible with neat PLDA homopolymer, as confirmed elsewhere [34], [35], [36].

In this work, polymer solubility parameters were calculated following *Hoftyzer-Van Krevelen Method* [37]. In this method the solubility parameters of the components can be calculated considering three group contributions: molecular dispersive force (δ_d), dipol-dipol permanent interaction (δ_p), and hydrogen bonding force (δ_h) using the Equation 2.2.

$$\delta = \sqrt{\delta_d^2 + \delta_p^2 + \delta_h^2} \quad \text{Equation 2. 2}$$

Table 2.8. summarized the polymer blend components solubility parameters together with the solvent parameter solubility to predict not only the miscibility between polymer blend components but also the solvent effect.

Table 2.8. Solubility parameters of PLDA, PCL and chloroform.	
Sample name	δ (MPa ^{1/2})
PLDA	20

PCL	23
Chloroform	19

All calculated solubility parameters are similar, which confirmed that chloroform is an adequate solvent for PLLA-b-PCL block copolymer as well as neat PLDA homopolymer. As can be seen from the AFM phase images shown in Figure 2.4 together with the δ showed in Table 2.8., the morphology of PLLA-b-PCL/PLDA polymer blends was not due to any immiscibility caused by non-solubility between solvent and each polymer blend components, however, the changes in the morphology were the effect of the increase of PCL block content in PLLA-b-PCL/PLDA polymer blends.

AFM phase images of PLLA-b-PCL/PLDA polymer blends with 20 wt% of DBC, which corresponds to 6.6 wt% of PCL block content, allowed to distinguish uniformly dispersed spherical PCL block rich phase micelles in the continuous PLLA block/PLDA matrix. The size of the spherical micelles separated domains, determined by AFM, was between 19 nm and 36 nm in diameter.

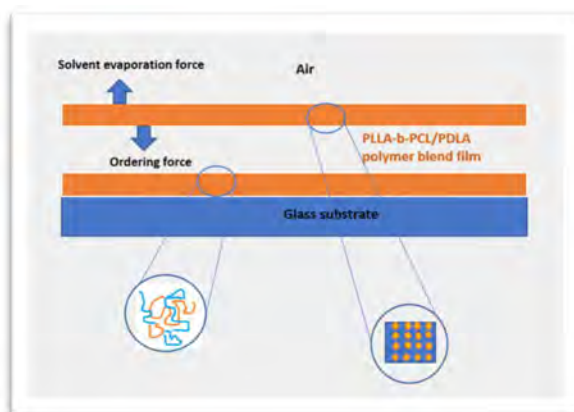
For PLLA-b-PCL/PLDA polymer blends with 30 wt% of DBC content, spherical micelles started to change, and finally interconnected micelles morphology can be detected, clearly observed for the polymer blend with 50 wt% of DBC content. The morphology of PLLA-b-PCL/PLDA polymer blends with 70 and 80 wt% of DBC content (PCL block content equal to 23 and 26 wt%, respectively) changed to a worm-like morphology, which could be a consequence of partial miscibility between the PLLA block of diblock copolymer and PLDA homopolymer matrix.

Taking into account that all nanostructured PLLA-b-PCL/PLDA polymer blends were prepared under the same experimental conditions, it can be concluded that the PCL block acts as a nanostructuring or nucleating agent and provokes the change in PLLA-b-PCL/PLDA polymer blends morphology [38]. Thus, as mentioned before, the morphology of PLLA-b-PCL/PLDA polymer blends changes from spherical micelles to wormlike micelles, passing through interconnected micelles.

To better understand the morphology of the investigated polymer blends surface tension (γ) was considered. The evaluation of both surface tension of each block which forms the diblock copolymer or the surface tension of neat homopolymers (PLDA and PCL) allow to predict the distribution of the PLLA-b-PCL diblock copolymer in the PLDA polymer matrix and on the substrate once the PLLA-b-PCL/PLDA polymer blends are spin coated. As it is described

elsewhere by *Jeon et al.* [39], the final morphology of nanostructured polymer blends depends on the solvent evaporation direction, time and temperature.

In this case, it was used glass substrate for the preparation of PLLA-b-PCL/PLDA polymer blend films, consequently the contact of investigated films with both, air and glass should be taken into account. one need to consider. The solvent used was chloroform and the possible mechanism of the film formation is schematically showed in Scheme 2.2.



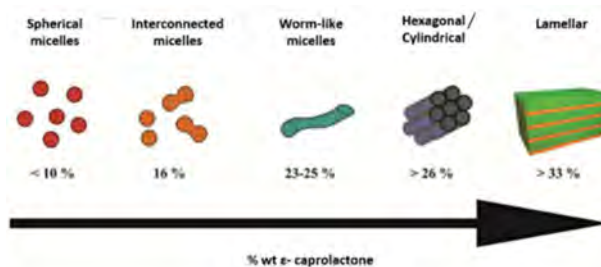
Scheme 2.2. Morphology formation of PLLA-b-PCL/PLDA polymer blends during the evaporation process.

Different steps can be distinguished during formation of the final morphology of the investigated polymer blends. At the beginning, the PLLA-b-PCL/PDLA polymer blend films contained chloroform used as solvent whereby the DBC in PLLA-b-PCL/PDLA polymer blend films were in a disordered state. Then, the concentration of polymer blend increased gradually due to continuous chloroform evaporation up to reach the critical value where the PCL block rich phase separation took place and the morphology is formed, therefore the DBC in PLLA-b-PCL/PDLA polymer blend films undergo a transition from a disordered state to an ordered state. Microphase separation occurred first on the surface, while within the interior of prepared PLLA-b-PCL/PDLA polymer blend film is still disordered due to a higher concentration of chloroform in this region of polymer blend film, generating an ordering front through the film which will be propagated from the film/air surface to the glass substrate. The nanostructure is reached since the evaporation of the chloroform occurred on the film/air surface. In the case of PLDA and PCL homopolymers, the γ extracted from bibliography are very similar, 50 and 51, theoretically, the maximum morphology that can be achieved in the

PLLA-b-PCL/PLDA polymer blends and which correspond to the most thermodynamic stability morphology will be a lamellar morphology, as it was predicted by several authors such as *Jeon et al.* [40] and *Hamley et al.* [41]. However, in PLLA-b-PCL/PLDA polymer blend films the lamellar morphology was not achieved. The γ parameters of investigated polymer blend components are listed in Table 2.9.

Sample name	γ (dina/cm)
PLDA homopolymer	50
PCL homopolymer	51

There are several causes which described why is not possible to achieve the theoretical lamellar morphology in this particular case. As is well known, up to 25 wt% of PCL immiscible block within the polymer blend, the expected morphology should be hexagonal or cylindrical one and from 33 wt% PCL block content should change to lamellar morphology as it is shown in Scheme 2.3.



Scheme 2.3. Different morphologies of PLLA-b-PCL diblock copolymer with increase of PCL block content. Source: *Scheme adapted from Ocando PhD work Nanostructured thermosetting systems from SBS block copolymers*”.

PLLA-b-PCL/PLDA polymer blends had up to 33 wt% of PCL segment block content (Table 2.1) however, the morphology achieved was interconnected micelles. This is due to the fact that in solution, block-solvent interactions dominated instead of block-polymer. Thus, PLDA polymer chains physically have been bounded within PLLA individual nanostructures of defined geometry. Much effort has been invested to identify the parameters which govern the diblock copolymer self-assembly in selective solvents into the different morphologies. *Müller et al.* [42] define the block length, NA , the molar volume, V_{mA} , and the density, ρ_A , of the solvophobic block together for giving the core volume, V_{core} , via the aggregation number, Z . In this work,

only the molar volume of the PCL immiscible block was evaluated. The theoretical density parameters ρ were $\rho_{\text{PCL}} 1.02 \text{ g/cm}^3$ and $\rho_{\text{PLA}} 1.24 \text{ g/cm}^3$. The vol% of the PCL block of each PLLA-b-PCL/PLDA polymer blend was calculated by Equation 2.3. and summarized in Table 2.10.

$$\rho = \frac{\text{weight (g)}}{\text{Volume (cm}^3\text{)}} \quad \text{Equation 2.3.}$$

Sample name	PLLA-b-PCL (wt%)	PCL (wt%)	PCL (vol %)
PLDA	0		
PLLA-b-PCL/PLDA 10:90	10	3.3	3.2
PLLA-b-PCL/PLDA 20:80	20	6.6	6.5
PLLA-b-PCL/PLDA 30:70	30	9.9	9.6
PLLA-b-PCL/PLDA 40:60	40	13.2	13
PLLA-b-PCL/PLDA 50:50	50	16.5	16
PLLA-b-PCL/PLDA 70:30	70	23	22.5
PLLA-b-PCL/PLDA 80:20	80	26.4	26
PLLA-b-PCL	100	33	32.3

Obtained results showed that the PCL vol% was only slightly lower than PCL wt%, which suggest that for 32.3 vol% the hexagonal/cylindrical morphology can be expected to be reached.

The morphology of a nanostructured polymer blends in which diblock copolymer is using as one of polymer blend components depends on three main factors:

1. Segregation forces of the diblock copolymer blocks.
2. Diblock copolymer crystallization.
3. Diblock copolymer molecular weight.

Several theoretical studies have been carried out to calculate the segregation force between PLLA and PCL blocks. The segregation force is usually expressed as combination of the χ_N , the χ_C , and with the M_n of the diblock copolymer. The study carried out by *Ho et al.* [32] identified χ_N values of around 2.9-4 in a temperature range between 50 °C to 180 °C for a PLLA-b-PCL diblock copolymer with a M_n of 22.600 g/mol and with 73.7 wt% of PCL block content corresponding to PLA block. These values are considering too by the *Mean field theory (MFT)* and the *Self-consistent field theory (SCFT)*. Both theories suggest that the diblock copolymer

microphase was separated from the melt state. As these values are too low it is easy to predict that diblock copolymers microphase separation is too weak, and it would be difficult to produce an ordered nanostructuration from the melt state. *Ho et al.* also confirmed that the driven force to define the final morphology in this case was from the PLA segment block crystallization. This effect was observed from the melt state.

Most of the research papers reviewed during this investigation were focus on the evaluation of the PLA diblocks copolymer morphology or crystallization behaviour (PLLA-b-PCL, PLLA-b-PEO, etc.) but not in the effect of the use of PLLA-b-PCL diblock copolymer as a main component for PLDA polymer blends. To clarify the influence of the crystallinity of each block of DBC on the final PLLA-b-PCL/PDLA polymer blends crystallinity and additional experiment was carried out. The PLLA-b-PCL/PDLA polymer blend with 20 wt% of DBC content was kept at 100 °C during 5 h and during this time the morphology was study. This experiment confirmed that at 100 °C only the PLLA block was crystallized. It corroborated that PLLA block drives final PLLA-b-PCL/PDLA polymer blend morphology.

2.3.4. Crystallinity of PLLA-b-PCL/PDLA polymer blends by DSC and WAXS

As it is well known, the crystallinity of PLLA-b-PCL/PDLA polymer blends has an strong effect on their thermal, mechanical and barrier properties. Consequently, the crystallinity of different PLLA-b-PCL/PDLA polymer blends was studied by DSC. The thermal transitions of PLLA-b-PCL/PDLA polymer blends were analysed and the effect of the addition of different DBC content on the PLLA-b-PCL/PDLA polymer blends was evaluated. The 2nd heating scan was taken into account to extract thermal transition of PLLA-b-PCL/PDLA polymer blends. Figure 2.5. represents DSC thermograms of neat PLDA and their polymer blends with different DBC content, from 10 wt% to 50 wt%.

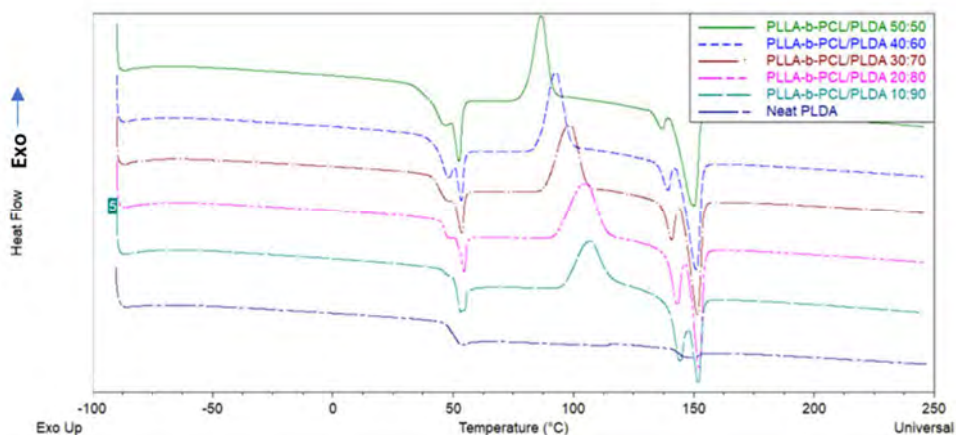


Figure 2.5. DSC thermograms of neat PLDA and PLLA-b-PCL/PLDA polymer blend films.

As can be observed, neat PLDA presented the T_g and a small peak of T_m which is related with a low crystallinity. PLLA-b-PCL/PLDA polymer blend films showed the T_g and T_{cc} shifted towards lower temperatures with the increase of DBC content. The T_g of PLLA-b-PCL/PLDA polymer blend decreases from 50 °C to 42 °C. It can be observed a peak at the same temperature of PLDA homopolymer and the PLLA segment block T_g in all the PLLA-b-PCL/PLDA polymer blends which could be confused with an enthalpy relaxation, but such peak corresponds with the T_m of PCL segment block. This shift of the T_g of PLDA/PLLA matrix to lower temperature if compared with the T_g of neat PLDA homopolymer was described by some authors and was identified as certain degree of compatibility between PLDA homopolymer and PLLA block with the PCL segment block. Observed changes in all PLLA-b-PCL/PLDA polymer blends T_{cc} are related with an increase of crystallinity in the nanostructured blends, and the double peak or bimodal melting temperature observed during PLDA homopolymer and PLLA segment block melting correspond to the two different crystalline forms or different crystal structures which melt at different temperatures. These crystalline forms melting behaviour was previously reported. α - crystals melts at high temperature and β - crystals [43] melts at low temperature. All these phenomes affect to crystallinity, and it was demonstrated by further crystallinity degree calculations. The degree of crystallinity was calculated using Equation 2.1. explained in Section 2.3.1.2 and shown in Table 2.11.

Table 2.11. Thermal transitions of PLLA-b-PCL/PLDA polymer blend compositions.

Sample name	PLDA/PLLA block phase						PCL block phase	
	T _g (°C)	T _{cc} (°C)	ΔH _c (J/mol)	T _m (°C) (PLDA+PLLA block)	ΔH _m (J/mol)	χ _c (%)	T _m (°C)	ΔH _m (J/mol)
Neat PLDA	51	124	1.45	146	1.47	0.00		
PLLA-b-PCL/PLDA 10:90	46	107	19.4	144 / 152	26.5	7.65	53	4.35
PLLA-b-PCL/PLDA 20:80	46	106	23.8	143 / 152	30.4	7.09	55	2.84
PLLA-b-PCL/PLDA 30:70	46	98	23.0	141 / 151	30.7	8.26	54	3.38
PLLA-b-PCL/PLDA 40:60	45	93	20.7	139 / 151	32.8	13.03	54	3.04
PLLA-b-PCL/PLDA 50:50	43	87	18.7	137 / 150	34.6	17.01	53	4.23

The maximum crystallinity reached for investigated PLLA-b-PCL/PLDA polymer blends was 17 % which correspond to polymer blends containing 50 wt% of DBC. This increase in crystallinity can be related to the fact that DBC can act as a nucleating agent changing the crystallinity of the PLLA block/PLDA matrix led to narrow T_{cc} peaks with the increase of DBC content. Similar phenomenon was observed also by *Hamley et al.*[44] for PLLA-b-PCL copolymers with different blocks ratio. Crystallinity results extracted from DCS results were corroborated by results obtained using WAXS technique.

Diffraction patterns represented in Figure 2.6. showed that PLDA neat sample exhibited very low diffraction peaks. However, when DBC was added into PLDA homopolymer, the crystallinity of the PLLA-b-PCL/PLDA polymer blends was increased. In addition, as DBC content increases in the blends main representative diffraction peaks intensity also increased.

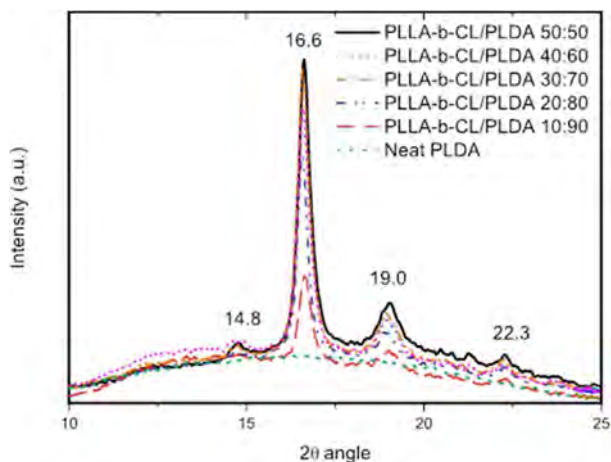


Figure 2.6. WAXS spectra of PLDA and PLLA-b-PCL/PLDA polymer blends containing different DBC contents.

From the literature, the first peak at $2\theta = 14.8^\circ$ was assigned to the 110/110/200 reflections of α -PLLA described as $2\theta = 15^\circ$ as corroborated *Kim et al.* [39]. A very intense peak at $2\theta = 16.6^\circ$ was close to the expected position for the α -form of PLLA crystals sets of 113 and 203 reflections at 17° . Moreover, as known from the literature peaks at 19° and 22° was related to the formation of other type of PLLA crystals. However, *Hamley et al.* [44] identified these peaks as the 110 reflections of PCL. All WAXS results corroborated that the inclusion of an PCL block in the PLLA-b-PCL/PLDA polymer blend controls the final crystallinity of the designed nanostructured materials and consequently other inherent final properties like thermal resistance that depend on morphology, as also pointed out by *Nakayama et al.* [45].

2.3.5. Thermogravimetical analyses

TGA curves of PLLA-b-PCL/PLDA polymer blends and neat PLDA homopolymer are shown in Figure 2.7. TGA thermograms showed two main steps, the first one corresponding to a weight loss between 80°C to 100°C related to the residual solvent in investigated polymer films and the second step corresponding to the onset of PLLA-b-PCL/PLDA T_{deg} , and then followed of the maximum of PLLA-b-PCL/PLDA T_{deg} . In Table 2.12. neat PLDA homopolymer and PLLA-b-PCL/PLDA polymer blend films TGA results were plotted.

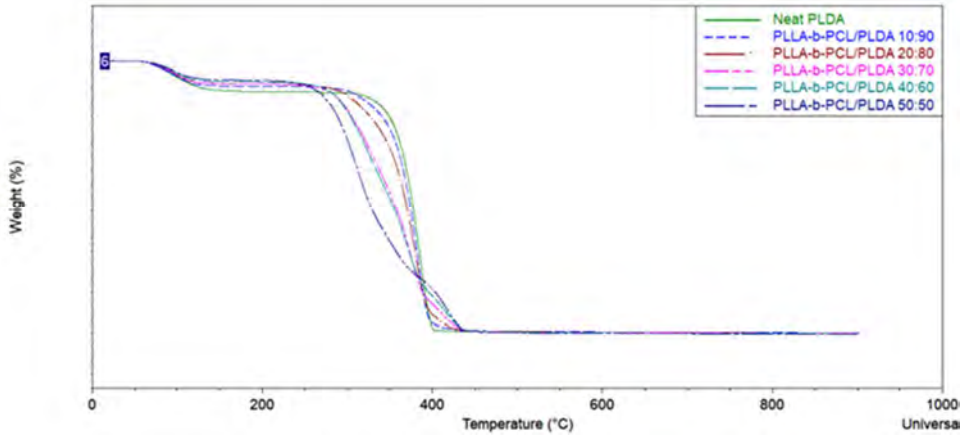


Figure 2.7. TGA curves of PLLA-b-PCL/PLDA polymer blend films.

Table 2.12. TGA curves of PLLA-b-PCL/PLDA polymer blend films.

Sample name	T _{onset} (°C)	T _{deg} (°C)
Neat PLDA	338	397
PLLA-b-PCL/PLDA 10:90	319	398
PLLA-b-PCL/PLDA 20:80	302	409
PLLA-b-PCL/PLDA 30:70	287	420
PLLA-b-PCL/PLDA 40:60	283	424
PLLA-b-PCL/PLDA 50:50	267	426

As can be observed in Figure 2.7. and Table 2.12 a clear trend took place, as much as the DBC amount increases as much as the thermal resistance to degradation increases. This effect was observed by other authors like *Navarro et al.* [46] confirming that PLLA-b-PCL addition decrease the thermal stability of PLA compared with the neat PLDA, however T_{deg} increases as DBC content increases. This effect could be explained by the nanostructuring effect which it caused by the DBC addition and then by the increase of crystallinity. Polymer blends presented an ordered morphological structure drive by a chemical blend which is the diblock copolymer plus a full miscibility of the PLDA homopolymer and the PLLA segment block, such composition is a thermodynamical stable morphology, and it caused the thermal resistance; also, PCL pristine polymer has a degradation temperature higher than PLA pristine polymer, so the increase of PCL causes an increase of thermal resistance.

2.3.6. Oxygen and water vapour barrier properties of PLLA-b-PCL/PLDA polymer blends

To evaluate the effect of the addition of PLLA-b-PCL diblock copolymer on the barrier properties of PLLA-b-PCL/PLDA polymer blend films, oxygen and water vapour transmission rate measurements were performed. Solvent casted PLLA-b-PCL/PLDA polymer blend films with dimensions of 5 cm x 5 cm were tested following the procedure described in Section 2.2.3.7.

Figure 2.8. showed the OTR results of the different PLLA-b-PCL/PLDA polymer blend films and in Table 2.13. calculated the OTR and oxygen permeability were listed. The oxygen permeability values were calculated by multiplying the oxygen transmission rate by the film thickness.

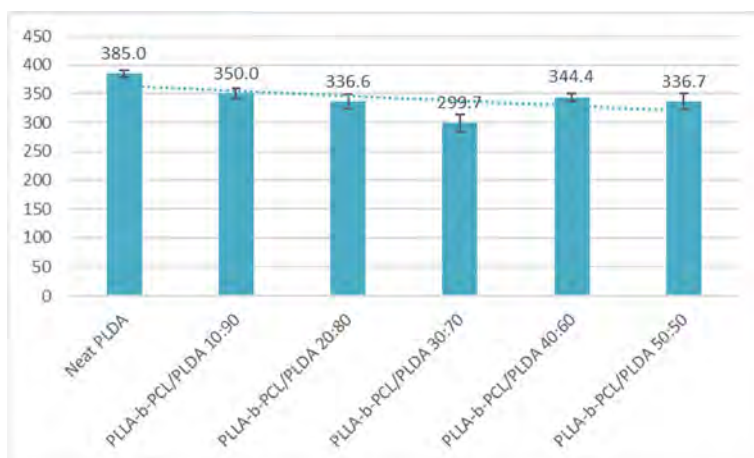


Figure 2.8. The OTR of solvent casted PLLA-b-PCL/PLDA polymer blend films.

Sample name	OTR (cm³/m².day.Pa)	Oxygen permeability (cm³.µm/m².day.Pa)
Neat PLDA	385 ± 6.2	38.500
PLLA-b-PCL/PLDA 10:90	350 ± 10.0	35.000
PLLA-b-PCL/PLDA 20:80	337 ± 12.1	33.660
PLLA-b-PCL/PLDA 30:70	300 ± 14.7	29.970
PLLA-b-PCL/PLDA 40:60	344 ± 7.3	34.440
PLLA-b-PCL/PLDA 50:50	337 ± 13.7	33.670

A slight decrease in the oxygen permeability was observed as visualized in the Figure 2.8. Similar results were also observed by *Plackett et al.* [4] and *Auras et al.*[3] for nanocomposites of PLDA modified with organomodified clays and also for copolymers of PLA modified with PCL. Neat PLDA film showed the OTR of 385 cc/m² day while the OTR of PLLA-b-PCL/PLDA polymer blend film with 30 wt% DBC content was equal to 300 cm³/ m² day Pa, this is a decrease of more than 20 % if compared to the OTR of neat PLDA homopolymer. These results once more confirmed that the addition of DBC into PLLA-b-PCL/PLDA polymer blends had strong affect not only on the final crystallinity but also on the barrier properties of investigated polymer blends. As mentioned before this behaviour can be related with the nanostructuring effect of DBC in investigated PLLA-b-PCL/PLDA polymer blends. Similar results have been published by *Drieskens et al.* [47]. They observed that crystallization of PLDA causes a decrease of oxygen permeability, however not in linear proportion with the decrease of amorphous volume size. Moreover, *Byun et al.* [48] observed a relation between the crystallinity and the correlation with the free volume. Authors showed that the increase of the crystallinity of investigated by them polymeric materials increased the barrier for the gases diffusion. Thus, higher amorphous phase content in polymeric materials higher will be free volume, which can facilitate the space for the oxygen diffusion. These previous works could explain the oxygen permeability decrease that was observed also in this investigation work for PLLA-b-PCL/PLDA polymer blend films prepared by extrusion.

Extruded samples showed higher increase of the oxygen barrier permeability than those PLLA-b-PCL/PLDA polymer blend films obtained by solvent casting. Surprisingly, the decrease in oxygen permeability reached values of 50 % for PLLA-b-PCL/PLDA polymer blend films with 10 wt% of DBC content and up to 70% of reduction for PLLA-b-PCL/PLDA polymer blend films with 50 wt% of DBC content. Achieved oxygen and water vapour barrier results represent an opportunity for PLLA-b-PCL/PLDA polymer blends as a future packaging material.

The OTR results obtained for extruded PLLA-b-PCL/PLDA polymer blend films are represented in Figure 2.9 and summarized in Table 2.14.

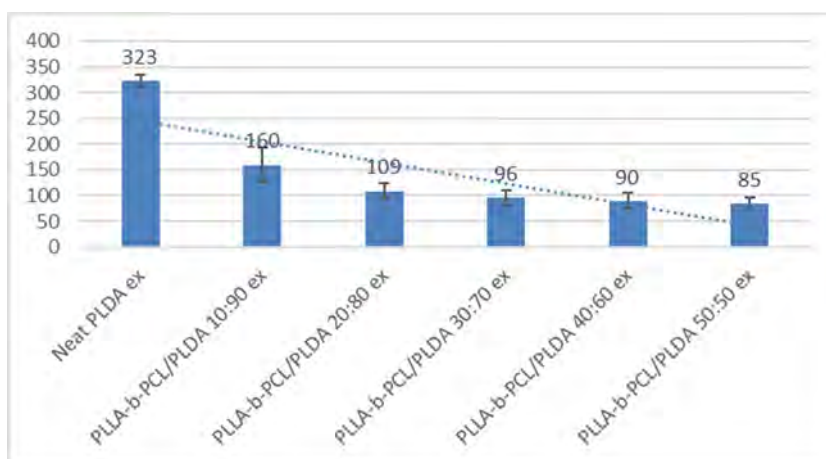


Figure 2.9. The OTR of extruded PLLA-b-PCL/PLDA polymer blend films.

Table 2.14. The OTR and oxygen permeability of extruded PLLA-b-PCL/PLDA polymer blend films.

Sample name	OTR (cm ³ /m ² .day.Pa)	Oxygen permeability (cm ³ .μm/m ² .day.Pa)
Neat PLDA ex	323 ± 11.6	32.301
PLLA-b-PCL/PLDA 10:90 ex	160 ± 32.8	16.001
PLLA-b-PCL/PLDA 20:80 ex	109 ± 15	10.880
PLLA-b-PCL/PLDA 30:70 ex	96 ± 15	9.600
PLLA-b-PCL/PLDA 40:60 ex	90 ± 15	9.000
PLLA-b-PCL/PLDA 50:50 ex	85 ± 12	8.500

The decrease of the oxygen permeability in extruded PLLA-b-PCL/PLDA polymer blend films surprisingly, was still better than those films obtained by solvent casting, reaching values of the OTR reduction of 74 % compared with the OTR for neat PLDA.

Water vapour permeability and water vapour transmission rate analyses were carried out according to ASTM F-1249 as it was explained in Section 2.2.3.7. The WVTR of solvent casted PLLA-b-PCL/PLDA polymer blend films results are represented in Figure 2.10 and the WVTR and the calculated water vapour permeability are summarized in Table 2.15.

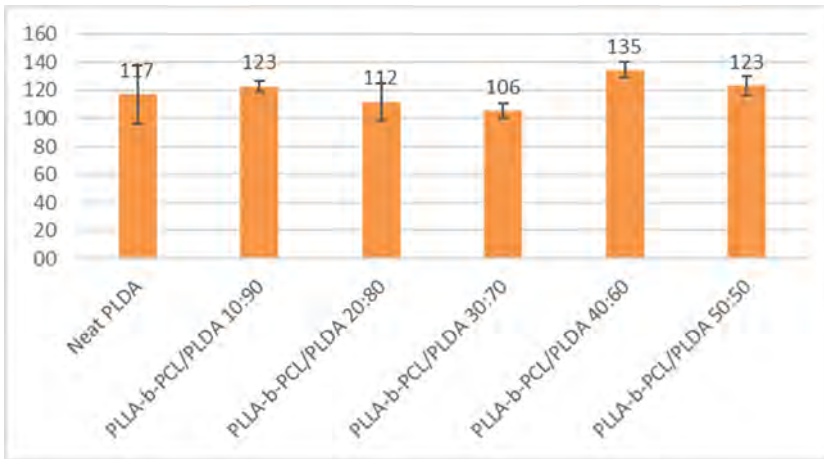


Figure 2.10. The WVTR of solvent casted PLLA-b-PCL/PLDA polymer blend films.

Table 2.15. The WVTR and water permeability results of solvent casted PLLA-b-PCL/PLDA polymer blend films.

Sample name	WVTR (g/m ² .day.Pa)	Water permeability (g.μm/m ² .day.Pa)
Neat PLDA	117 ± 20.8	18.770
PLLA-b-PCL/PLDA 10:90	123 ± 4.0	19.663
PLLA-b-PCL/PLDA 20:80	112 ± 13.4	17.880
PLLA-b-PCL/PLDA 30:70	106 ± 5.4	16.895
PLLA-b-PCL/PLDA 40:60	135 ± 5.5	21.528
PLLA-b-PCL/PLDA 50:50	123 ± 6.9	19.688

As it can be extracted from results a slight decrease of the WVTR was observed with the increase of DBC content in PLLA-b-PCL/PLDA polymer blends. The maximum decrease in the WVTR was obtained for PLLA-b-PCL/PLDA polymer blend films with 30 wt% of DBC content. As PLDA homopolymer is a hydrophilic polymer, it presents poor water vapour barrier properties. *Shogren et al.* [49] reported the correlation between water solubility, crystallinity, and their effect on T_g . Extruded PLLA-b-PCL/PLDA polymer blend films showed a decrease of the WVTR with the increase of the crystallinity, as directly related to the PCL block content with the increase of the DBC content in investigated polymer blends. However, in solvent casted samples this relation is not a linear relation, consequently, there are other factors which could drive the water vapour permeability. One of these factors could be the solvent residual content. The amount of solvent in a PLDA sample is related directly to higher amorphous phase

in polymer blend film which facilitates the space for the gases diffusion, but this effect was not observed in DSC thermograms.

Water vapour permeability of extruded PLLA-b-PCL/PLDA polymer blends was determined using the same conditions and equipment as for solvent casted polymer blends. The same effect was observed for oxygen permeability results when compared solvent casted polymer blends with extruded polymer blends. In Figure 2.11. WVTR of extruded PLLA-b-PCL/PLDA polymer blend films are plotted.

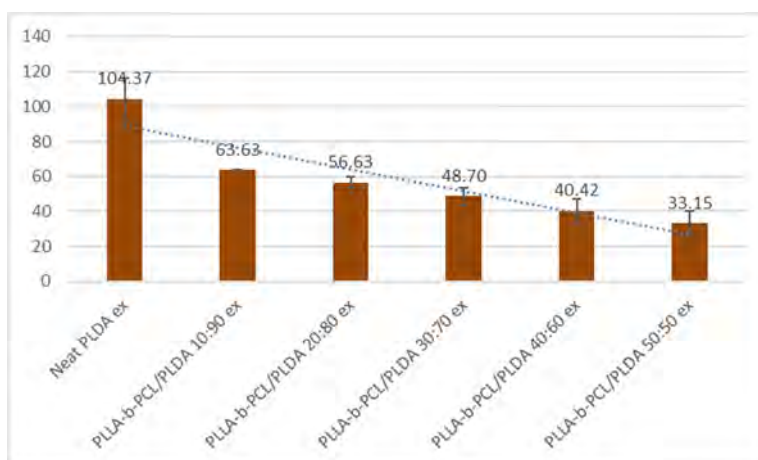


Figure 2.11. Water vapour transmission rate of extruded PLLA-b-PCL/PLDA-polymer blend films.

In Table 2.16 WVTR and calculated water vapour permeability are listed. The polymer blends thickness was 160 μm .

Table 2.16. The WVTR and water permeability results of extruded PLLA-b-PCL/PLDA polymer blends films.

Sample name	WVTR (g/m ² .day.Pa)	Water permeability (g. μm /m ² .day.Pa)
Neat PLDA ex	104 \pm 11.8	16.698
PLLA-b-PCL/PLDA 10:90 ex	64 \pm 0.13	10.181
PLLA-b-PCL/PLDA 20:80 ex	57 \pm 3.00	9.061
PLLA-b-PCL/PLDA 30:70 ex	49 \pm 5.00	7.792
PLLA-b-PCL/PLDA 40:60 ex	40 \pm 7.00	6.468
PLLA-b-PCL/PLDA 50:50 ex	33 \pm 7.00	5.303

In extruded PLLA-b-PCL/PLDA polymer blends, a linear decrease in the WVTR values was detected with the increase of the DBC content. As expected, also in the case of WVTR the

crystallinity has strong effect on the barrier properties of prepared polymer blend films due to crystalline domains can act as fillers that are impermeable to gas penetrants. Therefore, can be conclude that the permeability decreases with the increase of the crystallinity.

In addition, the different techniques used to fabricate the polymer blend films led to changes in the final properties. Extruded PLLA-b-PCL/PLDA polymer blends have not any solvent residue consequently the polymer chain is just ordered following the nanostructuration due to the immiscibility of the PCL block segment and driven by the PLLA block segment chain. For extruded PLLA-b-PCL/PLDA polymer blend films, the WVTR decreased linearly with the increase of DBC content. *Tsuji et al.*[50] observed an improvement on water vapour permeability up to 30 % compared with neat PLDA and indicated it as the maximum increase to be reached for investigated by them polymeric materials. This is due to the higher resistance of restricted amorphous regions. In this investigation field, *Duan and Thomas* [51], have reported the effect of the crystallinity on the water vapour permeability of PLDA polymer by means of the tortuous path model. Several papers explained the effect of the processing conditions, the molecular weight, or the final gas barrier properties differences by adding different nanoreinforcements [52], [53] and [54].

Nowadays, any paper has been found explaining the use of double crystallinity diblock copolymers as materials to reduce gas permeability on PLDA samples for packaging applications.

2.4. CONCLUSIONS

In this Chapter polymer blending technology was used to introduce PCL blocks into PLDA polymer matrix with the objective of improving its inherent weaknesses. A commercial and semi-crystalline PLLA-b-PCL diblock copolymer was used for this purpose.

PLLA-b-PCL/PLDA polymer blend films have been prepared using three different techniques, solvent casting, spin coating and extrusion cast. Results of characterization of the appearance, morphology, thermal and barrier properties lead to the following conclusions:

- Obtained PLLA-b-PCL/PLDA polymer blend films were transparent indicating the absence of macroscopic phase separation.
- AFM phase images clearly showed the effect of the addition of the PLLA-b-PCL diblock copolymer on the blend, concretely the immiscible PCL block of the DBC caused a

nanoscale separation and then different morphologies were reached with the increase of PCL block content in PLLA-b-PCL/PLDA polymer blends.

- The crystallinity of PLLA-b-PCL/PLDA polymer blends increased with the increase of PCL block content in PLLA-b-PCL/PLDA polymer blend reaching values up to 17% compared with 1% of the neat PLDA polymer.
- Thermal results showed a slight decrease of the T_g of the polymer blends suggesting partial miscibility of the DBC with the PLDA and a plasticizer effect.
- Finally, the most unexpected effect was the improvement of barrier properties, oxygen and water vapour barrier properties were increased by the addition of the DBC in the blend, reaching values of a decrease of 20 % of the value of oxygen transmission rate compared with the PLDA homopolymer. This effect was increased when the materials were prepared using an extruder, reaching values of a decrease of more than 50 % compared with the PLDA homopolymer values. Water vapour permeability results presented also a slight improvement reaching values of 30 % of a decrease of the water vapour transmission rate.

2.5. REFERENCES

1. Kfoury, G.; Raquez, J.M.; Hassouna, F.; Odent, J.; Toniazzo, V.; Ruch, D.; Dubois, P. Recent Advances in High Performance Poly(Lactide): From “Green” Plasticization to Super-Tough Materials via (Reactive) Compounding. *Front. Chem.* 2013, *1*, 1–46, doi:10.3389/fchem.2013.00032.
2. Raquez, J.M.; Habibi, Y.; Murariu, M.; Dubois, P. Poly(lactide (PLA)-Based Nanocomposites. *Prog. Polym. Sci.* 2013, *38*, 1504–1542, doi:10.1016/j.progpolymsci.2013.05.014.
3. Auras, R.; Harte, B.; Selke, S. An Overview of Poly(lactides) as Packaging Materials. *Macromol. Biosci.* 2004, *4*, 835–864, doi:10.1002/mabi.200400043.
4. N. Gontard, D.P. Food Packaging Applications of Biopolymer-Based Films. In *Biopolymers: New Materials for sustainable films and coatings.*; New York, 2011; pp. 211–232.
5. C. Johansson Bionanocomposites for Food Packaging Applications. In *Nanocomposites with biodegradable polymers*; Mittal V., Ed.; Oxford, 2011; pp. 348–367.
6. S. A, S.M. Industrial Production of High Molecular Weight Poly(Lactic Acid). In *Poly(lactic acid): synthesis, structures, properties, processing, and application*; Auras R, Lim LT, Selke SEM, Tsuji H, Ed.; New Jersey, 2010; pp. 27–41.
7. R. M. Rasal, A. V. Janorkar, D.E.H. No Title. *Prog. Polym. Sci.* 2010, *35*, 338–356.
8. Liu, H.; Zhang, J. Research Progress in Toughening Modification of Poly(Lactic Acid). *J. Polym. Sci. Part B Polym. Phys.* 2011, *49*, 1051–1083, doi:10.1002/polb.22283.
9. Lukic, I.; Vulic, J.; Ivanovic, J. Antioxidant Activity of PLA/PCL Films Loaded with Thymol and/or Carvacrol Using ScCO₂ for Active Food Packaging. *Food Packag. Shelf Life* 2020, *26*, 100578, doi:10.1016/j.fpsl.2020.100578.
10. Muller, J.; Casado Quesada, A.; González-Martínez, C.; Chiralt, A. Antimicrobial Properties and Release of Cinnamaldehyde in Bilayer Films Based on Poly(lactic Acid (PLA) and Starch. *Eur. Polym. J.* 2017, *96*, 316–325, doi:10.1016/j.eurpolymj.2017.09.009.
11. Ljungberg, N.; Wesslén, B. Preparation and Properties of Plasticized Poly(Lactic Acid) Films. *Biomacromolecules* 2005, *6*, 1789–1796, doi:10.1021/bm050098f.
12. Feijoo, J.L.; Cabedo, L.; Giménez, E.; Lagaron, J.M.; Saura, J.J. Development of Amorphous PLA-Montmorillonite Nanocomposites. *J. Mater. Sci.* 2005, *40*, 1785–1788,

doi:10.1007/s10853-005-0694-8.

13. Tenn, N. Effect of Nanoclay Hydration on Barrier Properties of PLA / Montmorillonite Based Nanocomposites. 2013.
14. ITENE Modified Phyllosilicate 2012.
15. ITENE Polymer Nanocomposite Comprising Polylactic Acid Reinforced with the Modified Phyllosilicate 2012.
16. Petersson, L.; Kvien, I.; Oksman, K. Structure and Thermal Properties of Poly(Lactic Acid)/Cellulose Whiskers Nanocomposite Materials. *Compos. Sci. Technol.* 2007, *67*, 2535–2544, doi:10.1016/j.compscitech.2006.12.012.
17. Mathew, A.P.; Oksman, K.; Sain, M. The Effect of Morphology and Chemical Characteristics of Cellulose Reinforcements on the Crystallinity of Polylactic Acid. *J. Appl. Polym. Sci.* 2006, *101*, 300–310, doi:10.1002/app.23346.
18. Tingaut, P.; Zimmermann, T.; Lopez-Suevos, F. Synthesis and Characterization of Bionanocomposites with Tunable Properties from Poly(Lactic Acid) and Acetylated Microfibrillated Cellulose. *Biomacromolecules* 2010, *11*, 454–464, doi:10.1021/bm901186u.
19. Semba, T.; Kitagawa, K.; Ishiaku, U.S.; Hamada, H. The Effect of Crosslinking on the Mechanical Properties of Polylactic Acid/Polycaprolactone Blends. *J. Appl. Polym. Sci.* 2006, *101*, 1816–1825, doi:10.1002/app.23589.
20. Builes, D.H.; Labidi, J.; Eceiza, A.; Mondragon, I.; Tercjak, A. Unsaturated Polyester Nanocomposites Modified with Fibrillated Cellulose and PEO-b-PPO-b-PEO Block Copolymer. *Compos. Sci. Technol.* 2013, *89*, 120–126, doi:10.1016/j.compscitech.2013.09.015.
21. Peponi, L.; Tercjak, A.; Torre, L.; Kenny, J.M.; Mondragon, I. Morphological Analysis of Self-Assembled SIS Block Copolymer Matrices Containing Silver Nanoparticles. *Compos. Sci. Technol.* 2008, *68*, 1631–1636, doi:10.1016/j.compscitech.2008.02.032.
22. Armentano, I.; Bitinis, N.; Fortunati, E.; Mattioli, S.; Rescignano, N.; Verdejo, R.; Lopez-Manchado, M.A.; Kenny, J.M. Multifunctional Nanostructured PLA Materials for Packaging and Tissue Engineering. *Prog. Polym. Sci.* 2013, *38*, 1720–1747, doi:10.1016/j.progpolymsci.2013.05.010.
23. N. Lopez-Rodriguez, A. Lopez-Arraiza, E. Meaurio, J.R.S. No Title. *Polym. Eng. Sci.* 2006, *46*, 1299.
24. Builes DH, Hernández-Ortiz JP, Corcuera MA, Mondragon I, T.A. Effect of Poly(Ethylene

- Oxide) Homopolymer and Two Different Poly(Ethylene Oxide-b- Poly(Propylene Oxide)-b-Poly(Ethylene Oxide) Triblock Copolymers on Morphological, Optical, and Mechanical Properties of Nanostructured Unsaturated Polyester. *ACS Appl Mater Interfaces*. 2014, 22, 1073–1081, doi:10.1021/am4046266.
25. Cano, L.; Builes, D.H.; Tercjak, A. Morphological and Mechanical Study of Nanostructured Epoxy Systems Modified with Amphiphilic Poly(Ethylene Oxide-b-Propylene Oxide-b-Ethylene Oxide)Triblock Copolymer. *Polymer (Guildf)*. 2014, 55, 738–745, doi:10.1016/j.polymer.2014.01.005.
 26. Navarro-Baena, I.; Marcos-Fernandez, A.; Kenny, J.M.; Peponi, L. Crystallization Behavior of Diblock Copolymers Based on PCL and PLLA Biopolymers. *J. Appl. Crystallogr*. 2014, 47, 1948–1957, doi:10.1107/S1600576714022468.
 27. Gomez-Hermoso-de-Mendoza, J.; Gutierrez, J.; Tercjak, A. Improvement of Macroscale Properties of TiO₂/Cellulose Acetate Hybrid Films by Solvent Vapour Annealing. *Carbohydr. Polym*. 2020, 231, 115683, doi:10.1016/j.carbpol.2019.115683.
 28. Wasanasuk, K.; Tashiro, K.; Hanesaka, M.; Ohhara, T.; Kurihara, K.; Kuroki, R.; Tamada, T.; Ozeki, T.; Kanamoto, T. Crystal Structure Analysis of Poly(L-Lactic Acid) α Form on the Basis of the 2-Dimensional Wide-Angle Synchrotron X-Ray and Neutron Diffraction Measurements. *Macromolecules* 2011, 44, 6441–6452, doi:10.1021/ma2006624.
 29. Navarro-Baena, I.; Marcos-Fernández, A.; Fernández-Torres, A.; Kenny, J.M.; Peponi, L. Synthesis of PLLA-b-PCL-b-PLLA Linear Tri-Block Copolymers and Their Corresponding Poly(Ester-Urethane)s: Effect of the Molecular Weight on Their Crystallisation and Mechanical Properties. *RSC Adv*. 2014, 4, 8510–8524, doi:10.1039/c3ra44786c.
 30. I.W.Hamley *The Physics of Block Copolymers*; Sons, J.W.&, Ed.; Oxford University Press: Oxford, 1998;
 31. A.J.Müller, V. Balsamo, M.L.A. Crystallization in Block Copolymers with More than One Crystallizable Block. In *Springer: Progress in understanding of polymer crystallization*; Reiter G, S.G., Ed.; Berlin, 2007.
 32. R-M.Ho, P-Y.Hsieh, W-H.Tseng, C-C. Lin, B-H.Huang, B.L. No Title. *Macromolecules* 2003, 36, 9085.
 33. Wu, X.; Qiao, Y.; Yang, H.; Wang, J. Self-Assembly of a Series of Random Copolymers Bearing Amphiphilic Side Chains. *J. Colloid Interface Sci*. 2010, 349, 560–564, doi:10.1016/j.jcis.2010.05.093.
 34. Maglio, G.; Migliozzi, A.; Palumbo, R. Thermal Properties of Di- and Triblock Copolymers of Poly(L-Lactide) with Poly(Oxyethylene) or Poly(ϵ -Caprolactone). *Polymer (Guildf)*. 2002, 44, 369–375, doi:10.1016/S0032-3861(02)00764-4.

35. Hamley, I.W.; Castelletto, V.; Castillo, R. V.; Müller, A.J.; Martin, C.M.; Pollet, E.; Dubois, P. Crystallization in Poly(L-Lactide)-b-Poly(ϵ -Caprolactone) Double Crystalline Diblock Copolymers: A Study Using x-Ray Scattering, Differential Scanning Calorimetry, and Polarized Optical Microscopy. *Macromolecules* 2005, *38*, 463–472, doi:10.1021/ma0481499.
36. J.M. Huang, P.P. Chu, F.C.C. No Title. *Polymer (Guildf)*. 2000, *41*, 1741.
37. VAN KREVELEN, D.W. *Properties of Polymers*; Ed. Elsevi.; Amsterdam, 1990;
38. Lazzari, M. Liu, G. Lecommandoux, S. *Block Copolymers in Nanoscience*; Verlag GmbH & Co. KGaA, Ed.; Wiley-VCH.; Weinheim, 2006;
39. Jeon, O.; Lee, S.-H.; Kim, S.H.; Lee, Y.M.; Kim, Y.H. Synthesis and Characterization of Poly(l-Lactide)-Poly(ϵ -Caprolactone) Multiblock Copolymers. *Macromolecules* 2003, *36*, 5585–5592, doi:10.1021/ma034006v.
40. Jeon, O.; Lee, S.H.; Kim, S.H.; Lee, Y.M.; Kim, Y.H. Synthesis and Characterization of Poly(L-Lactide)-Poly(ϵ -Caprolactone) Multiblock Copolymers. *Macromolecules* 2003, *36*, 5585–5592, doi:10.1021/ma034006v.
41. Müller, A.J.; Albuérne, J.; Marquez, L.; Raquez, J.M.; Degée, P.; Dubois, P.; Hobbs, J.; Hamley, I.W. Self-Nucleation and Crystallization Kinetics of Double Crystalline Poly(p-Dioxanone)-b-Poly(ϵ -Caprolactone) Diblock Copolymers. *Faraday Discuss.* 2005, *128*, 231–252, doi:10.1039/b403085k.
42. Castillo, R.V.; Müller, A.J.; Raquez, J.M.; Dubois, P. Crystallization Kinetics and Morphology of Biodegradable Double Crystalline PLLA- b -PCL Diblock Copolymers. *Macromolecules* 2010, *43*, 4149–4160, doi:10.1021/ma100201g.
43. K. Chavalitpanya, S.P. Energy Procedia, 2013, *34* 542 – 548. *Energy Procedia* 2013, *34*, 542–548.
44. Michell, R.M.; Müller, A.J.; Spasova, M.; Dubois, P.; Burattini, S.; Greenland, B.W.; Hamley, I.W.; Hermida-Merino, D.; Cheval, N.; Fahmi, A. Crystallization and Stereocomplexation Behavior of Poly(D - And L -Lactide)-b-Poly(N,N-Dimethylamino-2-Ethyl Methacrylate) Block Copolymers. *J. Polym. Sci. Part B Polym. Phys.* 2011, *49*, 1397–1409, doi:10.1002/polb.22323.
45. Nakayama, Y.; Aihara, K.; Yamanishi, H.; Fukuoka, H.; Tanaka, R.; Cai, Z.; Shiono, T. Synthesis of Biodegradable Thermoplastic Elastomers from ϵ -Caprolactone and Lactide. *J. Polym. Sci. Part A Polym. Chem.* 2015, *53*, 489–495, doi:10.1002/pola.27463.
46. Navarro-Baena, I.; Sessini, V.; Dominici, F.; Torre, L.; Kenny, J.M.; Peponi, L. Design of Biodegradable Blends Based on PLA and PCL: From Morphological, Thermal and

- Mechanical Studies to Shape Memory Behavior. *Polym. Degrad. Stab.* 2016, *132*, 97–108, doi:10.1016/j.polymdegradstab.2016.03.037.
47. M. Drieskens, R. Peeters, J. Mullens, D. Franco, P.L. Structure versus Properties Relationship of Poly (Lactic Acid). I. Effect of Crystallinity on Barrier Properties. *J. Polym. Sci. Part B Polym. Phys.* 2009, *47*, 2247–2258.
48. Y. Byun, S. Whiteside, R. Thomas, M. Dharmam, J. Hughes, Y.T.K. No Title. *J. Appl. Polym. Sci.* 2012, *124*, 3577–3582.
49. R. Shogren No Title. *J. Environ. Polym. Degrad.* 1997, *5*, 91–95.
50. Tsuji, H.; Okino, R.; Daimon, H.; Fujie, K. Water Vapor Permeability of Poly(Lactide)s: Effects of Molecular Characteristics and Crystallinity. *J. Appl. Polym. Sci.* 2006, *99*, 2245–2252, doi:10.1002/app.22698.
51. Duan, Z.; Thomas, N.L. Water Vapour Permeability of Poly(Lactic Acid): Crystallinity and the Tortuous Path Model. *J. Appl. Phys.* 2014, *115*, doi:10.1063/1.4865168.
52. Ortenzi, M.A.; Basilissi, L.; Farina, H.; Di Silvestro, G.; Piergiovanni, L.; Mascheroni, E. Evaluation of Crystallinity and Gas Barrier Properties of Films Obtained from PLA Nanocomposites Synthesized via “in Situ” Polymerization of L-Lactide with Silane-Modified Nanosilica and Montmorillonite. *Eur. Polym. J.* 2015, *66*, 478–491, doi:10.1016/j.eurpolymj.2015.03.006.
53. S. Shankar, L-F. Wang, J.-W.R. No Title. *Mater. Sci. Eng.* 2018, *93*, 289–298.
54. H. Faraj, N. Follain, C.S. No Title. *Polym. Test.* 2022, *113*, 107683.

CHAPTER 3

Preparation and characterization of polymer blends based on poly (L-D-lactic acid), poly(ϵ -caprolactone) homopolymers and a poly (L-lactic acid-b- ϵ -caprolactone) diblock copolymer as compatibilizer agent

In this Chapter the use of PLLA-b-PCL diblock copolymer as compatibilizer agent to improve the compatibility between PLDA and PCL homopolymer blends has been evaluated. The investigation developed in this Chapter has taken advantage of the fact that PLLA block of PLLA-b-PCL diblock copolymer could be partially miscible with PLDA homopolymer while PCL block of this diblock copolymer is partially miscible with PCL homopolymer. For this purpose, PLDA-PCL polymer blends with two different ratios between components, 70:20 and 80:20, have been chosen taken into account their good final properties showed in Chapter 2. The effect of the PLLA-b-PCL diblock copolymer addition has been investigated to check an improvement of final properties of prepared PLLA-b-PCL/PLDA-PCL polymer blends if compare with PLDA homopolymer.

.

CHAPTER 3. Preparation and characterization of polymer blends based on poly (L-D-lactic acid), poly(ϵ -caprolactone) homopolymers and a poly (L-lactic acid-b- ϵ -caprolactone) diblock copolymer as compatibilizer agent

3.1. INTRODUCTION AND OBJECTIVES	103
3.2. MATERIALS AND METHODS	106
3.2.1. Materials	106
3.2.2. Experimental methods	107
3.2.2.1. Preparation of PLLA-b-PCL/PLDA-PCL polymer blends by solvent casting	107
3.2.2.2. Preparation of PLLA-b-PCL/PLDA-PCL polymer blends by spin coating	108
3.2.2.3. Preparation of PLLA-b-PCL/PLDA-PCL polymer blends by extrusion	108
3.2.3. Characterization techniques	109
3.2.3.1. Appearance, transparency and thickness of PLLA-b-PCL/PLDA-PCL polymer blend films	109
3.2.3.2. Differential scanning calorimetry (DSC)	109
3.2.3.3. Wide Angle X-ray diffraction (WAXS)	109
3.2.3.4. Thermogravimetric analysis (TGA)	110
3.2.3.5. Atomic force microscopy (AFM)	110
3.3. RESULTS AND DISCUSSION.....	110
3.3.1. <i>Appearance, transparency, and thickness of PLLA-b-PCL/ PLDA-PCL polymer blend films</i>	110
3.3.2. <i>Thermal properties of PLLA-b-PCL/PLDA-PCL polymer blends by DSC</i>	113
3.3.3. <i>Crystallinity of PLLA-b-PCL/PLDA-PCL polymer blend films by WAXS</i>	118
3.3.4. <i>Thermogravimetric analysis</i>	120
3.3.5. <i>Morphology of PLLA-b-PCL/PLDA-PCL polymer blend films by AFM</i>	123
3.3.6. <i>Oxygen and water vapour barrier properties of PLLA-b-PCL/PLDA-PCL polymer blend films</i>	126
3.4. CONCLUSIONS	129
3.5. REFERENCES	131

3.1. INTRODUCTION AND OBJECTIVES

Biodegradable polymers are well known in the actual state of the art due to their environmental advantages and versatility. As part of the family of biodegradable polyesters, PLA is the most attractive due to its properties and ease production. As it has been described in the previous Chapters, PLDA, the most used enantiomer of PLA at industrial level, has many useful properties such as biodegradability, biocompatibility, and a non toxicity, which, as well with relatively low processing costs and desirable mechanical properties PLA makes it an attractive polymeric material for the polymer industry.

The use of PLDA is limited due to some shortcomings as its high brittleness, low elongation at break, poor processability by conventional thermoplastics processing techniques and inadequate mechanical properties for certain applications which require toughness. Therefore, there is a need to improve physico-mechanical PLDA properties. In this direction, many attempts have been made to develop new polymeric materials based on PLA with improved properties. However, the solutions found to date are still unsatisfactory since the improvement always requires an addition or mixture with another polymer and/or additive making the final product more expensive or in most of the cases is observed a decrease in other properties.

In Chapter 1, the miscibility of polymer blends based on PLDA and PCL homopolymers has been studied and the results showed that both homopolymers are immiscible. In Chapter 2 a PLLA-b-PCL diblock copolymer has been used to introduce PCL block on PLDA polymer matrix by polymer blending. Such PCL block of the diblock copolymer has been microphase separated from PLDA matrix leading to PLDA based nanostructured materials with enhanced properties. Successful results achieved in Chapter 2 provoke the interest in study the effect of the use of the PLLA-b-PCL diblock copolymer for improving compatibility between immiscible PLDA-PCL polymer blends.

Several authors have been study blending technology to improve PLA homopolymer properties, *Nofar et al.* [1] presented an exhaustive review about the different polymer blends which have been develop by blending PLA with different polymers, including binary blends with biopolymers (biodegradable and non-biodegradable), biobased polymers and conventional polymers. Moreover, ternary polymer blends and nanocomposites blends have been investigated looking for understand the effect of the polymer composition, the

processing technologies, and the morphology on the final properties of the developed blends. Figure 3.1. showed the different types of research works carried out during the last two decades as a function of the blend typologies.

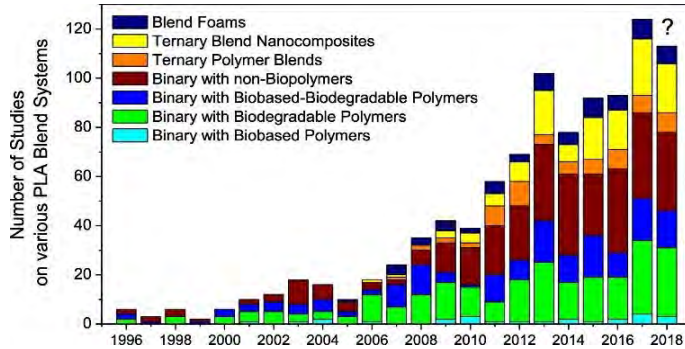


Figure 3.1. Reported studies on PLA based blends. (Source Reference [2]).

Same authors analyse the rate of the numbers of research which have been done for binary blends based on PLA blending with biodegradable and non-biodegradable biobased polymers.

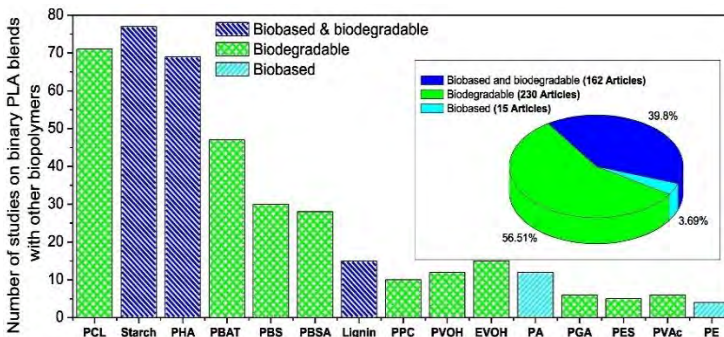


Figure 3.2. Studies carried out with PLA and other biopolymers. (Source Reference [2]).

Figure 3.2. showed that PCL is one of the most studied biodegradable polymers to be blend with PLA in order to improve its final properties, such as high toughness and because of ductility that brings to PLA [3]. Other authors have been study such blending technology to improve PLA homopolymer properties, such as *Berthe et al.* [4] and *Liang et al.* [5] who worked on the mixture of extruded blends of PLA and PCL with the aim of improving PLA water vapour permeability. However, the use of mixtures generally implies disadvantages or is subject to limitations of use. Blends of PLA with other thermoplastics like PCL must be prepared at high temperatures to ensure good homogenization of the mixture before blending. On the one hand, this limits the type of thermoplastics which can be combined with PLA and, on the other

hand, requires temperature control since as showed in the Chapter 1 and Chapter 2, the T_{deg} of PLDA is started at ~ 180 °C. Moreover, the results obtained in Chapter 1 proved that PLDA-PCL polymer blends are immiscible, consequently the used of compatibilizer seems to be interesting alternative.

Several works have been reported on the determination of the compatibilization between PCL and PLA polymer blend components. *Esmailzadeh et al.* [6] observed biphasic region for PLA-PCL polymeric blends from SEM images (see Figure 3.3) indicating the immiscibility between PCL phase and PLA matrix. *Wu et al.* [7] have also reported the immiscibility PLA-PCL polymer blends and the utility of the use of compatibilizers agents.

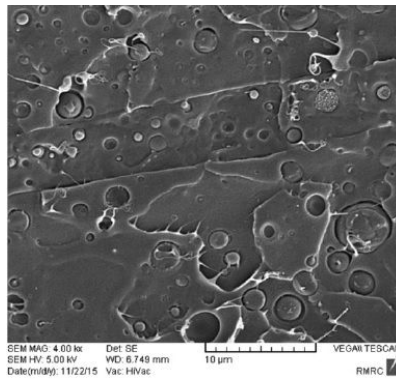


Figure 3.3. SEM micrographs of cryogenically fractured surface of an immiscible PLA-PCL polymer blend showing the *island effect*. (Source Reference [6])

Matta et al. [8] studied PLA-PCL blends with different ratio between components prepared by melt blending. Obtained different PLA-PCL polymer blends showed an increase of elongation at break and impact toughness but a decrease in strength and modulus. Such results corroborated that a full miscibility was not achieved in these polymer blends, which was confirmed by the fact that PLA-PCL polymer blends showed two T_g s at the same temperature as polymer blend components. *Cock et al.* [9] presented similar behaviour for PLA-PCL polymer blends obtained by melt blending. Nevertheless, they also observed the effect of the addition of PCL on the final crystallinity, and the results were similar to those observed for PLLA-b-PCL/PLDA polymer blends described in Chapter 2.

Another way to improve the PLA properties has been through the development of nanocomposites, with the aim of improving both the mechanical properties and the barrier properties to the OTR and the WVTR if compare with the neat PLA. However, the objective of

this research work was the preparation of polymeric materials based on PLDA with food safety and future quick industrialization avoiding the use of nanoparticles to reduce the industrialization drawbacks caused by nanoparticles uses.

As pointed out by many authors, one of effective way to improve final properties of PLA/PCL polymer blends is the use of the compatibilizer agents. In this research field, *Chien-Chung et al.* [10] studied the use of two different surfactants: both different copolymers based, one on poly (ethylene oxide) (PEO) and the other one on poly (propylene oxide) (PPO) to improve PLA toughness without losing the strength of neat PLDA. Authors reported that the elongation at break values of the blends of PLA-PCL with surfactants increased after adding both surfactants, however simultaneously the mechanical properties of these polymer blends became lower. Thus, follow the actual state of art [11], [12], [13] and [14] one can concluded that there is a need of looking for compatibilizer agents to improve the miscibility between component of PLA-PCL polymer blends to take advantages of both homopolymers properties and to solve the main PLA weakness just to obtain polymeric material based on PLDA as a reference polymer to be used for packaging applications among others.

The aim of this Chapter is to analyse the use of a PLLA-b-PCL diblock copolymer as a compatibilizer agent for polymer blends consist of PLDA and PCL. The compatibility of the PLLA-d-PCL diblock copolymer with the PLDA homopolymer matrix and its benefits on mechanical, barrier and thermal properties was demonstrated in Chapter 2. The main goal of this Chapter is to obtain polymer blends using PLLA-b-PCL diblock copolymer which is able to act as nanostructuring agent but also as compatibilizer agent since PLLA block of DBC is partially miscible with PLDA and PCL block of DBC is partially miscible with PCL. The supposed effect of compatibilization will be study for two specific PLDA-PCL polymer blends with the ratio of 80:20 and 70:30 with different DBC content from 1 wt% to 10 wt%.

3.2. MATERIALS AND METHODS

3.2.1. Materials

In this investigated work, the PLDA and PCL described in more details in Chapter 1, Section 1.2 were used. Moreover, PLLA-b-PCL diblock copolymer detailed in Chapter 2, Section 2.2 was also used as compatibilizer agent.

3.2.2. Experimental methods

Results obtained in Chapter 2 showed that PLLA-b-PCL/PLDA polymer blend films with 20 wt% and 30 wt% of PLLA-b-PCL diblock copolymer presented the best results in terms of processability, thermal and barrier properties. Both weight ratios, 70:30 and 80:20 were selected to be used as a reference for preparation of PLDA-PCL polymer blends modified with PLLA-b-PCL as compatibilizer agent. Different PLLA-b-PCL/PLDA-PCL polymer blends were prepared by varying the PLLA-b-PCL diblock copolymer content in the selected PLDA-PCL polymer blends. The contents varied from 1 wt% to 10 wt% of DBC as it is shown in Table 3.1.

Methods for preparing the different PLLA-b-PCL/PLDA-PCL polymer ternary blends were solvent casting, spin coating and extrusion. All polymer ternary blends were prepared at laboratory scale.

3.2.2.1. Preparation of PLLA-b-PCL/PLDA-PCL polymer blends by solvent casting

PLLA-b-PCL/PLDA-PCL polymer blends were prepared by dissolving 4 wt% of each polymer in chloroform under stirring (100 rpm) at 40 °C and 3.5 h. First, PLDA homopolymer and PCL homopolymer solutions were prepared. Then, a mixture of PLDA and PCL homopolymers with the weight ratio of 80:20 and 70:30, respectively, were prepared. After that, a solution of DBC of 10 g was prepared by dissolving the PLLA-b-PCL diblock copolymer in chloroform in the same conditions and then, the different amounts of DBC were added to the mixture of PLDA-PCL obtaining the final ternary polymer blends. Table 3.1. showed the different compositions of the PLLA-b-PCL / PLDA-PCL ternary blends.

Sample name	PLDA (wt%)	PCL (wt%)	PLLA-b-PCL (wt%)
Neat PLDA-PCL 70:30	70	30	-
PLLA-b-PCL/PLDA-PCL 70:30:1	69.3	29.7	1
PLLA-b-PCL/PLDA-PCL 70:30:3	67.9	29.1	3
PLLA-b-PCL/PLDA-PCL 70:30:5	66.5	28.5	5
PLLA-b-PCL/PLDA-PCL 70:30:7	65.1	27.9	7
PLLA-b-PCL/PLDA-PCL 70:30:10	63	27	10
Neat PLDA-PCL 80:20	80	20	-
PLLA-b-PCL/PLDA-PCL 80:20:1	79.2	19.8	1
PLLA-b-PCL/PLDA-PCL 80:20:3	77.6	19.4	3

PLLA-b-PCL/PLDA-PCL 80:20:5	76.0	19.0	5
PLLA-b-PCL/PLDA-PCL 80:20:7	74.4	18.6	7
PLLA-b-PCL/PLDA-PCL 80:20:10	72.0	18.0	10

Each mixture of PLLA-b-PCL/PLDA-PCL polymer blends was stirring at temperature of 25 °C until their final homogenization (~30 min). The solution was completely transparent. As in the previous Chapters, a non-selective solvent has been chosen to be use for all polymer blend components (PLDA, PCL and DBC). Moreover, as describe in more details in Chapter 2, chloroform was used, based on the calculation of the polymer-solvent interaction parameter.

Then, 5 mL of each solution mixture was cast onto Petri dishes and dried following protocol 2 explained in Chapter 1, Section 1.2.2.1.

Obtained PLLA-b-PCL/PLDA-PCL polymer blends films were stored in a silica gel desiccator during 24 h before being tested.

3.2.2.2. Preparation of PLLA-b-PCL/PLDA-PCL polymer blends by spin coating

PLLA-b-PCL/PLDA-PCL polymer blend films were spin coated using a P6700 spin-coater from Cookson Electronics. These films were prepared from a solution of chloroform at concentration 1 wt%. An amount of 20 μ L of each sample were coated onto a glass support, and the spin-coater cycle program was as follows: 1.000 rpm for 60 s and 4.000 rpm for 20 s. Residual chloroform was removed by evaporation at room temperature. As for polymer blend films prepared by solvent casting, films were stored in a silica gel desiccator during 24 h before the measurements.

3.2.2.3. Preparation of PLLA-b-PCL/PLDA-PCL polymer blends by extrusion

PLLA-b-PCL/PLDA-PCL polymer blend films were fabricated also by extrusion at laboratory scale. Previously to the processing step, PLDA and PCL homopolymers and PLLA-b-PCL diblock copolymer were dried in different conditions. The PLDA homopolymer and PLLA-b-PCL was dried in the same conditions describe in the Chapter 2, Section 2.2.2.3. while the PCL homopolymer was dried in the same condition as PLLA-b-PCL diblock copolymer.

To prepare the extruded mixtures, the different amounts of PLLA-b-PCL, PLDA and PCL were weighted and pre-mixed, then the mixtures were processed in a twin screw mini-extruder Micro 15 cc Twin Screw Compounder, (DSM Xplore). The processing conditions as well as the

variables to control PLLA-b-PCL/PLDA-PCL polymer blend films thickness are described in detail in Chapter 2, Section 2.2.2.3.

3.2.3. Characterization techniques

3.2.3.1. Appearance, transparency and thickness of PLLA-b-PCL/PLDA-PCL polymer blend films

The thicknesses of PLLA-b-PCL/PLDA-PCL polymer blend films obtained by solvent casting were measured using a micrometer (Mitutoyo) with a sensitivity of $\pm 2 \mu\text{m}$. The thickness was calculated as average value of measurements taken at five different locations on each film sample as it has been explained in Chapter 2, Section 2.2.3.3.

The appearance of solvent casted polymer blend films was visual analysed observing the solutions transparency before blending and in the final polymer blend films.

Transparency measurements of prepared polymer blend films were carried out on a UV-Vis-V-630 spectrophotometer described in more details in Chapter 2, Section 2.2.3.3.

3.2.3.2. Differential scanning calorimetry (DSC)

DSC was performed using a DSC Q 2000 from TA Instruments Inc. equipped with an autosampler. Nitrogen was used as purge gas (20 mL/min). DSC technique was used to determine the thermal transitions of PLLA-b-PCL/PLDA-PCL polymer blends. DSC measurement was performed with the heating/cooling scan rate equal to $10^\circ\text{C}/\text{min}$ in the temperature range was from -90°C to 250°C . The T_g , T_{cc} , T_c and T_m were calculated in the same way as describe in Chapter 2, Section 2.2.3.2.

T_{cc} and T_m were determined from heating scans while T_c was determined from the cooling scans. To avoid thermal history, the samples were heated above the melting temperature of polymer blend components priori to each measurement.

3.2.3.3. Wide Angle X-ray diffraction (WAXS)

WAXS analysis of PLLA-b-PCL/PLDA-PCL polymer blend films were performed using a Bruker AXS D5005 diffractometer equipped with Cu hollow cathode ($\lambda = 0.154 \text{ nm}$) and an oscillation detector. The WAXS spectra were measured from 10° to 25° (2θ) at a scan rate of $0.02^\circ/\text{min}$.

3.2.3.4. Thermogravimetical analysis (TGA)

TGA analyses of PLLA-b-PCL/PLDA-PCL polymer blend films were carried out using a TGA Q5000 from TA Instruments Inc. described in more details in Chapter 2, Section 2.2.3.6. The TGA data were plotted as the weight percentage loss versus temperature.

3.2.3.5. Atomic force microscopy (AFM)

The morphology of the investigated PLLA-b-PCL/PLDA-PCL polymer blend films was studied using AFM. AFM images were achieved by operating in tapping mode with a scanning probe microscope (Nanoscope IIIa, Multimode™ from Veeco) equipped with an integrated silicon tip/cantilever with a resonance frequency of ~ 300kHz from the same manufacturer. Height and phase images were obtained under ambient conditions with typical scan speeds of 0.8 - 1.6 line/s, using a scanner head with a maximum range of 16 µm x 16 µm. For analysis of the observed surface structures, Nanoscope image processing software was used.

3.2.3.6. Oxygen and water vapour permeability measurements (OTR and WVTR)

Permeability of PLLA-b-PCL/PLDA-PCL polymer blend films obtained by extrusion cast was tested. The OTR of investigated PLLA-b-PCL/PLDA-PCL polymer blend films was measured according to ASTM standard method D3985 using an OX-TRAN 2/21 ST (Mocon, Inc.).

The WVTR was measured according to ASTM F-1249 using a Permatran W 3/33 SG+ module (Mocon, Inc.). The OTR and the WVTR measurement conditions are described in detail in Chapter 2, Section 2.2.3.7.

3.3. RESULTS AND DISCUSSION

3.3.1. Appearance, transparency, and thickness of PLLA-b-PCL/PLDA-PCL polymer blend films

The appearance of the solutions before cast onto the Petri dishes was transparent and once the polymer blend films were formed remained transparent. The transparency of each investigated polymer blend films is shown in Figure 3.4.

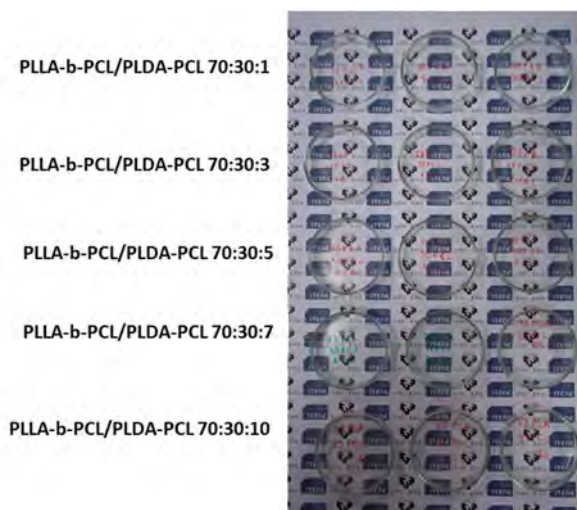


Figure 3.4. Digital images of transparency of solvent casted PLLA-b-PCL/PLDA-PCL 70:30 polymer blend films.

As it was described in Chapter 2, Section 2.2.3.1., the thickness of the polymer blend films was measured using a micrometer and calculated as an average value of measurements taken at five different points on each film sample as it is shown in Scheme 2.1 of Chapter 2. The average of the centered point was determined separately to the other measurements points.

Table 3.2. summarized the average thickness of solvent casted PLLA-b-PCL/PLDA-PCL 70:30 polymer blend films and Table 3.3. those corresponding to PLLA-b-PCL/PLDA-PCL 80:20 polymer blend films.

Table 3.2. Thickness of solvent casted PLLA-b-PCL/PLDA-PCL 70:30 polymer blend films measurements.		
Samples name	Thickness (mm)*	Centered point (mm)
PLDA-PCL 70:30	145 ± 9	147 ± 14
PLLA-b-PCL/PLDA-PCL 70:30:1	131 ± 10	148 ± 10
PLLA-b-PCL/PLDA-PCL 70:30:3	153 ± 10	156 ± 10
PLLA-b-PCL/PLDA-PCL 70:30:5	149 ± 7	140 ± 13
PLLA-b-PCL/PLDA-PCL 70:30:7	144 ± 10	145 ± 7
PLLA-b-PCL/PLDA-PCL 70:30:10	150 ± 6	152 ± 8

Table 3.3. Thickness of solvent casted PLLA-b-PCL/PLDA-PCL 80:20 polymer blend films measurements.

Samples name	Thickness (mm)*	Centered point (mm)
PLDA-PCL 80:20	148 ± 13	152 ± 14
PLLA-b-PCL/PLDA-PCL 80:20:1	133 ± 12	137 ± 17
PLLA-b-PCL/PLDA-PCL 80:20:3	135 ± 10	137 ± 2
PLLA-b-PCL/PLDA-PCL 80:20:5	138 ± 17	142 ± 3
PLLA-b-PCL/PLDA-PCL 80:20:7	137 ± 2	137 ± 7
PLLA-b-PCL/PLDA-PCL 80:20:10	133 ± 2	140 ± 6

Obtained thickness results indicated that the solvent casted polymer blend films had a non-homogeneous thickness. The thickness of the different polymer blend films was quite dispersed and there was a difference between the centered point and the measurements in the other points of the films. This dispersion can be related to the drying process of the PLLA-b-PCL/PLDA-PCL polymer blend films prepared by three different preparation techniques. On the one hand, the solvent evaporation process which drive the vitrification of the polymeric chains and the films formation can have effect. On the other hand, the phase separation between the polymer blend components (PLDA, PCL and PLLA-b-PCL) and finally, the compatibility or miscibility between the block of PLLA-b-PCL diblock copolymer with adequate homopolymer, PCL or PLDA, respectively.

Generally, the thickness values of polymer blend films prepared by solvent casting were between 130 μm -150 μm . The thickness of extruded PLLA-b-PCL/PLDA-PCL polymer blend films was controlled by adjusting extruder parameters and the final average thickness of each extruded ternary polymer blend films was around 160 μm .

As for PLLA-b-PCL/PLDA polymer blend films, UV-Vis measurements were carried out to determine the transmittance of PLLA-b-PCL/PLDA-PCL polymer blend films. Important to mentioned that the transmittance values of these ternary polymer blend films were compared with the transmittance values of binary polymer blends of PLDA-PCL 80:20 and PLDA-PCL 70:30. In Chapter 2, Section 2.3.2 the transmittance values of neat PLDA and PCL homopolymers were determined and as comparison those dates were also incorporated in Table 3.4 and Table 3.5. The transmittance values were taken at 600 nm. A slight reduction of the light transmission of PLDA-PCL 70:30 polymer blends was detected if compared with the light transmission of neat PLDA and also PLDA-PCL 80:20 polymer blends. This can be caused by the increases of the PCL content in these polymer blends. In both formulations, the addition

of DBC resulted in decrease of the transparency with the increase of DBC content in of PLLA-b-PCL/PLDA-PCL polymer blend films.

Table 3.4. Transmittance values of solvent casted PLLA-b-PCL/PLDA-PCL 70:30 polymer blend films.

Sample name	Transmittance (%)
Neat PLDA	99
PLDA -PCL 70:30	90
PLLA-b-PCL/PLDA-PCL 70:30:1	90
PLLA-b-PCL/PLDA-PCL 70:30:3	89
PLLA-b-PCL/PLDA-PCL 70:30:5	89
PLLA-b-PCL/PLDA-PCL 70:30:7	87
PLLA-b-PCL/PLDA-PCL 70:30:10	87
Neat PCL	84

Table 3.5. Transmittance values of solvent casted PLLA-b-PCL/PLDA-PCL 80:20 polymer blend films.

Sample name	Transmittance (%)
Neat PLDA	99
PLDA -PCL 80:20	92
PLLA-b-PCL/PLDA-PCL 80:20:1	92
PLLA-b-PCL/PLDA-PCL 80:20:3	92
PLLA-b-PCL/PLDA-PCL 80:20:5	90
PLLA-b-PCL/PLDA-PCL 80:20:7	90
PLLA-b-PCL/PLDA-PCL 80:20:10	90
Neat PCL	84

3.3.2. Thermal properties of PLLA-b-PCL/PLDA-PCL polymer blends by DSC

In this study, ternary polymer blends based on two different PLDA-PCL homopolymer blends with weight ratio 70:30 and 80:20 modified with different DBC content (from 1wt% to 7 wt% for PLLA-b-PCL/PLDA-PCL 70:30 polymer blends and from 1 wt% to 10 wt for PLLA-b-PCL/PLDA-PCL 80:20 polymer blends) were deeply analysed.

2nd heating scan of DSC measurement was taken into account. Figure 3.5. showed DSC thermograms for PLLA-b-PCL/PLDA-PCL 70:30 polymer blend films and Table 3.6. summarized the thermal transition temperature values as well as thermal transition enthalpies and degree

of crystallinity. Figure 3.6. and Table 3.7. showed the same date for PLLA-b-PCL/PLDA-PCL 80:20 polymer blend films.

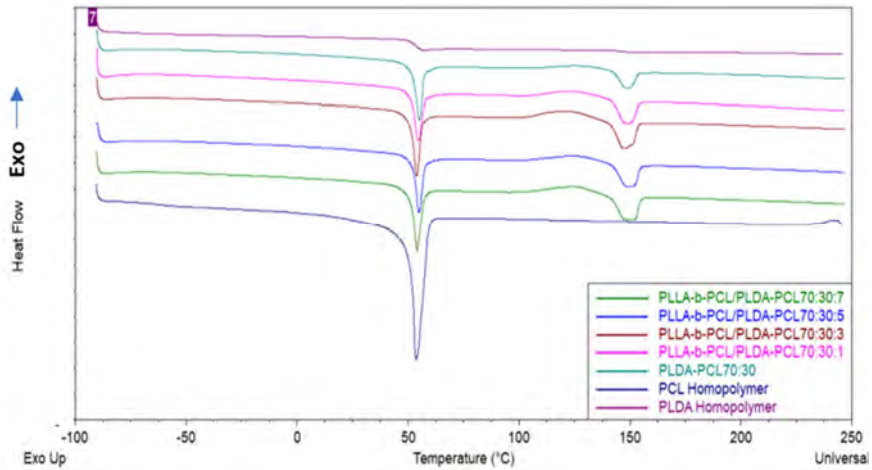


Figure 3.5. DSC thermograms of PLLA-b-PCL/PLDA-PCL 70:30 polymer blend films with different DBC content. The DSC thermograms of PLDA and PCL homopolymers were added for comparison.

Table 3.6. Thermal transitions of PLLA-b-PCL/PLDA-PCL 70:30 polymer blend films with different DBC content.

Sample names	PLLA block/PLDA						PCL block/PCL		
	T _g (°C)	T _{cc} (°C)	ΔH _c (J/mol)	T _m (°C)	ΔH _m (J/mol)	X _c (%)	T _g (°C)	T _m (°C)	ΔH _m (J/mol)
Neat PLDA	53	130	0.5	152	0.6	0.15	-	-	-
Neat PCL	-	-	-	-	-	-	-63	54	76.1
PLDA-PCL 70:30	-	128	3.9	148	7.3	3.74	-	55	18.0
PLLA-b-PCL/PLDA-PCL 70:30:1	-	125	6.8	148	10.9	4.38	-	55	17.7
PLLA-b-PCL/PLDA-PCL 70:30:3	-	123	10.7	148	13.4	2.96	-	54	18.6
PLLA-b-PCL/PLDA-PCL 70:30:5	-	127	7.6	149	11.2	3.88	-	55	18.5
PLLA-b-PCL/PLDA-PCL 70:30:7	-	126	9.4	148	12.9	3.70	-	54	21

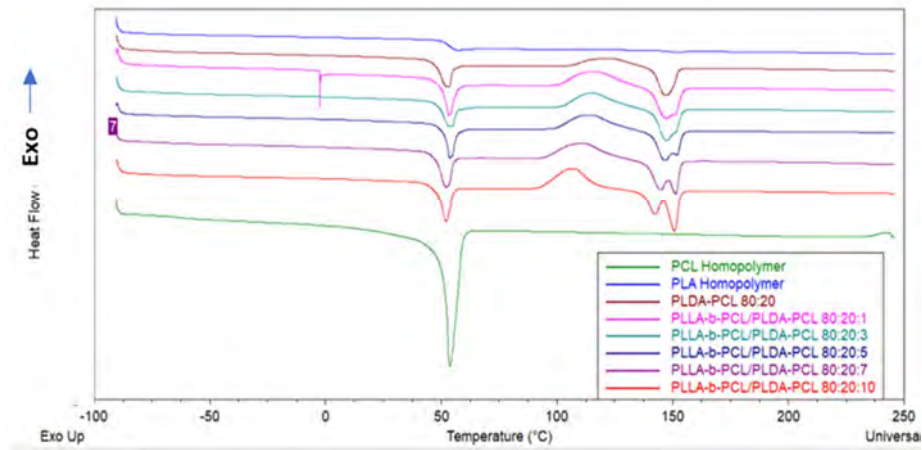


Figure 3.6. DSC thermograms of PLLA-b-PCL/PLDA-PCL 80:20 polymer blend films with different DBC content. The DSC thermograms of PLDA and PCL homopolymers were added for comparison.

Table 3.7. Thermal transitions of PLLA-b-PCL/PLDA-PCL 80:20 polymer blend films with different DBC content.

Sample names	PLDA+ PLLA block						PCL block		
	T_g (°C)	T_{cc} (°C)	ΔH_c (J/mol)	T_m (°C)	ΔH_m (J/mol)	X_c (%)	T_g (°C)	T_m (°C)	ΔH_m (J/mol)
Neat PLDA	53	130	0.5	152	0.65	0.15	-	-	-
Neat PCL	-	-	-	-	-	-	-63	54	76.1
PLDA-PCL 80:20	-	122	9.3	147	13.05	4	-	52	10.9
PLLA-b-PCL/PLDA-PCL 80:20:1	-	117	17	147	19.33	2.51	-	53	11.6
PLLA-b-PCL/PLDA-PCL 80:20:3	-	116	15.39	147	18.19	3.12	-	53	10.9
PLLA-b-PCL/PLDA-PCL 80:20:5	-	115	16.6	146/152	18.99	2.57	-	54	12.2
PLLA-b-PCL/PLDA-PCL 80:20:7	-	112	17.7	145/151	22.25	4.86	-	52	13.8
PLLA-b-PCL/PLDA-PCL 80:20:10	-	108	21.1	142/151	21.53	0.44	-	52	13.8

As can be deduced from obtained DSC results, the behaviour of both polymer blends was different. In the case of PLLA-b-PCL/PLDA-PCL 70:30 polymer blends, the influence of the

diblock copolymer was not significant. The PLDA-PCL 70:30 binary blend showed a slight decrease of the T_{cc} and an increase of the X_c value compared with correspond values for neat PLDA indicating that the crystallization of the blend was changed. The addition of different DBC content into the PLDA-PCL 70:30 binary blend did not provoke the same effect. In addition, the T_m s of both PLDA and PCL rich phase of PLDA-PCL 70:30 polymer blends remained at the same temperature as for PLDA and PCL homopolymers. The same behaviour possessed PLLA-b-PCL/PLDA-PCL 70:30 ternary polymer blends with different DBC content. The insignificant effect of the addition of DBC content on the changes in the T_m of each separated phase is probably due to the high PCL homopolymer content in the ternary polymer blends.

On the contrary, for PLLA-b-PCL/PLDA-PCL 80:20 ternary polymer blends several trends can be clearly observed. The increase of the DBC content led to a decrease of the T_{cc} being 122 °C for PLDA-PCL 80:20 binary polymer blends and 108 °C for PLLA-b-PCL/PLDA-PCL 80:20 ternary polymer blend with 10 wt% of DBC contents. This shift can indicate that the PLLA-b-PCL diblock copolymer encourages cold crystallization of the PLLA-b-PCL/PLDA-PCL 80:20 ternary polymer blends, forming increasingly crystallinity, given that the cold crystallization peaks were increasingly more defined and narrower and shifted towards low temperature as was reported by several authors who studied the cold crystallization kinetics adding different nucleating agents to PLA polymers such as *Battegazzore et al.* [15] and *Henricks et al.* [16].

This effect was significantly influenced by the addition of different DBC content and was different if compared to PLDA-PCL 80:20 binary polymer blend and PLDA homopolymer. A sudden change in the crystallinity of neat PLDA homopolymer was observed, leading to conclusion that the homopolymer prepared by the same processes was practically amorphous. Thus, any crystallization and melting transition was detected under employed DSC measurement conditions. These properties changed considerably after blending with neat PCL homopolymer, consequently strong effect of PCL addition was also observed in ternary polymer blends affecting properties of prepared blends if compared to neat PLDA homopolymer.

Regarding melting transition of PLLA block/PLDA matrix, two T_m s appeared for PLLA-b-PCL/PLDA-PCL 80:20 polymer blends if compared with one T_m for PLDA-PCL 80:20 polymer blend. The first T_m corresponded to the T_m of the PLDA homopolymer and the second one to the T_m of PLLA block of the PLLA-b-PCL diblock copolymer. In the case of the T_m of PCL, very defined peaks were observed, without the appearance of a second T_m corresponding to PCL

block, suggesting possible miscibility between PCL homopolymer and the PCL block of PLLA-b-PCL diblock copolymer or due to the low amount of PCL block in the final PLLA-b-PCL/PLDA-PCL polymer blend.

X_c of each sample was studied based on DSC results and was calculated for each block of the PLLA-b-PCL using the Equation 2.1, explained in more details in Chapter 2, Section 2.3.1.2.

This equation has been used by *Cock et al.* [9]. Authors reported that X_c depends strongly on values corresponding to post-melt crystallization (the crystallinity analysed from the cooling process), or cold crystallization ΔH_{cc} (the crystallinity analysed from the heating process). In this work the total crystallinity of PLDA was assumed and the total crystallinity corresponding to PLLA block of PLLA-b-PCL diblock copolymer was also assumed in Equation 3.1 where is explained how it was calculated the total value of enthalpy of melting transition for extracting crystallinity of semi-crystalline polymers.

$$\Delta H = \Delta H_m - \Delta H_{cc} \text{ Equation 3. 1.}$$

Theoretical enthalpy values for ΔH_m^0 of PLDA and PCL extracted from the literature were 93 J/g [17] and 156.8 J/g [18], respectively.

First, it is necessary the calculation of the weight content of each block in PLLA-b-PCL/PLDA-PCL polymer blend films according to the composition. The M_n of the PLLA-b-PCL diblock copolymer and each block as well as PDI was taken from Table 1.4, Chapter 1, Section 1.3.1.2. In Table 3.8 the wt% of each segment block is summarized.

Table 3.8. Weight content of each block of PLLA-b-PCL diblock copolymer in PLLA-b-PCL/PLDA-PCL polymer blend films.		
Sample name	PLLA (wt %)	PCL (wt%)
PLLA-b-PCL/PLDA-PCL 70:30:1	0.67	0.33
PLLA-b-PCL/PLDA-PCL 70:30:3	2.00	1.00
PLLA-b-PCL/PLDA-PCL 70:30:5	3.33	1.67
PLLA-b-PCL/PLDA-PCL 70:30:7	4.67	2.33
PLLA-b-PCL/PLDA-PCL 80:20:1	0.67	0.33
PLLA-b-PCL/PLDA-PCL 80:20:3	2.00	1.00
PLLA-b-PCL/PLDA-PCL 80:20:5	3.33	1.67
PLLA-b-PCL/PLDA-PCL 80:20:7	4.67	2.33
PLLA-b-PCL/PLDA-PCL 80:20:10	6.67	3.33

Once the compositions and the weight contribution of each segment block was calculated, it was possible to calculate the contribution of the crystallinity of each block in the correspondent PLLA-b-PCL/PLDA-PCL 70:30 and 80:20 polymer blends. Table 3.9 shows the calculated contribution of correspondent χ_c of each block of diblock copolymer in PLLA-b-PCL/PLDA-PCL 80:20 polymer blend films with different DBC content, which addition caused an effect on thermal transitions.

Table 3.9. Degree of crystallinity of each block in PLLA-b-PCL/PLDA-PCL polymer blend films.

Sample name	PLLA (wt %)	PCL (wt%)	X_{PLLA} (%)	X_{PCL} (%)
PLLA-b-PCL/PLDA-PCL 80:20:1	0.67	0.33	0.084	0.022
PLLA-b-PCL/PLDA-PCL 80:20:3	2.00	1.00	0.302	0.073
PLLA-b-PCL/PLDA-PCL 80:20:5	3.33	1.67	0.541	0.135
PLLA-b-PCL/PLDA-PCL 80:20:7	4.67	2.33	0.855	0.162
PLLA-b-PCL/PLDA-PCL 80:20:10	6.67	3.33	1.299	0.247

From results summarized in Table 3.9. higher contribution came from PLDA block of PLLA-b-PCL diblock copolymer. But it is observed that as increases DBC in the polymer blend increases χ_c . Both homopolymer are semi-crystalline polymer and thus a high χ_c was expected. On the contrary, authors like as *Cock et al.* [9] observed that the degree of crystallinity of PCL block of used in similar PLLA-b-PCL diblock copolymers was around 44.5 % compared with the degree of PLDA that was around 30 %.

3.3.3. Crystallinity of PLLA-b-PCL/PLDA-PCL polymer blend films by WAXS

WAXS technique was used to analyse the crystallinity of investigated PLLA-b-PCL/PLDA-PCL polymer blend films. Such technique together with DSC allow to study the crystallinity of the polymer blend films without any treatment like heating. The WAXS results reflect the real behaviour of the polymer blend films during their shelf-life and as was explained in Chapter 2 have a direct impact on the final barrier properties of investigated polymer blend films. WAXS of PLLA-b-PCL/PLDA-PCL 70:30 and 80:20 polymer blend films with different DBC content are shown in Figure 3.7 and Figure 3.8, respectively.

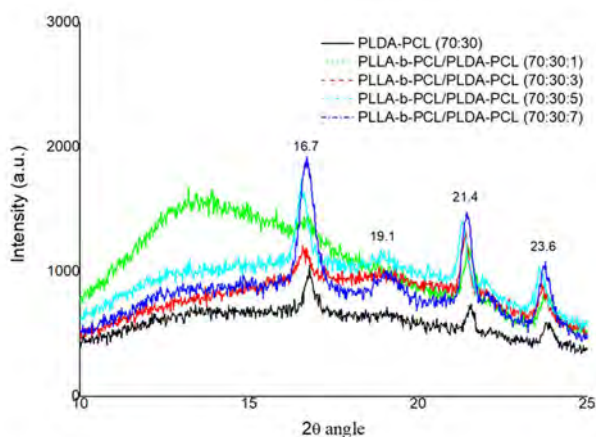


Figure 3.7. WAXS spectra of PLLA-b-PCL/PLDA-PCL 70:30 polymer blend films with different DBC content.

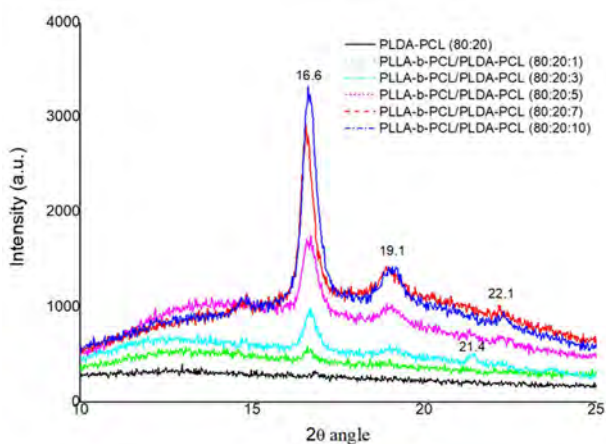


Figure 3.8. WAXS spectra of PLLA-b-PCL/PLDA-PCL 80:20 polymer blend films with different DBC content.

If compare the WAXS spectra of PLDA-PCL 80:20 polymer blend film with WAXS spectra of PLDA-PCL 70:30 polymer blend film, one can easily deduced that polymer blends with weight ratio 80:20 showed lower crystallinity if compare with polymer blends with weight ratio 70:30. As expected taken into account the PCL content in PLDA-PCL polymer blends, the addition of DBC into this polymer blends led to increase of the crystallinity of PLLA-b-PCL/PLDA-PCL polymer blends. Moreover, a part of strong increased of the intensity of the peaks, the increase of the DBC content resulted in the detection of additional peak.

Similarly, to values obtained in Chapter 2, the first peak at 2θ equal to 16.6° and 16.7° for PLDA-PCL 80:20 and PLDA-PCL 70:30 polymer blends, respectively, was close to the expected position for the α -form of PLLA crystals sets of (113) and (203) reflections at 17° . Also peaks at 19° were related to the formation of other type of PLLA crystals. *Carmona et al.* [19] reported that the PCL characteristics peaks at 2θ equal to 21.5° , 21.8° , and 23.7° corresponding to the (110), (111), and (200) plane reflections of the characteristic pattern of PCL crystalline structure, respectively.

PLLA-b-PCL/PLDA-PCL 70:30 showed those peaks at 21.4° and 23.6° and PLLA-b-PCL/PLDA-PCL 80:20 showed the last peak a slight shifted to lower values 22.1° instead of 23.6° this could be because of DBC into PLDA-PCL blends act as compatibilizer agent.

3.3.4. Thermogravimetric analysis

TGA curves of PLLA-b-PCL/PLDA-PCL 70:30 and 80:20 polymer blend films with different DBC content are presented in Figure 3.9 and Figure 3.10, respectively.

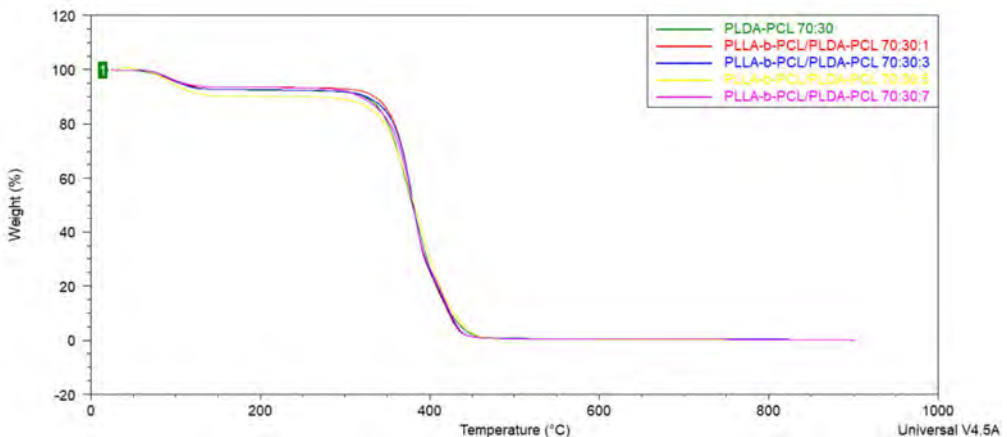


Figure 3.9. TGA curves of PLLA-b-PCL/PLDA-PCL 70:30 polymer blends films with different DBC content.

As can be clearly seen from TGA results reported in Figure 3.9 and Figure 3.10, both series of PLLA-b-PCL/PLDA-PCL polymer blends possessed three degradation steps. The first one related to the residual solvent evaporation, the second corresponding to degradation process of PLLA block/PLDA matrix and the third one to degradation of PCL block/PCL rich phase.

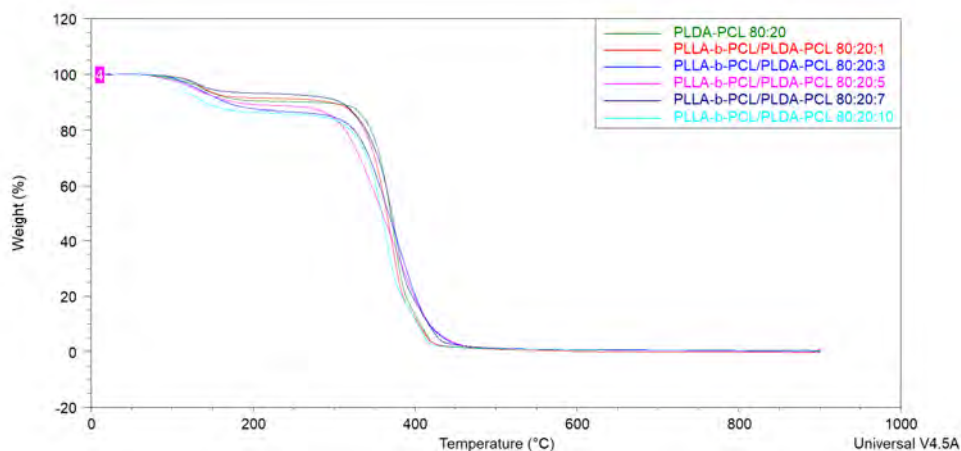


Figure 3.10. TGA curves of PLLA-b-PCL/PLDA-PCL 80:20 polymer blend films with different DBC content.

The main difference in the first degradation step was related to the fact that the increase of DBC content in ternary polymer blends reduced the residual solvent compared with the PLDA-PCL 70:30 and PLDA-PCL 80:20 binary polymer blends. This could be caused by the crystallization effect of the PCL in these blends. Thus, the crystallization affected the molecular chains conformation and avoid the occlusion of the solvent within the polymer chains, and as a consequence the amount of the occluded solvent is reduced. This effect was studied by *Hughes et al.* [20] who analysed the effect on other properties among thermal ones for solvent casted films of PLA. In this Chapter it can be observed that the effect was stronger for ternary polymer blends containing 30 wt% of PCL than in those polymer blends containing 20 wt%.

T_{onset} and T_{deg} were listed in Table 3.10 for PLLA-b-PCL/PLDA-PCL 70:30 polymer blend films and in Table 3.11 for the PLLA-b-PCL/PLDA-PCL 80:20 polymer blend films. The T_{onset} and T_{deg} of PLDA and PCL homopolymers were extracted from TGA results presented in Chapter 1.

Table 3.10. TGA curves of PLLA-b-PCL/PLDA -PCL 70:30 polymer blend films with different DBC content.

Sample name	T_{onset} (°C)	T_{deg} (°C)
Neat PLDA	342	391
Neat PCL	382	446
PLDA-PCL 70:30	339	431
PLLA-b-PCL/PLDA-PCL 70:30:1	339	432
PLLA-b-PCL/PLDA-PCL 70:30:3	337	433

PLLA-b-PCL/PLDA-PCL 70:30:5	334	434
PLLA-b-PCL/PLDA-PCL 70:30:7	325	434

Table 3.11. TGA curves of PLLA-b-PCL/PLDA -PCL 80:20 polymer blend films with different DBC content.

Sample name	T _{onset} (°C)	T _{deg} (°C)
Neat PLDA	342	391
Neat PCL	382	446
PLDA -PCL 80:20	333	418
PLLA-b-PCL/PLDA-PCL 80:20:1	320	416
PLLA-b-PCL/PLDA-PCL 80:20:3	327	425
PLLA-b-PCL/PLDA-PCL 80:20:5	320	418
PLLA-b-PCL/PLDA-PCL 80:20:7	317	430
PLLA-b-PCL/PLDA-PCL 80:20:10	301	414

Generally, the T_{onset} and T_{deg} of PCL homopolymer phase was higher than the T_{onset} and T_{deg} of PLDA homopolymer. Thus, consequently the T_{onset} and T_{deg} of PLDA-PCL polymer blends with both 20 wt% and 30 wt% of PCL increased if compare with these values correspond to neat PLDA homopolymers. Moreover, PLDA-PCL polymer blends with 30 wt% of PCL have higher T_{onset} and T_{deg} than PLDA-PCL polymer blends with 20 wt% of PCL. This effect corroborates that PLDA-PCL polymer blends containing the DBC slightly reduced the thermal stability as DBC increases. The decrease is lower in PLDA-PCL polymer blends containing 30 wt% of DBC compared with those containing 20 wt% of DBC. The T_{onset} of both ternary polymer blends 70:30 and 80:20 suffer a displaced to lower temperatures with the increase of DBC content. This effect is more penalized in PLLA-b-PCL/PLDA-PCL 80:20 ternary polymer blends reaching a decrease of 30 °C compared with the T_{deg} of PLDA-PCL 80:20 polymer blend when the addition of DBC was 10 wt%. However, if the comparison is due to PLDA neat homopolymer, the addition of DBC causes an increase on the thermal stability of prepared polymer blends.

Taking into account the effect of the PLLA-b-PCL diblock copolymer as compatibilizer agent on both PLDA-PCL polymer blend films, the forward investigation will be continued only with PLLA-b-PCL/PLDA-PCL 80:20 polymer blends with 1 wt% to 10 wt%. of DBC. Thus, morphology and barrier properties study will be analysed only for blends based on PLLA-b-PCL/PLDA-PCL 80:20.

3.3.5. Morphology of PLLA-b-PCL/PLDA-PCL polymer blend films by AFM

The morphology of investigated PLLA-b-PCL/PLDA-PCL 80:20 ternary polymer blend films with 1 wt% to 7 wt% of DBC content was analysed by AFM. All prepared by spin-coating polymer blend films were transparent at room temperature, indicating lack of the microphase separation. As shown in Figure 3.11 any significant changes in the morphologies were observed with the increases of the DBC content. The AFM phase image of PLDA-PCL 80:20 binary polymer blend was the same than AFM phase image a) (see Figure 3.11) allowed to distinguish typical phase separation, with the homogeneously distributed separated PCL rich phase with the average domains size 30 nm in diameter. As mentioned in Chapter 2, final morphology of the PLLA-b-PCL/PLDA polymer blends depends on the number of monomeric units of each block of DBC together with molar ratio of both blocks as well as the relation between χ , the molecular weight and the volume fraction of the immiscible block, in this case PCL block [21]. AFM phase images of PLLA-b-PCL/PLDA-PCL 80:20 ternary polymer blends confirmed microphase separation of immiscible PCL block/PCL rich phase from PLLA block/PLDA matrix. However, here it should be pointed out that the size of microphase separated domains was below 150 nm, as a consequence the final properties of these PLLA-b-PCL/PLDA-PCL 80:20 ternary polymer blends are not strongly affected if compared to the PDLA homopolymer. The AFM phase images allow to distinguish a continuous brighter region attributed to PLLA block/PLDA matrix. Simultaneously, the spherical, darker regions corresponded to PCL block/PCL rich phase. It can be also easy visualized that the increase of the DBC content resulted in decrease of the separated domains. (See Figure 3.11).

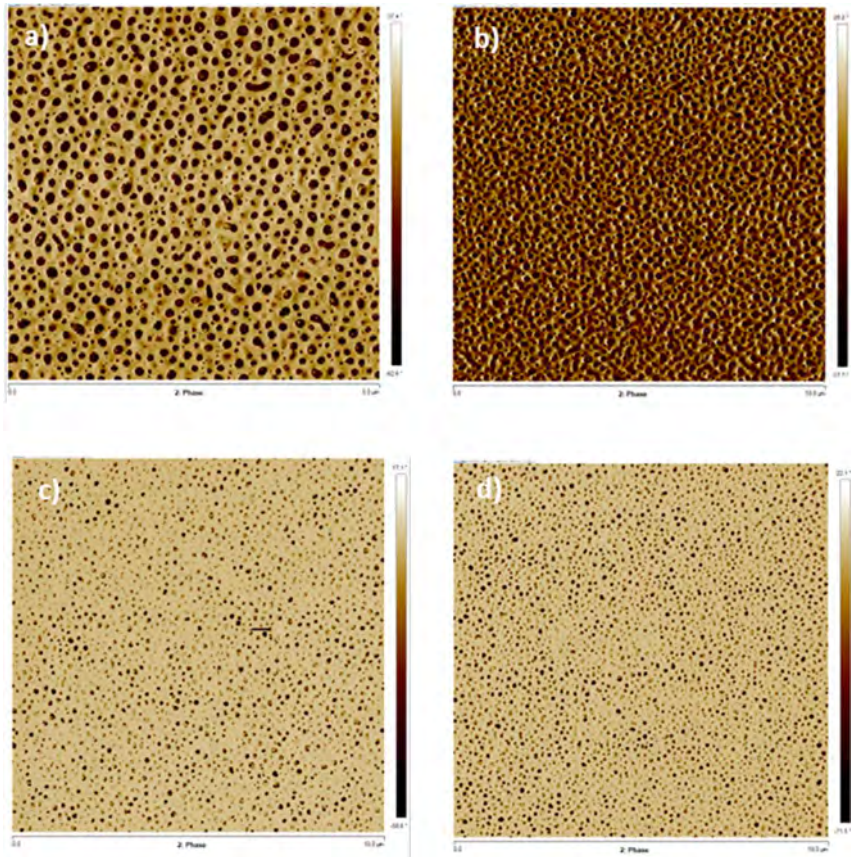


Figure 3.11. AFM phase images of PLLA-b-PCL/PLDA-PCL polymer blends containing different DBC content: a) 1, b) 3, c) 5, and d) 7 wt%.

The size of the spherical microphase separated domains of PLLA-b-PCL/PLDA-PCL 80:20 ternary polymer blend with 1 wt% of DBC varied from 15-52 nm to 130-140 nm. For ternary polymer blends with 3 wt% of DBC content the smallest spherical particles were clearly observed, being their size between 90 nm and 140 nm in diameter. Moreover, for these blends some interconnected spherical micelles can be distinguished. PLLA-b-PCL/PLDA-PCL 80:20 ternary polymer blend with 5 wt% and 7 wt% of DBC content showed similar domains size from 90 nm to 150 nm diameters. As shown in the Figure 3.12, interesting phenomenon was detected for PLLA-b-PCL/PLDA-PCL 80:20 ternary polymer blend with 7 wt% of DBC content. As can be shown in inset of Figure 3.12, inside the spherical phase separation of PCL block/PCL rich phase crystals of PCL can be identify that could correspond to the PCL segment block. Consequently, these results are in good agreement with DSC results, where the increase of

crystallinity in PLLA-b-PCL/PLDA-PCL 80:20 ternary polymer blend with the increase of the DBC content was reported.

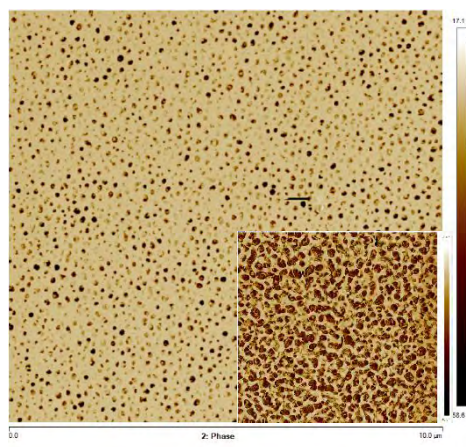


Figure 3.12. AFM phase images of PLLA-b-PCL/PLDA-PCL 80:20 with 7 wt% of PLLA-b-PCL diblock copolymer. Inset correspond to high magnification AFM phase image.

As also happened for PLLA-b-PCL/PLDA polymer blends, theoretical morphology predicted from molecular weight and volumetric rate between components was not reached. Thus, predicted lamellar morphology was not obtained. To better understand these results, a calculation of vol% PCL in each ternary polymer blends has been done using the theoretical density parameters extracted from bibliography which were ρ (PCL) equal to 1.02 g/cm^3 and ρ (PLA) equal to 1.24 g/cm^3 . The vol% PCL for each PLLA-b-PCL/PLDA-PCL polymer blend was summarized in Table 3.12.

Samples names	molar volume of blocks of each ternary blend	
	PLLA (vol %)	PCL (vol%)
PLDA-PCL 80:20		
PLLA-b-PCL/PLDA-PCL 80:20:1	0.54	0.33
PLLA-b-PCL/PLDA-PCL 80:20:3	1.61	0.98
PLLA-b-PCL/PLDA-PCL 80:20:5	2.69	1.63
PLLA-b-PCL/PLDA-PCL 80:20:7	3.76	2.29
PLLA-b-PCL/PLDA-PCL 80:20:10	5.38	3.27

As it has been observed the volume of immiscible segment block related to PCL is very low compared with the molar volume expected for changing the morphology as was explained in Table 2.10, Chapter 2, Section 2.3.3.

3.3.6. Oxygen and water vapour barrier properties of PLLA-b-PCL/PLDA-PCL polymer blend films

Taking into account the OTR and the WVTR results obtained for PLLA-b-PCL/PLDA polymer blends described in Chapter 2, Section 2.3.6, only PLLA-b-PCL/PLDA-PCL polymer blend films prepared by extrusion were analysed. As was described in Chapter 2, the films were masked, and the measure section was of 5 cm x 5 cm. The measurements were carried out according to ASTM standards for oxygen (ASTM D 3985) and water vapour permeability (ASTM F-1249).

Obtained OTR results are plotted in Figure 3.13 and the OTR and oxygen permeability of PLLA-b-PCL/PLDA-PCL ternary polymer blend films are summarized in Table 3.13. The OTR value of PLDA-PCL 80:20 polymer blends are higher than the oxygen barrier value of neat PLDA homopolymer films. The addition of DBC into PLDA-PCL 80:20 polymer blends results in continuous decrease of the OTR value with the increase of DBC content, reaching the OTR values 30% lower for PLLA-b-PCL/PLDA-PCL polymer blend films with 10 wt % of DBC content if compared with the OTR value of PLDA-PCL 80:20 polymer blends.

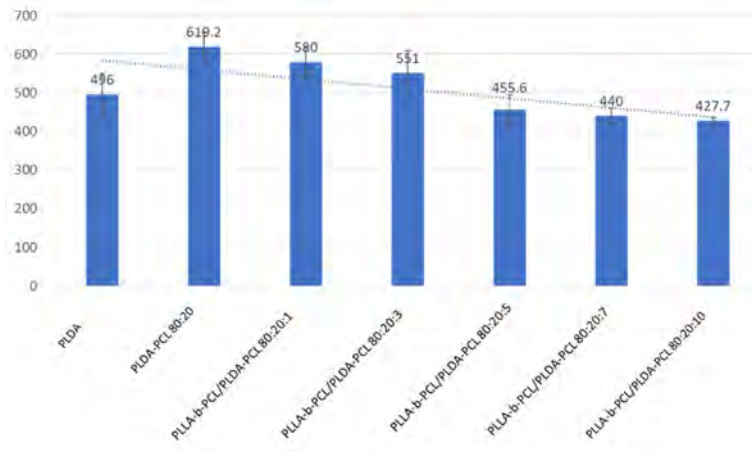


Figure 3.13. The OTR of PLLA-b-PCL/PLDA-PCL polymer blend films with different DBC content.

Sample name	OTR (cm ³ /m ² .day.Pa)	Oxygen permeability (cm ³ .µm/m ² .day.Pa)
Neat PLDA	385 ± 6.2	38.500

PLDA-PCL 80:20	620 ± 36.8	69.120
PLLA-b-PCL/PLDA-PCL 80:20:1	580 ± 40	58.000
PLLA-b-PCL/PLDA-PCL 80:20:3	551 ± 56.8	55.100
PLLA-b-PCL/PLDA-PCL 80:20:5	456 ± 38.5	45.560
PLLA-b-PCL/PLDA-PCL 80:20:7	440 ± 20	44.000
PLLA-b-PCL/PLDA-PCL 80:20:10	427 ± 8.4	42.770

In addition, the influence of time on the OTR values of PLLA-b-PCL/PLDA-PCL polymer blend films was evaluated and for some formulations the reduction up to 50 % of OTR value was observed. The digital images of investigated 1-month aged PLLA-b-PCL/PLDA-PCL polymer blend films are showed in Figure 3.14 and the OTR values are graphed in Figure 3.15. The reduction of OTR values after 1 month aged was probably related to the degree of crystallinity of the PLLA-b-PCL/PLDA-PCL polymer blend films. Thus, with time, the degree of crystallinity of PLLA-b-PCL/PLDA-PCL polymer blend films increased and as a consequence, the OTR values decreased. As it can be seen in Figure 3.14 investigated polymer blend films loss its transparency and are crystallized.

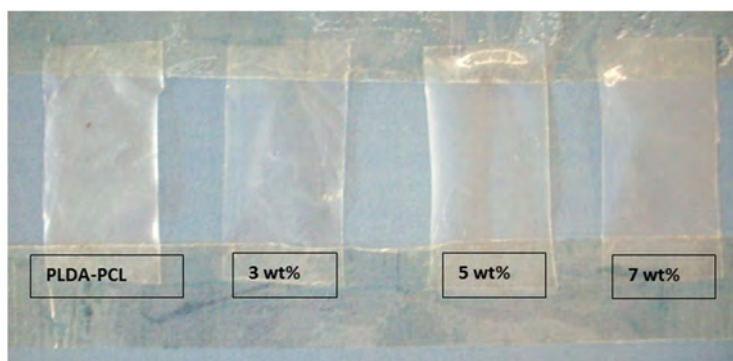


Figure 3.14. Digital images of 1-month aged PLLA-b-PCL/PLDA-PCL polymer blend films with different DBC content.

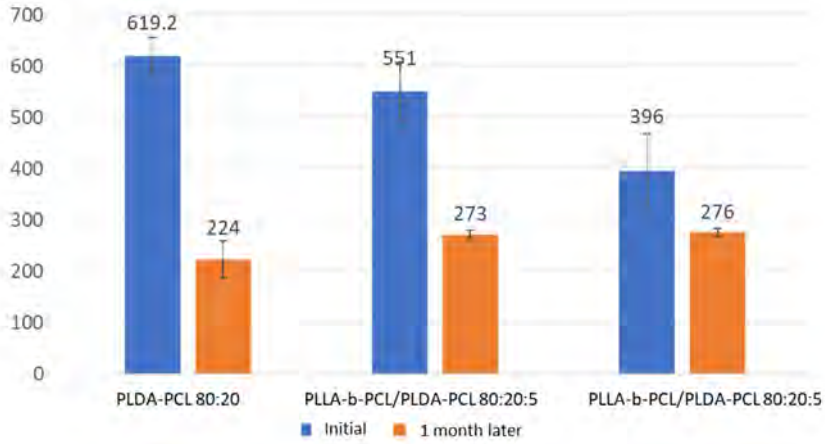


Figure 3.15. The OTR of 1-month aged PLLA-b-PCL/PLDA-PCL polymer blend films.

Figure 3.16 showed WVTR values of PLLA-b-PCL/PLDA-PCL polymer blends containing different DBC percentages.

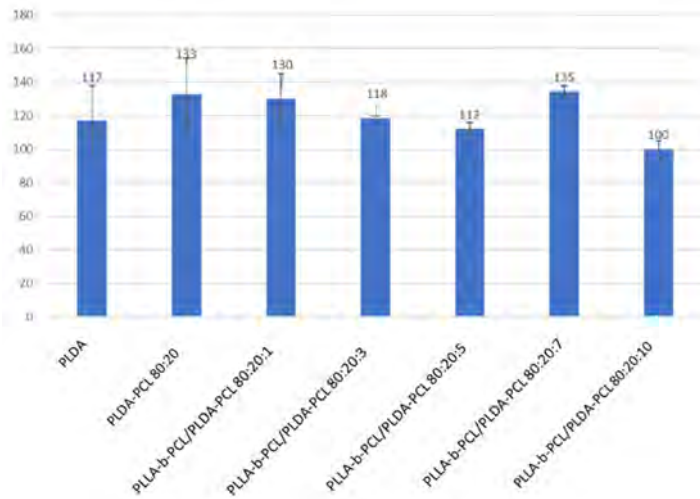


Figure 3.16. The WVTR of PLLA-b-PCL/PLDA-PCL polymer blend films with different DBC content.

As showed in Figure 3.16 and summarized in Table 3.14, the WVTR values decreased with the increase of DBC content in PLLA-b-PCL/PLDA-PCL polymer blend films, reaching the lowest WVTR value for PLLA-b-PCL/PLDA-PCL 80:20 polymer blend films with 10 wt% of DBC content.

The lower improvement of vapour water permeability if compare with oxygen water permeability was probably due to the hydrophilic character of PLDA.

Table 3.14. The WVTR and water permeability of PLLA-b-PCL/PLDA-PCL polymer blend films with different DBC content.

Sample name	WVTR (g/m ² .day.Pa)	Water permeability (g.µm/m ² .day.Pa)
Neat PLDA	117 ± 20.8	18.770.4
PLDA-PCL 80:20	133 ± 21.6	21.216
PLLA-b-PCL/PLDA-PCL 80:20:1	130 ± 15	20.800
PLLA-b-PCL/PLDA-PCL 80:20:3	118 ± 1.4	18.994
PLLA-b-PCL/PLDA-PCL 80:20:5	112 ± 4	17.920
PLLA-b-PCL/PLDA-PCL 80:20:7	135 ± 3.2	21.600
PLLA-b-PCL/PLDA-PCL 80:20:10	100 ± 5	16.000

The OTR and the WVTR results showed an improvement of the barrier properties of PLLA-b-PCL/PLDA-PCL polymer blend films with the increase of the DBC content. However, the improvement of the barrier properties is lower than those achieved for nanostructured PLLA-b-PCL/PLDA polymer blend films discussed in Chapter 2, this improvement corroborates that DBC can acted as compatibilizer agent in PLLA-b-PCL/PLDA-PCL polymer blends.

3.4. CONCLUSIONS

Results obtained in this Chapter indicated that the PLLA-b-PCL diblock copolymer acted as compatibilizer agent for PLDA and PCL homopolymer blends.

The following conclusions of this investigation can be drawn:

- The weight ratio between components of the PLDA-PCL polymer blend affected the final properties of these polymer blends if compare with PLDA and PCL homopolymer.
- The compatibilization effect of PLLA-b-PCL block copolymer was higher for PLDA-PCL 80:20 polymer blends than for PLDA-PCL 70:30 polymer blends due to higher PCL content in DBC.
- The addition of PLLA-b-PCL diblock copolymer into PLDA-PCL 80:20 polymer blends affected their final properties such as appearance, thermal, morphology and barrier properties.

- All PLLA-b-PCL/PLDA-PCL polymer blends based on PLDA-PCL 80:20 were transparent avoiding macrophase separation.
- DSC results showed an effect on the T_{cc} of PLDA being shifted to lower temperatures compared with the neat PLDA-PCL 80:20 polymer blend, this trend indicated a compatibility effect between the polymer blends strongly related with an increase of degree of crystallinity of PLLA-b-PCL/PLDA-PCL polymer blends., which corroborated by WAXS analyses.
- AFM results demonstrated lack of macrophase separation. Moreover, the increase of DBC content led to increase of the diameter of the PCL spherical particles microphase separated from PLLA-b-PCL/PLDA-PCL polymer blends.
- The oxygen and water vapour barrier properties increased linearly with the addition of the DBC into PLDA-PCL 80:20 polymer blends, reaching values of 30 % of improvement of oxygen permeability barrier compared with values for neat PLDA-PCL 80:20 polymer blend. Simultaneously, the water vapour permeability showed 24% of improvement if compared with the neat PLDA-PCL 80:20 polymer blend.
- The successful compatibilization effect of PLLA-b-PCL diblock copolymer resulted in improvement of barrier and thermal properties.
- PLLA-b-PCL diblock copolymer incorporated into PLLA-b-PCL/PLDA-PCL polymer blends can act as both compatibilizer agent for both PLDA and PCL homopolymer and as nanostructuring agent due to microphase separation of PCL block from PLLA block and the PLDA from the PLDA-PCL polymer blend.

3.5. REFERENCES

1. Nofar, M. PLLA/PDLA Blends: Stereocomplex Crystals. *Multiph. Polylactide Blends* 2021, 145–156, doi:10.1016/b978-0-12-824150-9.00004-2.
2. Nofar, M.; Sacligil, D.; Carreau, P.J.; Kamal, M.R.; Heuzey, M.C. Poly (Lactic Acid) Blends: Processing, Properties and Applications. *Int. J. Biol. Macromol.* 2019, *125*, 307–360, doi:10.1016/j.ijbiomac.2018.12.002.
3. Tsuji, H.; Ikada, Y. Blends of Aliphatic Polyesters. I. Physical Properties and Morphologies of Solution-Cast Blends from Poly(DL-Lactide) and Poly(ϵ -Caprolactone). *J. Appl. Polym. Sci.* 1996, *60*, 2367–2375, doi:10.1002/(SICI)1097-4628(19960627)60:13<2367::AID-APP8>3.0.CO;2-C.
4. Berthé, V.; Ferry, L.; Bénézet, J.C.; Bergeret, A. Ageing of Different Biodegradable Polyesters Blends Mechanical and Hygrothermal Behavior. *Polym. Degrad. Stab.* 2010, *95*, 262–269, doi:10.1016/j.polymdegradstab.2009.11.008.
5. Liang, J.Z.; Zhou, L.; Tang, C.Y.; Tsui, C.P. Crystalline Properties of Poly(L-Lactic Acid) Composites Filled with Nanometer Calcium Carbonate. *Compos. Part B Eng.* 2013, *45*, 1646–1650, doi:10.1016/j.compositesb.2012.09.086.
6. Esmaeilzadeh, J.; Hesarakhi, S.; Hadavi, S.M.M.; Esfandeh, M.; Ebrahimzadeh, M.H. Microstructure and Mechanical Properties of Biodegradable Poly (D/L) Lactic Acid/Polycaprolactone Blends Processed from the Solvent-Evaporation Technique. *Mater. Sci. Eng. C* 2017, *71*, 807–819, doi:10.1016/j.msec.2016.10.070.
7. Wu, D.; Zhang, Y.; Zhang, M.; Zhou, W. Phase Behavior and Its Viscoelastic Response of Polylactide/Poly(ϵ -Caprolactone) Blend. *Eur. Polym. J.* 2008, *44*, 2171–2183, doi:10.1016/j.eurpolymj.2008.04.023.
8. Matta, A.K.; Rao, R.U.; Suman, K.N.S.; Rambabu, V. Preparation and Characterization of Biodegradable PLA/PCL Polymeric Blends. *Procedia Mater. Sci.* 2014, *6*, 1266–1270, doi:10.1016/j.mspro.2014.07.201.
9. Cock, F.; Cuadri, A.A.; García-Morales, M.; Partal, P. Thermal, Rheological and Microstructural Characterisation of Commercial Biodegradable Polyesters. *Polym. Test.* 2013, *32*, 716–723, doi:10.1016/j.polymertesting.2013.03.015.
10. Chen, C.; Chueh, J.; Tseng, H.; Huang, H.; Lee, S. <1-S2.0-S0142961202004660-Main.Pdf>. 2003, *24*, 1167–1173.
11. Yang, W.; Qi, G.; Ding, H.; Xu, P.; Dong, W.; Zhu, X.; Zheng, T.; Ma, P. Biodegradable Poly (Lactic Acid)-Poly (ϵ -Caprolactone)-Nanolignin Composite Films with Excellent

- Flexibility and UV Barrier Performance. *Compos. Commun.* 2020, 22, 100497, doi:10.1016/j.coco.2020.100497.
12. Navarro-Baena, I.; Sessini, V.; Dominici, F.; Torre, L.; Kenny, J.M.; Peponi, L. Design of Biodegradable Blends Based on PLA and PCL: From Morphological, Thermal and Mechanical Studies to Shape Memory Behavior. *Polym. Degrad. Stab.* 2016, 132, 97–108, doi:10.1016/j.polymdegradstab.2016.03.037.
 13. Si, W.J.; Zhang, H.; Li, Y.D.; Huang, C.; Weng, Y.X.; Zeng, J.B. Highly Toughened and Heat Resistant Poly(L-Lactide)/Poly(ϵ -Caprolactone) Blends via Engineering Balance between Kinetics and Thermodynamics of Phasic Morphology with Stereocomplex Crystallite. *Compos. Part B Eng.* 2020, 197, 108155, doi:10.1016/j.compositesb.2020.108155.
 14. Akoumeh, R.; Elzein, T.; Martínez-Campos, E.; Reviriego, F.; Rodríguez-Hernández, J. Fabrication of Porous Films from Immiscible Polymer Blends: Role of the Surface Structure on the Cell Adhesion. *Polym. Test.* 2020, 91, doi:10.1016/j.polymertesting.2020.106797.
 15. Battezzatore, D.; Bocchini, S.; Frache, A. Crystallization Kinetics of Poly(Lactic Acid)-Talc Composites. *Express Polym. Lett.* 2011, 5, 849–858, doi:10.3144/expresspolymlett.2011.84.
 16. Henricks, J.; Boyum, M.; Zheng, W. Crystallization Kinetics and Structure Evolution of a Polylactic Acid during Melt and Cold Crystallization. *J. Therm. Anal. Calorim.* 2015, 120, 1765–1774, doi:10.1007/s10973-015-4460-0.
 17. Park, S.D.; Todo, M.; Arakawa, K.; Koganemaru, M. Effect of Crystallinity and Loading-Rate on Mode I Fracture Behavior of Poly(Lactic Acid). *Polymer (Guildf).* 2006, 47, 1357–1363, doi:10.1016/j.polymer.2005.12.046.
 18. Jiang, S.; Ji, X.; An, L.; Jiang, B. Crystallization Behavior of PCL in Hybrid Confined Environment. *Polymer (Guildf).* 2001, 42, 3901–3907, doi:10.1016/S0032-3861(00)00565-6.
 19. Carmona, V.B.; De Campos, A.; Marconcini, J.M.; Mattoso, L.H.C. Kinetics of Thermal Degradation Applied to Biocomposites with TPS, PCL and Sisal Fibers by Non-Isothermal Procedures. *J. Therm. Anal. Calorim.* 2014, 115, 153–160, doi:10.1007/s10973-013-3259-0.
 20. Hughes, J. The Effects of Solvent Mixture on the Thermal and Mechanical Properties of Solvent Cast Poly-Lactic Acid (PLA) Film. *All Theses* 2011.
 21. Wu, X.; Qiao, Y.; Yang, H.; Wang, J. Self-Assembly of a Series of Random Copolymers

Bearing Amphiphilic Side Chains. *J. Colloid Interface Sci.* 2010, 349, 560–564, doi:10.1016/j.jcis.2010.05.093.

Los capítulos 4, 5, 6 y 7 están sujetos a confidencialidad por parte de la autora

***IV. GENERAL CONCLUSIONS, FUTURE
WORKS AND SCIENTIFIC PRODUCTION***

IV. GENERAL CONCLUSIONS, FUTURE WORKS AND SCIENTIFIC PRODUCTION

IV.1. GENERAL CONCLUSIONS..... 301

IV.2. FUTURE WORKS 304

IV.3. SCIENTIFIC PRODUCTION..... 306

IV.3.1. List of Patents..... 306

IV.3.2. List of communications 307

IV.3.3. List of courses 308

IV.1. GENERAL CONCLUSIONS

The general conclusions of this investigation thesis were following:

The results obtained for PLDA/PCL polymer blends confirmed that these blends are immiscible. On the contrary, the used of commercial PLLA-b-PCL diblock copolymer allowed to prepare PLLA-b-PCL/PLDA polymer blends on laboratory scale with the promising properties for possible packaging applications.

The properties of PLLA-b-PCL/PLDA polymer blends was strongly related with the capability of self-assembly of PLLA-b-PCL diblock copolymer in these polymer blends. Thus, different morphologies were detected by AFM techniques due to microphase separation of PCL block in PLLA block/PLDA matrix.

The final properties of PLLA-b-PCL/PLDA polymer blends depends strongly on commercial PLLA-b-PCL diblock copolymer content. The crystallinity of PLLA-b-PCL/PLDA polymer blends increased with increased of DBC content without losing their transparency, corroborating self-assembly of diblock copolymer at nanoscale. Moreover, slight decrease of the T_g of PLLA-b-PCL/ PLDA polymer blends was observed, indicating a low plasticizer effect, which reduces the neat PLDA homopolymer brittleness.

The oxygen permeability barrier of solvent casted PLLA-b-PCL/PLDA polymer blends with commercial DBC was improved reaching a decrease of 20 % of the OTR if compared with neat PLDA. The same polymer blends obtained by extrusion cast showed a decrease of 50% of the OTR if compared with neat PLDA. Moreover, the WVTR values improved for polymer blends prepared by both processing techniques.

Commercial PLLA-b-PCL diblock copolymers acted as compatibilizer for PLDA-PCL polymer blends being PLLA block partially miscible with neat PLDA and PCL block partially miscible with neat PCL. The compatibilizer effect was higher for PLDA-PCL 80:20 polymer blend. Similarly, as for PLLA-b-PCL/PLDA polymer blends, the addition of commercial PLLA-b-PCL diblock copolymer into PLDA-PCL 80:20 polymer blend resulted in nanostructured polymeric materials.

The addition of commercial PLLA-b-PCL diblock copolymer into PLDA-PCL 80:20 improved 30 % of oxygen barrier permeability and 24 % of water vapour barrier permeability if compared with PLLA-b-PCL/PLDA-PCL polymer blend prepared in the same way.

The addition of commercial PLLA-b-PCL diblock copolymer into PLDA-PCL 80:20 improved 30 % of oxygen barrier permeability and 24 % of water vapour barrier permeability if compared with PLLA-b-PCL/PLDA-PCL polymer blend prepared in the same way.

The synthesis of PLLA-b-PCL diblock copolymer was successfully done on a laboratory scale by ROP of ϵ -CL and subsequently L-LA monomer incorporation. Synthesized PLLA-b-PCL diblock copolymer with weight ratio between blocks 2:1 possessed similar properties to commercial PLLA-b-PCL and maintained self-assembly capability in PLLA-b-PCL/PLDA polymer blends leading to nanostructured materials. PLLA-b-PCL/PLDA polymer blends with synthesized DBC maintained barrier properties if compare with the same polymer blends with commercial DBC and showed elongation at break improvement of 40% if compared to neat PLDA.

Obtained results confirmed that it was possible not only to upscale the PLLA-b-PCL diblock copolymer synthesis on preindustrial scale without purification step, but also it was possible to improve the chemical synthesis yield. Synthesized in the ITENE pilot plant PLLA-b-PCL diblock copolymer possessed similar properties if compared to commercial PLLA-b-PCL diblock copolymer and the one synthesized on a laboratory scale.

DBC/PLDA polymer blends prepared using synthesized on preindustrial scale DBC were also successfully produced in pilot plant of ITENE facilities. A specific screw configuration for extrusion compound allowed to avoid DBC degradations and improving the DBC and PLDA mixing index. Results obtained for different DBC/PLDA polymer blends confirmed that synthesized DBC, on the one hand, acted as plasticizer for PLDA matrix and, on the other hand, acted as a nucleating agent increasing DBC/PLDA polymer blends crystallinity if compared with the neat PLDA polymer. Improvements on thermal and permeability barrier properties were maintained.

Food safety analyses (overall and specific migration tests) according to EU Regulation N^o 10/2011 demonstrated that developed DBC/PLDA polymer blends are safe to be used as a packaging material for different foodstuffs and in different conservation conditions, from short time to long time.

Biodegradability and compostability tests done according to UNE EN 13432:2000 confirmed that DBC/PLDA polymer blends with up to 20 % of DBC content are biodegradable and compostable.

DBC/PLDA polymer blends could be used as packaging materials as was confirmed used them for two specific applications such as thermoformed trays and vacuum flexible bags. From the point of view of converting technologies, the processability of DBC/PLDA polymer blends was successful and both types of packages were produced.

The validation with foodstuffs, concretely, croissants for the thermoformed trays and sliced cured ham for the vacuum flexible bags, showed a limited functionality. Both products packed in the developed biodegradable and compostable packages fulfilled with the commercial shelf-life but with a loss of properties. In both products the most identified change was the dryness compared with the products packaged with the commercial packages. However, it can be concluded that 70 % of the internal panellist didn't identified changes in the flavour of the sliced cured ham packed with the developed DBC/PLDA polymer blends. Finally, developed during this investigation work polymer blends could be a new alternative for PLA uses in a short time on industrial scale.

IV.2. FUTURE WORKS

The knowledge developed during this investigation work has been used to continue with the research on the synthesis of tailored made block copolymers to improve biodegradable and compostable polymers focus on packaging applications.

In the first place, an identification of the packaging market niches in which biodegradable materials present a competitive advantage has been carried out. Then, two specific types of packaging and processing technologies have been selected. The selected types were:

- Flexible packaging processed by extrusion: for applications which require thermal resistance to be used for single-use flexible materials to contain sauces such as mayonnaise or for individual thermoformed trays for jam. In this case the material selected will be PBS.
- Rigid packaging processed by injection: to be used for applications such as small bottles or coffee capsules. For this market the selected polymer family will be poly(hydroxialkanoates). In particular, the poly(3-hydroxybutyrate-co-3-hydroxyvalerate) (PHBV) due to PHBV grade is still the unique approved for food contact applications.

Preliminary work for the synthesis of both types of block copolymers have been started. The first one is a triblock copolymer of PLLA-b-PBS-b-PLLA with the aim to improve PLDA thermal resistance and to reduce the cost of PBS homopolymer. In addition, the effect of the developed triblock copolymer will be test as a compatibilizer for PLDA/PBS polymer blends. The second one is a diblock copolymer of PLA-b-PHBV with the aim to improve PLDA toughness and PHB flexibility and to test its properties as compatibilizer for future PLDA/PHB polymer blends.

The current state and next steps for each BCP is detailed:

- *Development of PLLA-b-PBS-b-PLLA triblock copolymer*

The synthesis of the PLLA-b-PBS-b-PLLA triblock copolymer by using dimethylsuccinate and diethylsuccinate as prepolymers to obtain PBS by transesterification and to synthesize the triblock by ROP using L-LA as monomer, is being study at laboratory scale. Preliminary results showed a low M_n of the triblock copolymer and very long time for the reaction (20 h). Preliminary blends of PBS of the triblock copolymer have been obtained by extrusion cast al

laboratory scale and low improvement in mechanical and thermal properties have been observed. For the future is proposed:

- To evaluate different prepolymers such as alkylsuccinate and new catalyst materials and its percentages to reduce the time of the polymerization step
- To evaluate different ratios between the blocks of PLLA and PBS (current 3:1)
- To select the best PLLA-b-PBS-PLLA triblock copolymer and to blend in different weight ratio with both selected matrices, PLDA and PBS following the procedure described in Chapter 2 and Chapter 4.

- Development of PLA-b-PHB diblock copolymer

The synthesis of PLA-b-PHB diblock copolymer is being study on laboratory scale. This synthesis route consists of two steps, the first one is the preparation of PHBV oligomers by methanolysis and the second one the polymerization with L-LA monomer by using an organometallic catalyst. Preliminary results obtained low M_n prepolymers of PHBH-OH leading to low M_n of the PHBV-b-PLLA diblock copolymers. Furthers steps should be:

- Selection of different catalyst to obtain best results in the PHBV methanolysis or to look for other monomers extracted from fermentation steps of the PHBV to be used as precursors
- Once the synthesis of the PHBV-b-PLLA will be set up. Several polymer blends of the synthesized PHBV-b-PLLA diblock copolymer with both, PHBV and PLDA homopolymers will be studied following the procedures described in Chapter 2 and Chapter 4.

IV.3. SCIENTIFIC PRODUCTION

IV.3.1. List of Patents

Title: COMPOSITIONS FOR THE PREPARATION OF A NANOSTRUCTURED BIODEGRADABLE POLYMERIC MATERIAL

Number: EP13382126.4

Inventors: Miriam Gallur Blanca, Natalia Ortuño Mansilla, Susana Aucejo Romero, Maria Jordá Beneyto, Ana Domingo Galet, Mercedes Hortal Ramos.

Solicitant: INSTITUTO TECNOLÓGICO DEL EMBALAJE, TRANSPORTE Y LOGÍSTICA (ITENE)

Year: 2013

Title: COPOLÍMERO TRIBLOQUE Y COMPOSICIONES QUE LO COMPREDEN Y PROCEDIMIENTO DE OBTENCIÓN DE LOS MISMOS

Number: PCT/ES2022/070377

Inventors: Miriam Gallur Blanca, Maria Jose Jimenez Pardo, Soraya Carmen Sánchez Ballester

Solicitant: INSTITUTO TECNOLÓGICO DEL EMBALAJE, TRANSPORTE Y LOGÍSTICA (ITENE)

Year: 2021

Title: A DIBLOCK COPOLYMER COMPRISING POLY(L-LACTIDE) AND POLY (ϵ -CAPROLACTONE)

Number: EP21382526.8

Inventors: Miriam Gallur Blanca, Alejandro Aragón Gutiérrez, Antonio Montesinos Ramírez, María Amparo Verdú Solís.

Solicitant: INSTITUTO TECNOLÓGICO DEL EMBALAJE, TRANSPORTE Y LOGÍSTICA (ITENE)

Year: 2021

IV.3.2. List of communications

Title: IMPROVED BIODEGRADABLE MATERIALS FOR PACKAGING

Authors: Susana Aucejo, Miriam Gallur, Maria Jordá, Jose Maria Alonso.

Congress: COMATCOMP. V International Conference on Science and Technology of Composite Materials

Participation: Oral presentation

Year: 2009

Place: San Sebastián, España

Title: IMPROVED BIODEGRADABLE BLENDS PROPERTIES OF PLLA-PCL VIA BLOCK COPOLYMER SELF-ASSEMBLY

Authors: Miriam Gallur, Natalia Ortuño, Agnieszka Tercjak, Susana Aucejo, Iñaki Mondragon.

Congress: 7th International ECNP Conference on Nanostructured Polymers and Nanocomposites.

Participation: Poster Presentation

Year: 2012

Place: Prague, Czech Republic.

Title: NANOSTRUCTURED BIODEGRADABLE THERMOPLASTIC BLENDS BASED ON POLY (L-LACTIC ACID) AND A POLY (ϵ -CAPROLACTONE-B-L-LACTIDE) DIBLOCK COPOLYMER

Authors: Miriam Gallur, Natalia Ortuño, Agnieszka Tercjak, Susana Aucejo, Iñaki Mondragon.

Congress: 11th European Symposium on Polymer Blends.

Participation: Poster Presentation

Year: 2012

Place: San Sebastián, España.

Title: NANOSTRUCTURED BIODEGRADABLE THERMOPLASTIC BLENDS BASED ON POLY (L-LACTIC ACID) AND A POLY(ϵ -CAPROLACTONE-B-L-LACTIDE) DIBLOCK COPOLYMER

Authors: Miriam Gallur, Natalia Ortuño, Agnieszka Tercjak, Susana Aucejo, Iñaki Mondragon.

Congress: 8th ECNP International Conference on Nanostructured Polymers and Nanocomposites.

Participation: Oral presentation

Year: 2014

Place: Dresden, Germany.

IV.3.3. List of courses

Title: Course of nanostructured polymer introduction

Attendees: Miriam Gallur, Maria Jordá, Jose Maria Alonso.

Organization: POLYMAT

Year: 2018

Place: San Sebastián, España

V. ANNEXES

V. ANNEXES LIST

V.1. LIST OF FIGURES	313
V.2. LIST OF TABLES	320
V.3. LIST OF ABBREVIATIONS.....	327
V.4. LIST OF SYMBOLS	330
V.5. LIST OF EQUATIONS.....	333
V.6. LIST OF SCHEMES.....	334

V.1. LIST OF FIGURES

Introduction

Figure I.1. Conventional polymer materials production by industries in Europe. Source: PlasticsEurope Market Research Group (PEMRG) and Conversio Market & Strategy.GmbH.

7

Figure I.2. Forecast of bioplastics up to 2025. Source: European Bioplastics, nova-Institute (2021). 10

Figure I. 3. Phase diagram of a symmetric diblock copolymer [23]. 17

Chapter 1.

Figure 1.1. Stereoisomers of L-lactic acid and D-lactic acid monomers. Source: adapted from Auras et al. [6]. 35

Figure 1.2. Stereoisomers of lactide dimers, a) D-lactide, b) meso-lactide, c) L-lactide. Source: adapted from Auras et al. [6]. 36

Figure 1.3. Chemical structure of PLDA. 40

Figure 1.4. Chemical structure of PCL..... 40

Figure 1.5. DSC thermograms of a) PLDA and b) PCL homopolymers. 44

Figure 1.6. DSC thermograms of PLDA homopolymer films prepared by solvent casting using chloroform as solvent..... 47

Figure 1.7. DSC thermograms of PLDA homopolymer films prepared by solvent casting using dichloromethane as solvent. 48

Figure 1.8. TGA curves of PLDA homopolymer films prepared by protocol 1. 49

Figure 1.9. TGA curves of PLDA homopolymer films prepared by protocol 2. 50

Figure 1.10. TGA curves of PLDA homopolymer films prepared by protocol 3..... 50

Figure 1.11. DSC thermograms of PLDA/PCL polymer blends during 1st heating scan. 52

Figure 1.12. DSC thermograms of PLDA/PCL polymer blends during 2nd heating scan. 54

Chapter 2.

Figure 2.1. Chemical structure of PLLA-b-PCL diblock copolymer. 66

Figure 2.2. DSC thermogram of PLLA-b-PCL diblock copolymer..... 73

Figure 2.3. Digital image of the transparency of solvent casted PLLA-b-PCL/PLDA polymer blend films.	75
Figure 2.4. AFM phase images of PLLA-b-PCL/PLDA polymer blends with different contents of DBC: (a) 20, (b) 30, (c) 50, (d) 70 and (e) 80 wt%.	77
Figure 2.5. DSC thermograms of neat PLDA and PLLA-b-PCL/PLDA polymer blend films.	83
Figure 2.6. WAXS spectra of PLDA and PLLA-b-PCL/PLDA polymer blends containing different DBC contents.	85
Figure 2.7. TGA curves of PLLA-b-PCL/PLDA polymer blend films.	86
Figure 2.8. The OTR of solvent casted PLLA-b-PCL/PLDA polymer blend films.	87
Figure 2.9. The OTR of extruded PLLA-b-PCL/PLDA polymer blend films.	89
Figure 2.10. The WVTR of solvent casted PLLA-b-PCL/PLDA polymer blend films.	90
Figure 2.11. Water vapour transmission rate of extruded PLLA-b-PCL/PLDA-polymer blend films.	91
 Chapter 3.	
Figure 3.1. Reported studies on PLA based blends. (Source Reference [2]).	104
Figure 3.2. Studies carried out with PLA and other biopolymers. (Source Reference [2]). ...	104
Figure 3.3. SEM micrographs of cryogenically fractured surface of an immiscible PLA-PCL polymer blend showing the island effect. (Source Reference [6])	105
Figure 3.4. Digital images of transparency of solvent casted PLLA-b-PCL/PLDA-PCL 70:30 polymer blend films.	111
Figure 3.5. DSC thermograms of PLLA-b-PCL/PLDA -PCL 70:30 polymer blend films with different DBC content. The DSC thermograms of PLDA and PCL homopolymers were added for comparison.	114
Figure 3.6. DSC thermograms of PLLA-b-PCL/PLDA-PCL 80:20 polymer blend films with different DBC content. The DSC thermograms of PLDA and PCL homopolymers were added for comparison.	115
Figure 3.7. WAXS spectra of PLLA-b-PCL/PLDA-PCL 70:30 polymer blend films with different DBC content.	119
Figure 3.8. WAXS spectra of PLLA-b-PCL/PLDA-PCL 80:20 polymer blend films with different DBC content.	119
Figure 3.9. TGA curves of PLLA-b-PCL/PLDA-PCL 70:30 polymer blends films with different DBC content.	120

Figure 3.10. TGA curves of PLLA-b-PCL/PLDA-PCL 80:20 polymer blend films with different DBC content. 121

Figure 3.11. AFM phase images of PLLA-b-PCL/PLDA-PCL polymer blends containing different DBC content: a) 1, b) 3, c) 5, and d) 7 wt%. 124

Figure 3.12. AFM phase images of PLLA-b-PCL/PLDA-PCL 80:20 with 7 wt% of PLLA-b-PCL diblock copolymer. Inset correspond to high magnification AFM phase image. 125

Figure 3.13. The OTR of PLLA-b-PCL/PLDA-PCL polymer blend films with different DBC content. 126

Figure 3.14. Digital images of 1-month aged PLLA-b-PCL/PLDA-PCL polymer blend films with different DBC content. 127

Figure 3.15. The OTR of 1-month aged PLLA-b-PCL/PLDA-PCL polymer blend films. 128

Figure 3.16. The WVTR of PLLA-b-PCL/PLDA-PCL polymer blend films with different DBC content. 128

Chapter 4.

Figure 4.1. *Experimental set up of PCL-OH prepolymer polymerization.*..... 144

Figure 4.2. *Improved experimental set up to produce PCL-OH prepolymer by mechanical stirring.* 146

Figure 4.3. *Digital picture of PCL-OH sample after filtering and drying.* 147

Figure 4.4. *Experimental set up of the PCL-b-PLLA diblock copolymers synthesis by mechanical stirring.* 148

Figure 4.5. *¹H-NMR spectrum of PCL-OH prepolymer prepared using magnetic stirring.*.... 152

Figure 4.6. *FTIR spectrum of PCL-OH prepolymer prepared using magnetic stirring.* 154

Figure 4.7. *TGA and DTG curves of PCL-OH prepolymer prepared using magnetic stirring.*. 154

Figure 4.8. *DSC thermograms of PCL-OH prepolymer prepared using magnetic stirring.*.... 155

Figure 4.9. *¹H-NMR spectrum of synthesized PLLA-b-PCL II diblock copolymer prepared using magnetic stirring.*..... 157

Figure 4.10. *FTIR spectra of synthesized PLLA-b-PLA diblock copolymers prepared using magnetic stirring. For comparison FTIR spectra of PCL-OH prepolymer was added.* 158

Figure 4.11. *TGA and DTG curves of synthesized PLLA-b-PCL diblock copolymers prepared using magnetic stirring. For comparison TGA and DTG curves of PCL-OH prepolymer were added.*..... 159

Figure 4.12. DSC thermograms of synthesized PLLA-b-PCL diblock copolymers prepared by magnetic stirring	160
Figure 4.13. AFM phase images of spin-coated PLLA-b-PCL/PLDA polymer blends with different synthesized PLLA-b-PCL diblock copolymer content: a) 10, b) 20, c) 30, d) 40, e) 50, f) 60, g)70 and h) 80 wt%.	163
Figure 4.14. ¹ H-NMR spectrum of PCL-OH prepolymer used in synthesis of PLLA-b-PCL diblock copolymers prepared by mechanical stirring.	164
Figure 4.15. TGA and DTG curves of PCL-OH prepolymer prepared by mechanical stirring.	165
Figure 4.16. DSC thermograms of PCL-OH prepolymer prepared by mechanical stirring.	166
Figure 4.17. ¹ H-NMR spectrum of synthesized PCL ₂₀ -b-PLLA ₄₀ diblock copolymer prepared by mechanical stirring.	167
Figure 4.18. TGA and DTG curves of PCL-b-PLLA diblock copolymers prepared by mechanical stirring.	169
Figure 4.19. DSC thermograms of synthesized PCL-b-PLLA diblock copolymers using mechanical stirring.	170
Figure 4.20. Digital images of transparency of injected PCL-b-PLLA/PLDA polymer blend. .	172
Figure 4.21. TGA and DGT curves of different PCL-b-PLLA/PLDA polymer blends with synthesized PCL-b-PLLA diblock copolymers using mechanical stirring.	172
Figure 4.22. DSC thermograms of different PCL-b-PLLA/PLDA polymer blends during (a) cooling and (b) heating scans.	174
Figure 4.23. Stress-strain curves of PCL-b-PLLA/PLDA polymer blends.	176
Figure 4.24. The OTR values of extruded PCL-b-PLLA/PLDA polymer blends with different synthesized PCL-b-PLLA diblock copolymers.	178
Figure 4.25. The WVTR values of PLDA/PCL-b-PLLA polymer blends with different synthesized PCL-b-PLLA diblock copolymers.	179
Chapter 5.	
Figure 5.1. Digital images of the pilot plant polymerization reactors at ITENE facilities.	192
Figure 5.2. ε-CL monomer conversion as a function of time.	194
Figure 5.3. Evolution of molecular weight as a function of time of PCL-OH I prepolymer synthesized with 0.1 wt% of Sn(Oct) ₂	195

Figure 5.4. Evolution of molecular weight as a function of time of PCL-OH II prepolymer synthesized with 0.05 wt% of Sn(Oct) ₂ .	196
Figure 5.5. Evolution of molecular weight as a function of time of PCL-OH III prepolymer synthesized with 0.025 wt% of Sn(Oct) ₂ .	196
Figure 5.6. ¹ H-NMR spectrum of the PCL-OH prepolymers.	197
Figure 5.7. Representative TGA and DTG curves of PCL-OH III synthesized on preindustrial scale.	199
Figure 5.8. Representative DSC thermogram of PCL-OH synthesized on preindustrial scale.	200
Figure 5.9. L-LA monomer conversion as a function of time during synthesis of PLLA-b-PCL diblock copolymers on preindustrial scale.	201
Figure 5.10. Evolution of the amperage (indirect measure of viscosity) as a function of time of PLLA-b-PCL diblock copolymers synthesized in the 100 L polymerization reactor.	203
Figure 5.11. Representative TGA and DTG curves of synthesized DBC ₃ PLLA-b-PCL diblock copolymer on preindustrial scale.	204
Figure 5.12. Representative DSC thermograms of DBC ₃ PLLA-b-PCL diblock copolymer synthesized on preindustrial scale.	205
Chapter 6.	
Figure 6.1. Evolution since 2006-2020 of plastic waste treatment. Source: Conversio Market & Strategy GmbH.	216
Figure 6.2. Production, consumption, and end-of-life of biodegradable polymer from renewable resources via composting [6].	219
Figure 6.3. Schematic representative use of Ludovic® software made at ITENE.	222
Figure 6.4. Types of injected DBC/PLDA polymer blend probes produced on preindustrial scale.	225
Figure 6.5. Example of theoretical biodegradation curve.	231
Figure 6.6. Digital images of DBC/PLDA polymer blends with 20 wt% of DBC for disintegration test.	231
Figure 6.7. Comparison of different screw configurations type ADBio with ITENE 3B screw configurations.	235
Figure 6.8. Temperatures profile of ITENE 3B and new designed screw configurations.	236
Figure 6.9. Pressures profile of ITENE 3B and new designed screw configurations.	236

Figure 6.10. MFI results of DBC/PLDA polymer blends with different DBC content.	240
Figure 6.11. DSC thermograms of DBC/PLDA polymer blends with different DBC content. .	241
Figure 6.12. TGA curves of DBC/PLDA polymer blends with different DBC content.	243
Figure 6.13. The HDT of DBC/PLDA polymer blends with different DBC content produced on preindustrial scale.	244
Figure 6.14. Flexural modulus of DBC/PLDA polymer blends with different DBC content produced on preindustrial scale.	246
Figure 6.15. The OTR values of DBC/PLDA polymer blends with different DBC content produced on preindustrial scale.	247
Figure 6.16. The WVTR of DBC/PDLA polymer blends with different DBC content produced on preindustrial scale.	248
Figure 6.17. Accumulation biodegradation degree of DBC/PLDA polymer blends with 20 wt% of DBC.	255
Figure 6.18. Digital images of DBC/PLDA polymer blends with 20 wt% of DBC during the disintegration test.	255
Figure 6.19. Digital images of Garden Cress without DBC/PLDA polymer blend with 20 wt% of DBC in the compost in a) Mixture 1 and c) Mixture 2 and with DBC/PLDA polymer blend with 20 wt% of DBC in the compost in b) Mixture 1 and d) Mixture 2.	257
Figure 6.20. Digital images of Summer Barley without DBC/PLDA polymer blend with 20 wt% of DBC in the compost in a) Mixture 1 and c) Mixture 2 and with DBC/PLDA polymer blend with 20 wt% of DBC in the compost in b) Mixture 1 and d) Mixture 2.	257

Chapter 7.

Figure 7.1. Digital images of croissants packed in a) DBC/PLDA polymer blend clamshell tray and b) in PET commercial tray.	272
Figure 7.2. Digital images of sliced cured ham packed in a) DBC/PLDA polymer blend with 20 wt% DBC monomaterial film and b) in PET/EVOH/PET multilayer film.	273
Figure 7.3. Digital images of thermoformed clamshell trays of DBC/PLDA polymer blend film with 20 wt% of DBC produced on preindustrial scale.	278
Figure 7.4. Digital images of DBC/PLDA polymer blend film with 20 wt% of DBC clamshell tray dropped from 1 m after DIR test.	278
Figure 7.5. Digital images of PET clamshell tray dropped from 1 m after DIR test.	279

- Figure 7.6.** Digital images of a) DBC/PLDA polymer blend film with 20 wt% of DBC b) PET clamshell trays after compression test at 10 mm. 280
- Figure 7.7.** Digital image of 60 µm thick extruded DBC/PLDA polymer blend film with 20 wt% of DBC of for vacuum bags applications. 280
- Figure 7.8.** Digital images of thermosealing samples of a) DBC/PLDA polymer blend film with 20 wt% of DBC and b) neat commercial PLA..... 284
- Figure 7.9.** The AW of the croissants packed in DBC/PLDA polymer blend film with 20 wt% of DBC if compared with PET clamshell trays. 285
- Figure 7.10.** Weight loss of the croissants packed in DBC/PLDA polymer blend film with 20 wt% of DBC if compared with PET clamshell trays. 285
- Figure 7.11.** Compressed force of the croissants packed in DBC/PLDA polymer blend clamshell trays with 20 wt% of DBC if compared with PET clamshell trays. 286
- Figure 7.12.** Water activity evolution of cured ham packed in DBC/PLDA polymer blend film with 20 wt% of DBC and commercial film vacuum bags. 287
- Figure 7.13.** Sliced cured ham packed in a) DBC/PLDA polymer blend film with 20 wt% of DBC and b) commercial multilayer vacuum bags during 9 days. 288
- Figure 7.14.** Comparative digital images of a) sliced cured ham packed in DBC/PLDA polymer blend film with 20 wt% of DBC and b) commercial multilayer vacuum bags at day 40. 289
- Figure 7.15.** Lipid oxidation evolution of sliced cured ham packed in DBC/PLDA polymer blend film with 20 wt% of DBC and commercial film vacuum bags. 290
- Figure 7.16.** pH evolution of sliced cured ham packed in DBC/PLDA polymer blend film with 20 wt% of DBC and commercial film vacuum bags. 291
- Figure 7.17.** Acceptance preferences of the panelist of both vacuum bag types. 291
- Figure 7.18.** Flavour and smell differences of sliced cured hams packed in both vacuum bag types. 292
- Figure 7.19.** Texture evaluation of sliced cured ham packed in both vacuum bag types. 293

V.2. LIST OF TABLES

Introduction

Table I.1. Polymer types used for packaging applications..... **9**

Table I.2. Commercial bioplastics available at industrial scale, producers, and brand names.
..... **12**

Chapter 1.

Table 1.1. PLA stereoisomers configurations..... 36

Table 1.2. Different conditions tested for preparation of PLDA homopolymer films by solvent casting method. S1 correspond to step 1 and S2 correspond to step 2. 41

Table 1.3. PLDA/PCL polymer blend films and its weight relation between blend components.
..... 41

Table 1.4. PLDA and PCL homopolymers molecular weights obtained by GPC. 44

Table 1.5. PLDA and PCL homopolymers thermal transitions by DSC..... 45

Table 1.6. PLDA homopolymer films used to evaluate the optimal preparation conditions. .. 45

Table 1.7. PLDA homopolymer films thermal transitions using different protocols. 47

Table 1.8. Tonset and Tdeg of PLDA homopolymer films obtained by protocol 1. 49

Table 1.9. Tonset and Tdeg of PLDA homopolymer films obtained by protocol 2. 50

Table 1.10. Tonset and Tdeg of PLDA homopolymer films obtained by protocol 3. 51

Table 1.11. PLDA/PCL polymer blends thermal transitions during 1st heating scan. 53

Table 1.12. PLDA/PCL polymer blends thermal transitions during 2nd heating scan. 54

Chapter 2.

Table 2.1. PLLA-b-PCL/PLDA polymer blend formulations..... 67

Table 2.2. PLLA-b-PCL/PLDA polymer blends extrusion conditions..... 69

Table 2.3. PLLA-b-PCL diblock copolymer molecular weights obtained by GPC. 72

Table 2.4. PLLA-b-PCL diblock copolymer thermal transitions..... 72

Table 2.5. Thermal transitions of PLLA-b-PCL diblock copolymer obtained by DSC..... 73

Table 2.6. Thickness of solvent casted PLLA-b-PCL/PLDA polymer blend films.....	75
Table 2.7. Transparency of PLLA-b-PCL/PLDA polymer blend films taken at 600 nm wavelength.	76
Table 2.8. Solubility parameters of PLDA, PCL and chloroform.	77
Table 2.9. Surface tension of the PLDA and PCL.	80
Table 2.10. PCL volume molar percentage in PLLA-b-PCL/PLDA polymer blends.	81
Table 2.11. Thermal transitions of PLLA-b-PCL/PLDA polymer blend compositions.....	84
Table 2.12. TGA curves of PLLA-b-PCL/PLDA polymer blend films.....	86
Table 2.13. The OTR and oxygen permeability of solvent casted PLLA-b-PCL/PLDA polymer blend films.87	
Table 2.14. The OTR and oxygen permeability of extruded PLLA-b-PCL/PLDA polymer blend films.....	89
Table 2.15. The WVTR and water permeability results of solvent casted PLLA-b-PCL/PLDA polymer blend films.....	90
Table 2.16. The WVTR and water permeability results of extruded PLLA-b-PCL/PLDA polymer blends films.	91
 Chapter 3.	
Table 3.1. PLLA-b-PCL/PLDA-PCL ternary polymer blend compositions.....	107
Table 3.2. Thickness of solvent casted PLLA-b-PCL/PLDA-PCL 70:30 polymer blend films measurements.	111
Table 3.3. Thickness of solvent casted PLLA-b-PCL/PLDA-PCL 80:20 polymer blend films measurements.	111
Table 3.4. Transmittance values of solvent casted PLLA-b-PCL/PLDA-PCL 70:30 polymer blend films.....	113
Table 3.5. Transmittance values of solvent casted PLLA-b-PCL/PLDA-PCL 80:20 polymer blend films.....	113
Table 3.6. Thermal transitions of PLLA-b-PCL/PLDA-PCL 70:30 polymer blend films with different DBC content.....	114
Table 3.7. Thermal transitions of PLLA-b-PCL/PLDA-PCL 80:20 polymer blend films with different DBC content.....	115
Table 3.8. Weight content of each block of PLLA-b-PCL diblock copolymer in PLLA-b-PCL/PLDA-PCL polymer blend films.....	117

Table 3.9. Degree of crystallinity of each block in PLLA-b-PCL/PLDA-PCL polymer blend films.	118
Table 3.10. TGA curves of PLLA-b-PCL/PLDA -PCL 70:30 polymer blend films with different DBC content.....	121
Table 3.11. TGA curves of PLLA-b-PCL/PLDA -PCL 80:20 polymer blend films with different DBC content.....	122
Table 3.12. PCL vol% in PLLA-b-PCL/PLDA-PCL polymer blends.....	125
Table 3.13. The OTR and oxygen permeability of PLLA-b-PCL/PLDA-PCL polymer blend films with different DBC content.....	126
Table 3.14. The WVTR and water permeability of PLLA-b-PCL/PLDA-PCL polymer blend films with different DBC content.....	129

Chapter 4.

Table 4.1. Reagent quantities used to synthesize PCL-OH prepolymers.....	143
Table 4.2. L-LA and ϵ -CL ratio and catalyst amounts to synthesize PLLA-b-PCL.....	145
Table 4.3. Spin coated PLLA-b-PCL/PLDA polymer blend films composition.....	145
Table 4.4. Amounts of PCL-OH prepolymer prepared by mechanical stirring.	147
Table 4.5. PCL-b-PLLA diblock copolymers theoretical molecular weight and reagents used for copolymerization synthesis.....	148
Table 4.6. PLDA/PCL-PLLA polymer blends extrusion conditions.....	149
Table 4.7. Mn, Mw and PDI of PCL-OH prepolymer prepared using magnetic stirring calculated by ^1H NMR and GPC.....	153
Table 4.8. Thermal parameters extracted from TGA and DTG curves of PCL-OH prepolymer prepared using magnetic stirring.....	155
Table 4.9. Thermal parameters extracted from DSC thermograms of PCL-OH prepolymer prepared using magnetic stirring.....	155
Table 4.10. Molecular weights of PLLA-b-PCL diblock copolymers calculated by ^1H NMR and GPC.....	157
Table 4.11. Thermal parameters extracted from TGA and DTG curves of synthesized PLLA-b-PCL diblock copolymers and PCL-OH prepolymer.....	160
Table 4.12. Thermal parameters extracted from heating scan of DSC curves of synthesized PLLA-b-PCL diblock copolymers prepared using magnetic stirring.....	161

Table 4.13. Degree of crystallinity of synthesized PLLA-b-PCL diblock copolymers prepared using magnetic stirring and used PCL-OH prepolymer.....	162
Table 4.14. Molecular weights of PCL-OH prepared by mechanical stirring calculated by ¹ H NMR.	165
Table 4.15. Thermal stability parameters extracted from TGA and DTG curves of PCL-OH prepolymer prepared by mechanical stirring.	166
Table 4.16. Thermal parameters extracted from DSC curve of PCL-OH prepolymer prepared by mechanical stirring.....	166
Table 4.17. Molecular weight of PCL and PLLA blocks calculated by ¹ H-NMR for the different PCL-b-PLLA diblock copolymers prepared by mechanical stirring.	168
Table 4.18. Molecular weight by GPC for the different PCL-b-PLLA diblock copolymers prepared by mechanical stirring.	168
Table 4.19. Thermal stability parameters extracted from TGA and DTG curves of different PCL-b-PLLA diblock copolymers prepared by mechanical stirring.	169
Table 4.20. Thermal parameters extracted from DSC curves of synthesized PCL-b-PLLA diblock copolymers using mechanical stirring.....	171
Table 4.21. Data extracted from TGA and DTG of different PCL-b-PLLA/PLDA polymer blends.	173
Table 4.22. Thermal parameters extracted from DSC curves of PLDA/PCL-PLLA diblock copolymers.....	175
Table 4.23. Mechanical properties of different PLDA/PCL-PLLA polymer blends.	176
Table 4.24. The OTR and oxygen permeability of extruded PLDA/PCL-PLLA polymer blends with different synthesized PCL-b-PLLA diblock copolymer.	178
Table 4.25. The WVTR and water vapour permeability of extruded PCL-b-PLLA/PLDA polymer blends with different synthesized PCL-b-PLLA diblock copolymer.....	179

Chapter 5.

Table 5.1. PCL-OH prepolymers reaction conditions on preindustrial scale varying catalyst wt%.	193
Table 5.2. Molecular weights of PCL-OH prepolymer after 4 h of reaction calculated by ¹ H NMR and GPC.	198
Table 5.3. Thermal stability parameters extracted from TGA and DTG curves of PCL-OH prepolymer synthesized on preindustrial scale. ...	199

Table 5.4. Thermal parameters extracted from DSC curve of PCL-OH prepolymer synthesized on preindustrial scale...	200
Table 5.5. Synthesized PLLA-b-PCL diblock copolymers on preindustrial scale.....	201
Table 5.6. Molecular weight of PLLA-b-PCL diblock copolymers synthesized on preindustrial scale.	203
Table 5.7. Thermal stability parameters extracted from TGA and DTG curves of different PCL-b-PLLA diblock copolymers synthesized on preindustrial scale.	205
Table 5.8. DSC thermal parameters of synthesized PLLA-b-PCL diblock copolymers.....	206
 Chapter 6.	
Table 6.1. Definitions of parameters extracted from Ludovic® software.	218
Table 6.2. DBC properties.	221
Table 6.3. DBC/PLDA polymer blend compositions selected to analyse optimum screws configurations.	222
Table 6.4. DBC/PLDA polymer blend compositions selected to analyse optimum screws configurations.	222
Table 6.5. DBC/PLDA polymer blends extrusion compounding conditions at pilot scale.....	224
Table 6.6. Injection moulding conditions of DBC/PLDA polymer blends on preindustrial scale.	225
Table 6.7. Single extrusion cast conditions of DBC/PLDA polymer blends on preindustrial scale.	226
Table 6.8. Description of the analyses carried out according to EN 13432:2000 for testing biodegradability and compostability of DBC/PLDA polymer blends.	229
Table 6.9. Biodegradability test composition for DBC/PLDA polymer blend with 20 wt% of DBC.....	230
Table 6.10. Ecotoxicity test compositions for DBC/PLDA polymer blend with 20 wt% of DBC.	232
Table 6.11. Thermal and rheological properties of DBC/PLDA polymer blend with 20 wt% DBC content used for Ludovic simulation.	233
Table 6.12. Types of elements used for designing extruder screw configurations.	234
Table 6.13. Ludovic simulation software outputs about the theoretical screw configurations.	237

Table 6.14. Thermal and rheological properties of DBC/PLDA polymer blend samples processed using ITENE 3B and ADBio 2 screw configurations.....	237
Table 6.16. MFI results of DBC/PLDA polymer blends.	239
Table 6.17. Thermal transitions of DBC/PLDA polymer blends with different DBC content. .	242
Table 6.18. TGA curves of DBC/PLDA polymer blends with different DBC content.....	243
Table 6.19. The HDT results of DBC/PLDA polymer blends with different DBC content produced on preindustrial scale.....	244
Table 6.20. Mechanical results of DBC/PLDA polymer blends varying the DBC content produced on preindustrial scale.....	244
Table 6.21. Oxygen permeability of DBC/PLLA polymer blends with different DBC content produced on preindustrial scale.....	247
Table 6.22. The WVTR values of DBC/PLDA polymer blends with different DBC content produced on preindustrial scale.....	248
Table 6.23. Global migration test results of DBC/PLDA polymer blends with 10 wt% and 20 wt% of DBC produced on preindustrial scale for different food simulants.	249
Table 6.24. The specific migration conditions for conventional plastics materials if compared to adapted condition for DBC/PLDA polymer blends.	250
Table 6.25. The specific migration results using different food simulants in contact with DBC/PLDA polymer blend with 10 wt% of DBC content.....	251
Table 6.26. The specific migration results using different food simulants in contact with DBC/PLDA polymer blend with 20 wt% of DBC.	251
Table 6.27. Dry and volatile solids of DBC and DBC/PLDA polymer blend with 20 wt% of DBC produced on preindustrial scale.....	253
Table 6.28. Metal and hazardous substances content in selected DBC produced on preindustrial scale.....	253
Table 6.29. Metal and hazardous substances content of extrusion cast DBC/PLDA polymer blend produced on preindustrial scale.....	254
Table 6.30. Disintegration rate of DBC/PLDA polymer blends with 20 wt% of DBC produced on preindustrial scale.....	256
Table 6.31. Ecotoxicity test results for DBC/PLDA polymer blends with 20 wt% of DBC.	256

Chapter 7

Table 7.1. Properties of DBC/PLDA 20:80.	269
--	-----

Table 7.2. Extrusion cast processing conditions to produce DBC/PLDA polymer blends with 20 wt% sheet reel on preindustrial scale.	270
Table 7.3. Extrusion cast processing conditions to produce DBC/PLDA polymer blends with 20 wt% of DBC film reel on preindustrial scale.	270
Table 7.4. Thermoforming parameters to be adjusted during sheets thermoforming trials on preindustrial scale.	271
Table 7.5. Thermoforming sheets final parameters to produced clamshells trays on preindustrial scale.	271
Table 7.6. Compression test results of thermoformed clamshell trays produced on preindustrial scale.	279
Table 7.7. Mechanical properties of extruded DBC/PLDA polymer blend film with 20 wt% of DBC produced on preindustrial scale.	281
Table 7.8. The COF results extruded DBC/PLDA polymer blend film with 20 wt% of DBC produced on preindustrial scale.	281
Table 7.9. Tear resistance results of extruded DBC/PLDA 20:80 polymer blend film with 20 wt% of DBC produced on preindustrial scale.	282
Thermosealing study of DBC/PLDA polymer blends with 20 wt% if comparison with commercial PLDA vacuum bags.	283

V.3. LIST OF ABBREVIATIONS

AFM	Atomic force microscopy
ATR	Attenuated total reflectance
AW	Water activity
BCP	Block copolymers
COF	Coefficient of friction
DBC	Diblock copolymer
DIR	Drop impact resistance
DMA	Dynamomechanical mechanical analysis
DP	Degree of polymerization
DS	Dry solids
DSC	Differential scanning calorimetry
DTG	First derivative thermogravimetric
ε-CL	ε-caprolactone monomer
EDTA	Ethylenediaminetetraacetic acid
EFSA	European Food Safety Authority
EVOH	Ethylene vinyl alcohol
FTIR	Fourier Transform infrared spectroscopy
GPC	Gel permeation chromatography
HDT	Heat reflection temperature
¹H-NMR	Proton nuclear magnetic resonance
HPLC	High-performance liquid chromatography
ICP-MS	Inductively coupled plasma mass spectrometry
LA	L-lactide monomer
MDA	Malonadialdehyde

MFI	Melt flow index
MFT	Mean field theory
NMR	Nuclear magnetic resonance
OTR	Oxygen transmission rate
PBAT	Poly (butylene adipate-co-terephthalate)
PBS	Poly (butylene succinate)
PBSA	Poly (butylene succinate adipate)
PCL	Poly (ϵ -caprolactone)
PCL-OH	Hydroxy-terminated poly (ϵ -caprolactone) prepolymer
PDI	Polydispersity index
PE	Polyethylene
PET	Polyethylene terephthalate
P3HB	Poly (3-hydroxybutyrate)
PHBV	poly (hydroxybutyrate-co-3-hydroxyvalerate)
PLA	Poly (lactic acid)
PLDA	Poly (L-D-lactic acid)
PLLA	Poly (L-lactic acid)
PLLA-b-PCL	Poly (L-lactic acid-b- ϵ -caprolactone) diblock copolymer
PMMA	Poly (methyl methacrylate)
PP	Polypropylene
PS	Polystyrene
PTFE	Polytetrafluoroethylene
PVC	Poly (vinyl chloride)
RH	Relative humidity
ROP	Ring opening polymerization

SCFT	Self-consistent field theory
SD	Standard deviation
SEM	Scanning electron microscope
SME	Specific mechanical energy
TBA	2-thiobarbituric acid
TCA	Trichloroacetic acid
TGA	Thermogravimetical analysis
THF	Tetrahydrofurane
UV-Vis	Ultraviolet-visible
WAXS	Wide angle X-ray diffraction
WVTR	Water vapour transmission rate
XRD	X-ray diffraction
ZME	Zester mixing element

V.4. LIST OF SYMBOLS

°	Degree
%	Percentage
°C	Degree Celsius
γ	Surface tension
cc	Cubic centimeter
cm	Centimeter
dm	Decimeter
δ	Solubility parameters
δ_d	Molecular dispersive force
δ_h	Hydrogen bonding force
δ_p	Dipol-dipol permanent interaction
ϕ	Volume fraction of the immiscible block
g	Gram
GPa	Giga Pascal
ΔH_c	Enthalpy of crystallization transition
ΔH_{cc}	Enthalpy of cold crystallization transition
ΔH_m	Enthalpy of melting transition
ΔW	Difference in weight loss
h	Hour
J	Joule
K	Kelvin
kg	Kilograms
kHz	Kilohertz
kJ	Kilojoules

kWh	Kilowatt-hour
L	Liter
L/D	Length/diameter ratio
μL	Microliter
μm	Micrometer
M_n	Number average molecular weight
M_w	Weight average molecular weight
m	Meter
min	Minutes
mbar	Milibar
mg	Miligram
mL	Mililiter
mm	Milimeter
MPa	Mega Pascal
N	Newton
N_A	Block length
nm	Nanometer
Pa	Pascal
ppm	Parts per million
psi	Pounds per square inch
ρ	Theoretical density
ρ_A	Density
rpm	Revolutions per minute
s	Second
T	Transmittance
T_c	Crystallization temperature

T_{cc}	Cold crystallization temperature
T_{deg}	Degradation temperature
T_g	Glass transition temperature
T_m	Melting temperature
T_{onset}	Onset temperature
V_{core}	Core volume
$V_{m,A}$	Molar volume
W	Watts
w	Mass fraction
w_x	Weight percent
wt%	Percentage by weight
wt/vol	Weight/volume
X_c	Degree of crystallinity
χ	Flory-Huggins interaction parameter
χN	Chain length
Z	Aggregation number

V.5. LIST OF EQUATIONS

Chapter 1

$$Tg12 = Tg1 w1 + Tg2 w2 \quad \text{Equation 1.1 } \mathbf{38}$$

$$Xc = \frac{\Delta Hm - \Delta Hcc}{\Delta Hm} \times 100 \quad \text{Equation 1.2..... } \mathbf{43}$$

Chapter 2

$$X_c = \frac{(\Delta H_{m(block)})}{\Delta H_m} \times W_{block} \quad \text{Equation 2.1}$$

..... **72**

$$\delta = \delta d2 + \delta p2 + \delta h2 \quad \text{Equation 2.2}$$

..... **77**

$$\rho = \frac{\text{weight (g)}}{\text{Volume (cm}^3\text{)}} \quad \text{Equation 2.3. } \mathbf{81}$$

Chapter 3

$$\Delta H = \Delta Hm - \Delta Hcc \quad \text{Equation 3.1..... } \mathbf{117}$$

Chapter 7

$$\Delta E = (\Delta a^*)^2 + (\Delta b^*)^2 + (\Delta L^*)^2 \quad \text{Equation 7.1 } \mathbf{276}$$

V.6. LIST OF SCHEMES

Chapter 2

Scheme 2.1. *Scheme of points to measure thickness of solvent casted PLLA-b-PCL/PLDA polymer blend films. 74*

Scheme 2.2. *Morphology formation of PLLA-b-PCL/PLDA polymer blends during the evaporation process. 79*

Scheme 2.3. *Different morphologies of PLLA-b-PCL diblock copolymer with increase of PCL block content. Source: Scheme adapted from Ocando PhD work Nanostructured thermosetting systems from SBS block copolymers". 80*

Chapter 4

Scheme 4.1. *The synthesis route of PCL-OH prepolymer. 143*

VI. ACKNOWLEDGEMENTS

VI. ACKNOWLEDGEMENTS

AGRADECIMIENTOS

Todos tenemos sueños. Pero para convertir los sueños en realidad, se necesita una gran cantidad de determinación, dedicación, autodisciplina y esfuerzo (Jesse Owens) y con esta frase comienzo los agradecimientos de mi Tesis Doctoral, a la que he dedicado una gran parte de la que por ahora es la década de mayor crecimiento tanto a nivel profesional, en la que he crecido como investigador a través de distintos puestos, como a nivel personal, ya que empecé la tesis siendo una y la acabo siendo una familia de cuatro.

Mis primeros agradecimientos son para una de mis dos directoras de tesis, Dr. Agnieszka Tercjak, gracias por todo tu apoyo, por enseñarme a plasmar de manera clara todos los desarrollos llevados a cabo, gracias por guiarme, darme ánimos y ayudarme, sean vacaciones, fines de semana o la hora que sea, por toda tu dedicación admirable, he aprendido mucho a tu lado, te estaré agradecida siempre.

Y a continuación, para la Dr. Susana Aucejo, gracias de corazón por ver en mí todo lo que ni siquiera aún sabía yo que era capaz de hacer. Gracias por contagiarme tu inquietud y gracias por apoyarme en mis iniciativas aún sin estar seguras de cuál iba a ser el resultado. Contigo he aprendido que en la ciencia hay que lanzarse, hay que probar y sobre todo no hay que tener miedo a asumir riesgos. Y gracias a tu confianza llegué al Dr. Iñaki Mondragón, no puedo escribir una línea sin emocionarme al pensar en él. Aún recuerdo cuando mi búsqueda por ampliar mi formación en materiales renovables me llevó al Master de Ingeniería en Materiales Renovables de la UPV/EHU y mi primera entrevista con él. En el Sport, un café, (era la primera vez que tenía una reunión de trabajo fuera de una sala de reuniones), recuerdo sus palabras: ¿pero tu valenciana entonces de qué dices que sabes? ¿de envases? Aquí solo trabajamos con copolímeros de bloque. Recuerdo mi cara de sorpresa. Habrá que pensar que hacemos para sacar de aquí una Tesis. ¿tú crees en la ciencia disruptiva? Y tanto que creo contesté, y hasta ahora. Espero que me veas por algún agujerito de la capa de ozono.

Así mismo me gustaría agradecer especialmente a mis jefes de ITENE, sin ellos no hubiera sido imposible ni iniciar, ni terminar este trabajo. Mis primeros agradecimientos a Dr. Javier Zabaleta por creer en este desarrollo aun cuando los números no lo acompañaban, muchas gracias de corazón, por haberme apoyado siempre y haberme ido dando pequeños empujones para poder llegar hasta aquí, he aprendido mucho de este proceso y también de planes de

negocio y de start ups, si tú no hubieras creído no habiéramos llegado hasta aquí. A mi jefa, Dr. Carmen Sánchez, por hacerlo posible, por ponerme los medios, por hacerme priorizar, sacar el tiempo y coger el toro por los cuernos, por ofrecerme su mano para lo que necesitara, sobre todo en estos meses de redacción, gracias por tu confianza. Y a mi equipo de ITENE, a mis chic@s de la Gerencia de Materiales y Envases y compañer@s en general, gracias a tod@s porque de una manera u otra habéis sufrido que mi dedicación a la tesis os haya restado dedicación a vosotr@s, pero en especial quiero agradecer a mi hermano mayor de ITENE, Jose Alonso, gracias por tu ayuda incansable, por tranquilizarme cuando colapso y por estar siempre ahí, y espero que por muchos años más. Ampí por darme ánimos, apoyo y poner tu hombro, siempre. Alejandro, Soraya, M^a Jose y Natalia, porque aquí hay un trocito vuestro. A mis compañeros de la Uni, porque a pesar de la distancia cuando vuelvo es como si no me hubiera ido, gracias a tod@s y en especial a Loli por tu ayuda, Raquel mi compi de banco, Junkal y Maria. También quiero agradecer a mi quinta de Master, nunca olvidaré nuestras vivencias dentro y fuera de la Uni.

Finalmente siempre se ha dicho que el último párrafo de la tesis es el más importante, así que os lo dedico a vosotros, a mi familia. A mis padres, papá, mamá, gracias por haberme dado siempre seguridad, demostrarme que con esfuerzo lo que uno desea es posible conseguirlo. Gracias a los dos por darme alas para volar desde bien pequeña y raíces para saber siempre volver a casa. Ahora sé lo que habréis sufrido en mis estancias fuera de Valencia. A mi hermano, por estar siempre que te necesito, aunque regruñas mil veces. A ti, Edu, por tu apoyo incondicional, por creer en mí y por poner mis sueños por delante de los tuyos, imposible tener mejor compañero de vida. Y a vosotras, Marta y Blanca, por haber aguantado como campeonas las ausencias de mamá, me encanta oírlos hablar de los plásticos que hace mamá para que no hayan plásticos en el mar, espero que cuando seáis mayores os leáis esta tesis. A la familia que uno elige, en especial a Sux, no sé cómo has sacado fuerzas estos meses para apoyarme, gracias, gracias, gracias. Y al resto de mis amig@s por aguantar mis rollos de tesinanda. Y un recuerdo para todas las personas queridas que se me han ido en 2022 y sobre todo a una a la que por muy poquito no he podido decirle, tía que ya he terminado la tesis, ya puedo salir! .

He tardado diez años en cumplir este sueño, pero no cambiaría nunca todos los que he podido cumplir por el camino y que ni siquiera soñaba con ellos cuando inicié esta tesis. Gracias.

Miriam

